

**CALIBRATION OF VEHICLE AND DRIVER  
CHARACTERISTICS FOR VISSIM MODEL,  
ANN-BASED SENSITIVITY ANALYSIS,  
TRAFFIC MANAGEMENT, AND SIGNAL  
DESIGN USING GA FOR MANGALORE  
CITY**

Thesis

Submitted in partial fulfilment of the requirements for the degree of  
**DOCTOR OF PHILOSOPHY**

by

**MARSH M. BANDI**  
**(Reg. No. 138005CV13F06)**



**DEPARTMENT OF CIVIL ENGINEERING  
NATIONAL INSTITUTE OF TECHNOLOGY KARNATAKA,  
SURATHKAL, MANGALORE – 575025**

**OCTOBER, 2021**

**CALIBRATION OF VEHICLE AND DRIVER  
CHARACTERISTICS FOR VISSIM MODEL,  
ANN-BASED SENSITIVITY ANALYSIS,  
TRAFFIC MANAGEMENT, AND SIGNAL  
DESIGN USING GA FOR MANGALORE  
CITY**

Thesis

Submitted in partial fulfilment of the requirements for the degree of

**DOCTOR OF PHILOSOPHY**

by

**MARSH M. BANDI**

**(Reg. No. 138005CV13F06)**

Under the guidance of

**Dr. VARGHESE GEORGE**

Research Supervisor



**DEPARTMENT OF CIVIL ENGINEERING  
NATIONAL INSTITUTE OF TECHNOLOGY KARNATAKA  
SURATHKAL, MANGALORE – 575025**

**OCTOBER, 2021**

## DECLARATION

*by the Ph.D. Research Scholar*

I hereby *declare* that the Research Thesis entitles "**CALIBRATION OF VEHICLE AND DRIVER CHARACTERISTICS FOR VISSIM MODEL, ANN-BASED SENSITIVITY ANALYSIS, TRAFFIC MANAGEMENT, AND SIGNAL DESIGN USING GA FOR MANGALORE CITY**" which is being submitted to National Institute of Technology Karnataka, Surathkal in partial fulfillment of the requirements for the award of the Degree of Doctor of Philosophy in Traffic and Transportation Engineering in the Department of Civil Engineering is a *bonafide report of the research work carried out by me*. The material contained in this Research Thesis/Synopsis has not been submitted to any University or Institution for the award of any degree.



138005CV13F06, MARSH M. BANDI

---


(Register Number, Name & Signature of the Research Scholar)  
Department of Civil Engineering

Place: NITK-Surathkal

Date: 29<sup>th</sup> October 2021

CERTIFICATE

This is to *certify* that the Research Thesis entitles "**CALIBRATION OF VEHICLE AND DRIVER CHARACTERISTICS FOR VISSIM MODEL, ANN-BASED SENSITIVITY ANALYSIS, TRAFFIC MANAGEMENT, AND SIGNAL DESIGN USING GA FOR MANGALORE CITY**" submitted by MARSH M. BANDI (Register Number: 138005CV13F06) as the record of the research work carried out by him, is *accepted as the Research Thesis/Synopsis submission* in partial fulfillment of the requirement for the award of degree of Doctor of Philosophy.

 (DR. VARGHESE GEORGE)  
29/10/2021

Research Guide  
(Name and Signature with Date and Seal)



  
01/11/2021

Chairman - DRPC  
(Signature with Date and Seal)

Chairman (DRPC)

Department of Civil Engineering  
National Institute of Technology Karnataka, Surathkal  
Mangalore - 575 025, Karnataka, INDIA

## ACKNOWLEDGEMENTS

*I take this opportunity to thank **GOD Almighty** for enabling me to complete this research. I hereby express my sincere thanks and gratitude to my esteemed research guide **Dr. Varghese George**, Professor in the Department of Civil Engineering, for his expert guidance, valuable suggestions, reference material provided, and continuous encouragement throughout the course of my thesis work.*

*I am grateful to **Dr. K. Swaminathan**, Professor and Head of Civil Engineering Department, for giving me the permission to do my dissertation work in the institute.*

*I record my sincere thanks to the **Commissioner of Police, Mangalore**, for having provided us the necessary permission for conducting video-graphic surveys at important junctions. Thanks are also due to the **Regional Transport Officer, Mangalore** for having provided us the necessary statistical data on traffic in Mangalore city.*

*I am also indebted to **Mr. Akash Anand** (NITK Alumni 2014), Research Scholar, NITK, Surathkal, **Dilipkumar and Aida** (NITK Alumni 2015), NITK, Surathkal, **Ishaan and Sreeja** (NITK Alumni 2016), NITK, Surathkaland other M.Tech Students of 2015 & 2016 batch for having provided necessary support in the Data Collection work.*

*I am also indebted to all **teaching and non-teaching staff** of the department of Civil Engineering, NITK, Surathkal and my **classmates and friends** who helped me directly and indirectly in the completion of this dissertation work.*

*Last but never the least; I would like to state my deepest gratitude to the support and love given to me by my Parents, **Mr&Mrs M. R. Bandi**, I am also highly indebted to my spouse, **Mrs Sharon M. Bandi** for her constant encouragement and moral support during the course of my research work.*

*Once again, I acknowledge with gratitude, one and all who helped me directly or indirectly in the completion of the research work related to my PhD.*

**MARSH M. BANDI**

## ABSTRACT

The field of traffic flow modeling has emerged as an important multi-disciplinary area with contributions from traffic-engineers, city-planners, mathematicians, and specialists in the field of computer sciences. Traffic engineers and planners constantly strive to alleviate problems that arise due to bottlenecks in traffic movement. One of the major challenges to traffic management lies in minimizing congestion and facilitating efficient traffic flow.

The study of traffic congestion requires a proper understanding of the relationship between vehicle characteristics and driver characteristics to mimic existing traffic flows on urban streets. Simulation approaches permit traffic engineers of developing countries to evolve reliable models to investigate the influence of various factors related to roadways, and driver and vehicle characteristics on traffic flow on urban roads characterized by heterogeneous traffic conditions. These modeling techniques assist in gaining insight into the underlying relationships between the above factors involved.

The primary scope of this study is focused on performing investigations using micro-simulation on understanding the traffic characteristics of Mangalore city in India, for heterogeneous traffic composition using *VISSIM*. A very important traffic circuit of the city connecting Hampankatta Circle, Navbharat Circle, PVS Circle, Bunts Hostel Circle, and Jyothi Circle, was considered for analysis, in addition to the nearby important locations such as Bendoorwell Junction, Balmatta Junction, and St. Theresa's School Junction.

In the *initial phase* of the study, the links and connectors representing the road network of the city were assigned in the *VISSIM* modeling environment on a template comprising a 1:5000 high-resolution base-map of the city overlaid with the layout of the roads and junctions using *AutoCAD*. Data on turning movements of traffic at various junctions was collected for 80 minutes during the peak-hour between 17:00 - 18.30 hours on Tuesday 10<sup>th</sup> March 2015 as part of this study. In this phase of the study, a number of simulation experiments were performed using the above data for default vehicle and driver characteristics, and the best random seed to be used for simulation was identified as 25, and 42 from among the random seeds from 1-50s tested.

In the *calibration exercise*, the driver and vehicle parameters were fine-tuned in fourteen major stages to minimize errors between the observed data and the simulated results. 75% of the video-graphic data was used for performing testing and calibration, while the remaining 25% of the data was used for validation studies. An *ANN-based sensitivity analysis* was then performed to identify the relative importance of various vehicle and driver characteristics. A *modified Garson's approach* was adopted in this study for the computation of relative sensitivity based on connection weights between the input layer, the three hidden layers, and the output layer for the optimized *ANN* configuration. Based on the results of the sensitivity analysis, the predictive capability of the simulation model was further enhanced by performing a *multi-level extended calibration* procedure that provided reliable results as per prescribed standards for traffic simulation. This finalized model was again validated successfully.

The fully calibrated *VISSIM* model was used in the later phase of the study, to study the effect of implementing *short-term* strategies such as widening of existing road-widths, and *long-term* improvement strategies such as introduction of flyovers at selected critical locations in the city. Additionally, studies were performed using the *genetic algorithm (GA)* based approach in the design of traffic signal timings for streamlining traffic flows across four important junctions in the city. The objective function in the *GA* module was formulated based on the *HCM average delay model* (TRB 2000).

The overall approach towards performing calibration studies evolved through the present study is expected to provide the basic framework for calibration and fine-tuning of vehicle and driver characteristics in the development of micro-simulation models. The findings of this study are expected to assist transport planners in developing innovative solutions to urban traffic management, analysis, design, and operation of vehicles on roadways.

*Keywords:* *VISSIM*, Micro-simulation, Calibration, *ANN*, Sensitivity, *Genetic Algorithm*, *HCM Average Delay Model*

# CONTENTS

	Page No.
<i>Title Page</i>	i
<i>Declaration</i>	ii
<i>Certificate</i>	iii
<i>Acknowledgements</i>	iv
<i>Abstract</i>	v
<i>List of Figures</i>	xi
<i>List of Tables</i>	xiv
<b>Chapter 1 INTRODUCTION</b>	
1.1 General	1
1.2 Problem Scenario and the Need for the Study	6
1.3 Additional Problems Due to Heterogeneous Traffic	9
1.4 Role of Modeling Techniques and Microsimulation in the Analysis of Urban Traffic Scenario	10
1.5 Transportation Scenario in Mangalore City and Need for the Present Study	11
1.6 Scope and Objectives of the Work	13
1.7 Organization of the Project	16
<b>Chapter 2 LITERATURE REVIEW</b>	
2.1 General	19
2.2 Review of Earlier Microsimulation Models for Speed Flow Studies	20
2.3 Studies on Applications of VISSIM in Traffic and Transportation	22
2.4 Studies on Applications of ANN on Traffic Flow Modeling and Discussions on ANN Applications in Sensitivity Analysis	27
2.4.1 <i>Additional Studies on the Application of ANN in Sensitivity Analysis in the Field of Transportation Engineering</i>	29
2.5 Genetic Algorithm (GA) Applications in Traffic and Transportation	29
2.6 Selected Studies on Isolated Signal Design and Delays	31
2.7 Summary	34
<b>Chapter 3 THEORETICAL BACKGROUND</b>	
3.1 General	41
3.2 Importance of Simulation-Based Traffic Flow Modeling and Types of Simulation Modeling Approaches	42
3.2.1 <i>Microscopic Simulation Models</i>	43
3.2.2 <i>Sub-Microscopic Simulation Models</i>	44
3.2.3 <i>Mesosopic Models</i>	44
3.2.4 <i>Macroscopic Models</i>	44
3.3 Macro-Models for Speed-Density-Flow Relationships	45
3.3.1 <i>Speed Vs Density Relationship</i>	45
3.3.2 <i>Speed Vs Flow Relationship</i>	46
3.3.3 <i>Flow Vs Density Relationships</i>	47
3.3.4 <i>Speed - Flow - Density Relationship</i>	48

3.3.5	<i>Speed Vs Flow Relationship and Capacity Estimation</i>	48
3.4	Basic Aspects on the Design of Isolated Traffic Signals using the HCM 2000 Design Method	49
3.4.1	<i>Theoretical Considerations in the Design of Pre-timed Isolated Signals for 2 or More Phases Using the HCM 2000 Design Method (TRB, 2000)</i>	52
3.5	Theoretical Aspects on Traffic Delay, Basic Aspects of Webster's Approach, and HCM 2000 Average Delay Model	54
3.5.1	<i>Steady State Stochastic Delay Model (Webster's Delay Equation)</i>	55
3.5.2	<i>Deterministic Delay Models (for Under-saturated and Over-saturated Flows)</i>	57
3.5.3	<i>Time-dependent Stochastic Delay Models (for Under-saturated and Over-saturated Flows)</i>	58
3.5.3.1	<i>HCM average delay model (TRB, 2000)</i>	60
3.6	General Theoretical Aspects of GA Operations	62
3.6.1	<i>Functioning of Genetic Algorithm Applications</i>	62
3.6.2	<i>Fundamental Genetic Operations</i>	63
<b>Chapter 4</b>	<b>METHODOLOGY OF THE STUDY</b>	
4.1	Introduction	65
4.2	Overall Methodology Adopted in the Study	66
4.3	An Overview of VISSIM 7.0	70
4.4	Basic Steps for Model Development in VISSIM	73
<b>Chapter 5</b>	<b>DETAILS OF THE STUDY AREA, DATA COLLECTION APPROACH, AND CREATION OF A TEMPLATE TO BE INTERFACED TO VISSIM</b>	
5.1	Introduction	77
5.2	Study Area Characteristics	77
5.2.1	<i>Details of the Study Area</i>	77
5.2.2	<i>Important Roads and Intersections in the City</i>	84
5.2.3	<i>Existing Scenario of Traffic and Transportation in Mangalore</i>	84
5.3	Creation and Updating of AutoCAD Drawings of Road, Junctions, and Development of A Composite High-Resolution Base Map	87
5.4	Traffic Data Collection at Selected Mid-blocks and Junctions	92
<b>Chapter 6</b>	<b>RESULTS AND DISCUSSIONS ON TESTING, CALIBRATION AND VALIDATION OF VISSIM MODEL FOR EXISTING SCENARIO</b>	
6.1	Introduction	95
6.2	Results and Discussions on Testing, Calibration, and GEH Statistics	96
6.2.1	<i>Interfacing the Composite .dwg File, and Field Data to Create a Network Map in VISSIM, Initial Default Settings, and Selection of the Best Random Seed</i>	98
6.2.1.1	<i>setting of the default values for vehicle and driving characteristics</i>	100
6.2.1.2	<i>selection of the best random seed using default settings</i>	102
6.2.2	<i>First Level of Refinement of Vehicle and Driver Characteristics for Calibrations Using Random Seed 42</i>	106
6.2.3	<i>Second Level of Refinement of Vehicle and Driver Characteristics for Calibrations Using Random Seed 42</i>	109



6.2.4	<i>Third Level of Refinement of Vehicle and Driver Characteristics for Calibration Using Random Seed 42</i>	112
6.2.5	<i>Fourth Level of Refinement of Vehicle and Driver Characteristics for Calibration Using Random Seed 42</i>	114
6.2.6	<i>Fifth Level of Refinement of Vehicle and Driver Characteristics for Calibration Using Random Seed 42</i>	115
6.2.7	<i>Sixth Level of Refinement of Vehicle and Driver Characteristics for Calibration Using Random Seed 42</i>	116
6.2.8	<i>Seventh Level of Refinement of Vehicle and Driver Characteristics for Calibration Using Random Seed 42</i>	118
6.2.9	<i>Eighth Level of Refinement of Vehicle and Driver Characteristics for Calibration Using Random Seed 42</i>	120
6.2.10	<i>Ninth Level of Refinement of Vehicle and Driver Characteristics for Calibration Using Random Seed 42</i>	121
6.2.11	<i>Tenth Level of Refinement of Vehicle and Driver Characteristics for Calibration Using Random Seed 42</i>	122
6.2.12	<i>Eleventh Level of Refinement of Vehicle and Driver Characteristics for Calibration Using Random Seed 42</i>	123
6.2.13	<i>Twelfth Level of Refinement of Vehicle and Driver Characteristics for Calibration Using Random Seed 42</i>	124
6.2.14	<i>Thirteenth Level of Refinement of Vehicle and Driver Characteristics for Calibration Using Random Seed 42</i>	125
6.2.15	<i>Fourteenth or Final Level of Refinement of Vehicle and Driver Characteristics for Calibration Using Random Seed 42</i>	126
6.3	Validation of VISSIM Model After Calibration	129
6.3.1	<i>Validation of Traffic Volumes after the Fourteenth Level of Calibration</i>	129
6.4	Sensitivity Analysis	131
6.4.1	<i>Preparation of Datasets for ANN-Based Sensitivity Analysis</i>	131
6.4.2	<i>Determination of Ideal Configuration of ANN Model for Sensitivity Analysis</i>	133
6.4.3	<i>Method Adopted in the Study of Sensitivity Analysis</i>	134
6.5	Extended Multi-Level Calibration Based on Results of Sensitivity Analysis	139
6.5.1	<i>Extended First Level of Simulation Based on Sensitivity Analysis</i>	139
6.5.2	<i>Extended Second Level of Simulation Based on Results of Sensitivity Analysis</i>	140
6.5.3	<i>Extended Third Level of Simulation Based on Results of Sensitivity Analysis</i>	141
6.5.4	<i>Extended Fourth Level of Simulation Based on Results of Sensitivity Analysis</i>	142
6.5.5	<i>Extended Fifth Level of Simulation Based on Results of Sensitivity Analysis</i>	143
6.5.6	<i>Extended Sixth Level of Simulation Based on Results of Sensitivity Analysis</i>	144
6.6	Extended Validation Based on Results of Sensitivity Analysis	147
6.6.1	<i>Extended Validation of Volumes</i>	147

<b>Chapter 7</b>	<b>ANALYSES USING VISSIM FOR SHORT-TERM AND LONG-TERM IMPROVEMENTS</b>	
7.1	Introduction	149
7.2	Analysis of Short-term Improvement Strategy-1	150
7.3	Analysis of Short-term Improvement Strategy-2	158
7.4	Analysis of Long-term Improvement Strategy-1	165
7.5	Analysis of Long-term Improvement Strategy-2	170
<b>Chapter 8</b>	<b>DESIGN OF 3-PHASE SIGNALS IN MANGALORE CITY USING HCM 2000 METHOD AND GA APPROACH WITH VERIFICATION USING VISSIM MODEL</b>	
8.1	Introduction	175
8.2	Design of 3-Phase Pre-Timed Signals for Selected Junctions in Mangalore City Using <i>HCM 2000</i> Design Method	177
8.2.1	<i>Design of 3-Phase Isolated Traffic Signal Using HCM 2000 Design Method: PVS Junction</i>	177
8.2.2	<i>Summary of the Design of 3-Phase Isolated Traffic Signals for the Remaining Three Junctions Using HCM 2000 Design Method</i>	180
8.3	Design of 3-Phase Isolated Signals for Selected Junctions Using GA Approach Based on <i>HCM</i> Average Delay Model	185
8.3.1	<i>A Summary of Theoretical Considerations in HCM Average Delay Model</i>	185
8.3.2	<i>Theoretical Considerations in the Formulation of the Objective Function, Constraints, and Defining of the Fitness Index for the GA Approach</i>	188
8.3.2.1	<i>constraint related to cycle length</i>	189
8.3.2.2	<i>constraints related to green time</i>	189
8.3.2.3	<i>non-negativity constraints</i>	190
8.3.2.4	<i>constraints related to off-set time</i>	190
8.3.2.5	<i>formulation of the constraint violation coefficient</i>	190
8.3.2.6	<i>formulation of the modified objective function</i>	191
8.3.2.7	<i>establishing the fitness index (FI)</i>	192
8.3.2.8	<i>normalization of the fitness value (NFV) - an alternative approach</i>	192
8.3.3	<i>Design of 3-Phase Isolated Signals Using GA-Based Approach for Optimal Design Using HCM Average Delay Model: PVS Junction</i>	192
8.3.3.1	<i>input data to be assigned to the GA algorithm</i>	193
8.3.3.2	<i>explanation on encoding of binary strings for a hypothetical set of binary strings and computation of actual string values based on green time variable bounds</i>	195
8.3.3.3	<i>computations in the GA for setting the proportions for effective green times</i>	198
8.3.3.4	<i>computations in the GA for of the value of the objective function <math>f(x)</math></i>	198
8.3.3.5	<i>computation of constraint violation coefficients for the effective green times</i>	201
8.3.3.6	<i>computation of constraint violation coefficient for cycle length</i>	202
8.3.3.7	<i>computation of constraint violation coefficients for phase priority</i>	202
8.3.3.8	<i>computation of constraint violation coefficient for non-negativity</i>	203
8.3.3.9	<i>computation of the sum of constraint violation coefficients</i>	203
8.3.3.10	<i>computation of the values of modified objective function <math>\eta(x)</math> for</i>	203

	<i>each string</i>	
8.3.3.11	<i>computation of the values of the fitness index (FI) for each string</i>	204
8.3.3.12	<i>selection of the best string to form the next generation by the principle of elitism</i>	204
8.3.4	<i>Results on the Design of 3-Phase Isolated Traffic Signals for the Remaining 3 Junctions Using the GA Approach</i>	208
8.4	Performing Simulations Using VISSIM and Assessment of Delays at Selected Junctions in Mangalore City	209
8.4.1	<i>Comparisons between the Performance of Existing Manually Controlled Signal Timings Vs Signal Timings Computed Based on HCM 2000 Design Method</i>	209
8.4.2	<i>Comparisons between the Performance of Existing Manually Controlled Signal Timings Vs Optimized Signal Timings Computed Using the GA Approach</i>	210
<b>Chapter 9</b>	<b>CONCLUSIONS</b>	
9.1	Introduction	213
9.2	Conclusions Based on Testing and Calibration of VISSIM Model	214
9.2.1	<i>Conclusions Based on Multi-Stage Calibrations Performed</i>	215
9.2.2	<i>Conclusions Based on Model Validation (after the 14<sup>th</sup> Stage of Calibration)</i>	217
9.2.3	<i>Conclusions Based on the Sensitivity Analysis</i>	217
9.2.4	<i>Conclusions Based on Extended Calibration after Sensitivity Analysis</i>	218
9.2.5	<i>Conclusions Based on Extended Validation after Sensitivity Analysis</i>	220
9.3	Conclusions on Short-term and Long-term Traffic Management Strategies	220
9.3.1	<i>Conclusions Based on Short-Term Improvements at Selected Locations in the City</i>	220
9.3.2	<i>Conclusions on Long-Term Improvements at Selected Locations in the City</i>	221
9.4	Conclusions Based on the Design of 3-Phase Traffic Signals Using HCM2000 Design Method and Genetic Algorithm Approach for the Selected Junctions	222
9.5	Major Contributions of the Study	223
9.6	Limitations and Scope for Future Studies	223
	<b>REFERENCES</b>	225
	<b>LIST OF PUBLICATIONS</b>	241
	<b>BIO-DATA</b>	243
	<b>APPENDIX I</b>	

## LIST OF FIGURES

<b>Figure. No.</b>	<b>Description</b>	<b>Page No.</b>
Fig.3.1a	Greenshield's Speed-Density Relationship	45
Fig.3.1b	Basic Speed-Flow Relationship	46
Fig.3.2	Flow- Density Relationship	47
Fig.3.3	Capacity Estimation from Speed-Flow Curve	49
Fig.3.8a	Steady State and Deterministic Delay Models	58
Fig.3.8b	Stochastic Steady State, Deterministic, and Time-Dependent Delay Model	60
Fig.4.1	A Schematic Diagram on Various Steps in the Methodology Adopted	76
Fig.5.1a	Graphical Representation of Growth of Mangalore City	79
Fig.5.1b	Ward Map of Mangalore City	81
Fig.5.2a	Percentage of Registered Vehicles in 2019	82
Fig.5.2b	Map of the Study Area	83
Fig.5.3a	Previous AutoCAD Drawing of the Road Network under Study	88
Fig.5.3b	Updated AutoCAD Drawing of the Road Network for the Present Study	89
Fig.5.4	Digitized High Resolution Base-Map of the City with Details on the Road Network	90
Fig.5.5	Composite .dwg Image Created in AutoCAD by Superimposing AutoCAD Drawing of Roads and Junctions on the High Resolution .jpg Base-Map of Mangalore City	91
Fig.5.6	Links and Connectors for the City Road Network Drawn on the Template	92
Fig.6.1	Graphical Representation of the Calibration Process Adopted for the Development of the VISSIM-based Simulation Model	99
Fig.6.2a	AutoCAD Drawing Superimposed on High Resolution Base-map of Mangalore City Road Network with 18 Mid-Block Sections Marked	103
Fig.6.2b	Comparisons between Observed and Simulated Traffic Volumes at the 18 Mid-Block Sections for Experiments Using Different Random Seeds	104
Fig.6.3	Comparison of Observed and Simulated Flows at 18 Mid-block Locations for the Seventh level of Refinement Using Random Seed 42	119
Fig.6.4	Comparison of Observed and Simulated Flows at 18 Mid-block Locations at the Fourteenth Level of Refinement Using Random Seed 42	128
Fig.6.5	Reduction in the Mean Absolute Prediction Errors Over Fourteen Stages of Calibration	128
Fig.6.6	Comparison of Observed and Simulated Flows at 18 Mid-block Locations for Validation after the Fourteenth Level of Calibration Using Random Seed 42	130
Fig.6.7	Structure of ANN Showing the Optimized Ideal Configuration	135
Fig.6.8a	Reduction in the Mean Absolute Prediction Errors for Multi-level Refinement Over Six Stages Based on Results of Sensitivity Analysis	146
Fig.6.8b	A Graphical Representation of the Reduction in the Mean Absolute Errors	146

Fig.6.9	Comparison of Observed and Simulated Flows at 18 Mid-block Locations for Extended Validation after Extended Calibration Using Random Seed 42	148
Fig.7.1a	Layout of the Existing Road Alignment between Karangalpady Junction and Bunt's Hostel Junction	151
Fig.7.1b	Link 1, Link 2, and Link3 between Karangalpady Junction and Bunt's Hostel Junction	152
Fig.7.1c	Short-Term Improvement Strategy-1: Comparison of Simulated Stopped Delays for Flows between Karangalpady and Jyothi Junctions via Bunt's Hostel Junction	153
Fig.7.1d	Short-Term Improvement Strategy-1: Comparison of Simulated Volumes for Flows between Karangalpady and Jyothi Junctions via Bunt's Hostel Junction	153
Fig.7.1e	Short-Term Improvement Strategy-1: Comparison of Simulated Speeds for Flows between Karangalpady and Jyothi Junctions via Bunt's Hostel Junction	155
Fig.7.1f	Short-Term Improvement Strategy-1: Comparison of Simulated Stopped Delays for Flows between Karangalpady and Kadri Junctions via Bunt's Hostel Junction	156
Fig.7.1g	Short-Term Improvement Strategy-1: Comparison of Simulated Volumes for Flows between Karangalpady and Kadri Junctions via Bunt's Hostel Junction	157
Fig.7.1h	Short-Term Improvement Strategy-1: Comparison of Simulated Speeds for Flows between Karangalpady and Kadri Junctions via Bunt's Hostel Junction	157
Fig.7.2a	Layout of the Existing Road Alignment at Bendoorwell Junction	159
Fig.7.2b	Link 1 and Link 2 at Bendoorwell Junction for Approach from Kankanady Junction to Balmatta Junction	160
Fig.7.2c	Short-Term Improvement Strategy-2: Comparison of Simulated Stopped Delays for Flows between Kankanady and St. Theresa's School Junction for Various Vehicle Types	161
Fig.7.2d	Short-Term Improvement Strategy-2: Comparison of Simulated Volumes for Flows between Kankanady and St. Theresa's School Junction for Various Vehicle Types	161
Fig.7.2e	Short-Term Improvement Strategy-2: Comparison of Simulated Speeds for Flows between Kankanady and St. Theresa's School Junction for Various Vehicle Types	163
Fig.7.3a	Simulation of Traffic Movement over the Proposed Flyover at Bunt's Hostel Junction	166
Fig.7.3b	Long-Term Improvement Strategy-1: Comparison of Simulated Volumes for Flows between PVS Junction and Jyothi Junction via Bunt's Hostel Junction	167
Fig.7.3c	Long-Term Improvement Strategy-1: Comparison of Simulated Speeds for Flows between PVS Junction and Jyothi Junction via Bunt's Hostel Junction	168
Fig.7.3d	Long-Term Improvement Strategy-1: Comparison of Simulated Volumes for Flows between PVS Junction and Kadri Junction via Bunt's Hostel Junction	169
Fig.7.3e	Long-Term Improvement Strategy-1: Comparisons of Simulated Speeds for Flows between PVS Junction and Kadri Junction via Bunt's	170

	Hostel Junction	
Fig.7.4a	Simulation of Traffic Movement over the Proposed Flyover at Bendoorwell Junction	171
Fig.7.4b	Long-Term Improvement Strategy-2: Comparison of Simulated Volumes for Flows between Kankanady and St. Theresa's School Junction via Bendoorwell Junction	173
Fig.7.4c	Long-Term Improvement Strategy-2: Comparison of Simulated Speeds for Flows between Kankanady and St. Theresa's School Junction via Bendoorwell Junction	173
Fig.8.1a	Layout and Phasing Diagram for 3-Phase Traffic Signal: PVS Junction	177
Fig.8.1b	Three Phase Signal Timing Diagram Using <i>HCM 2000</i> Design Method: PVS Junction	180
Fig.8.1c	Layout and Phasing Diagram for 3-Phase Traffic Signal: Jyothi Junction	181
Fig.8.1d	Layout and Phasing Diagram for 3-Phase Traffic Signal: Bunt's Hostel Junction	181
Fig.8.1e	Layout and Phasing Diagram for 3-Phase Traffic Signal: St. Theresa's School Junction	182
Fig.8.1f	Three Phase Signal Timing Diagram Using <i>HCM 2000</i> Design Method: Jyothi Junction	184
Fig.8.1g	Three Phase Signal Timing Diagram Using <i>HCM 2000</i> Design Method: Bunt's Hostel Junction	185
Fig.8.1h	Three Phase Signal Timing Diagram Using <i>HCM 2000</i> Design Method: St. Theresa's School Junction	185
Fig.8.2	A Flowchart of Important Stages in the Genetic Algorithm (GA) Approach	194

## LIST OF TABLES

<b>Table. No.</b>	<b>Description</b>	<b>Page No.</b>
Table 1.2a	Total Road Lengths and Road Densities for Selected Countries	7
Table 1.2b	Growth of Road Network in India from 1947 to 2016	7
Table 1.2c	Growth of Vehicles on Indian Roads from 1951 to 2016 (in Thousands)	8
Table 1.3a	Important Software's Used in Macro and Micro Simulation	12
Table 1.3b	Details on Land Usage (%) in Mangalore	13
Table 2.1a	Framework for Fundamental Characteristics of Traffic Flow	20
Table 2.1b	A Brief Review of Literature on Applications of VISSIM and Soft Computing in Micro-Simulation Modeling of Traffic Flow	37
Table 3.5	Saturation Flows for Straight Road Sections of Widths 3-5.5m	56
Table 5.1a	Details on Growth of Mangalore City	79
Table 5.1b	Details of Wards in Mangalore City Corporation (2011)	80
Table 5.2a	Details on Vehicle Registrations: 2012-2019	82
Table 5.2b	List of Important Junctions in Mangalore City	85
Table 5.3a	Important Mid-Block Sections Considered for Volume and Speed Studies	93
Table 6.1	Setting Default Values for Driving and Vehicle Characteristics	101
Table 6.2a	<i>GEH</i> Calibration for Volumes at 18 Mid-Blocks for Default Settings: Random Seed 25	104
Table 6.2b	<i>GEH</i> Calibration for Volumes at 18 Mid-Blocks for Default Settings: Random Seed 28	105
Table 6.2c	<i>GEH</i> Calibration for Volumes at 18 Mid-Blocks for Default Settings: Random Seed 42	105
Table 6.2d	<i>GEH</i> Calibration for Volumes at 18 Mid-Blocks for Default Settings: Random Seed 50	106
Table 6.3a	Lateral Clearances for Each Vehicle-Type with Respect to Other Vehicle-Types	107
Table 6.3b	Maximum and Minimum Lateral Clearances: Arasan and Krishnamurthy (2008)	107
Table 6.3c	Lateral Clearances for Standing and Moving Vehicles: Manjunatha et al. (2013)	107
Table 6.3d	Lateral Clearances for Standing and Moving Vehicles: Bains et al. (2013)	107
Table 6.4	Comparison of Actual and Simulated Traffic Volumes at 18 Mid-Block Locations for First Level Refinements: Random Seed 42	108
Table 6.5a	Desired Acceleration Rates Assigned for Different Vehicle Types	109
Table 6.5b	Maximum Acceleration Rates Assigned for Different Vehicle Types	109
Table 6.5c	Acceleration Rates for Various Vehicle Types: Arasan and Krishnamurthy (2008)	110
Table 6.5d	Deceleration Rates Assigned for Different Vehicle Types	110
Table 6.5e	Deceleration Rates for Various Vehicle Types: Suggested by Mathew and Radhakrishnan (2010)	111
Table 6.6	Comparison of Actual and Simulated Traffic Volumes at 18 Mid-Block Locations for Second Level Refinements: Random Seed 42	112

Table 6.7a	Combined Desired and Maximum Acceleration Distributions for Various Vehicle Types	113
Table 6.7b	Acceleration Rates for Various Vehicle Types: Suggested in Various Studies	113
Table 6.8	Comparison of Actual and Simulated Traffic Volumes at 18 Mid-Block Locations for Third Level Refinements: Random Seed 42	114
Table 6.9	Driving Behaviour (Car Following) Characteristic Assigned	114
Table 6.10	Comparison of Actual and Simulated Traffic Volumes at 18 Mid-Block Locations for Fourth Level Refinements: Random Seed 42	115
Table 6.11	Maximum Acceleration Rates Assigned for Different Vehicle Types	116
Table 6.12	Comparison of Actual and Simulated Traffic Volumes at 18 Mid-Block Locations for Fifth Level Refinements: Random Seed 42	116
Table 6.13	Desired Acceleration Rates Assigned for Different Vehicle Types	117
Table 6.14	Comparison of Actual and Simulated Traffic Volumes at 18 Mid-Block Locations for Sixth Level Refinements: Random Seed 42	117
Table 6.15a	Free Speeds Assigned for Different Vehicle Types	118
Table 6.15b	Free Speeds for Various Vehicle Types: Arasan and Krishnamurthy (2008)	118
Table 6.16	Comparison of Actual and Simulated Traffic Volumes at 18 Mid-Block Locations for Seventh Level Refinements: Random Seed 42	118
Table 6.17a	Eighth Level of Refinement of Vehicle and Driver Characteristics for Calibration Using Random Seed 42	120
Table 6.17b	Comparison of Actual and Simulated Traffic Volumes at 18 Mid-Block Locations for Eighth Level Refinements: Random Seed 42	121
Table 6.18a	Driving Behavior Characteristic (Car Following) Assigned	121
Table 6.18b	Comparison of Actual and Simulated Traffic Volumes at 18 Mid-Block Locations for Ninth Level Refinements: Random Seed 42	122
Table 6.19a	Driving Behavior Characteristic (Car Following) Assigned	122
Table 6.19b	Comparison of Actual and Simulated Traffic Volumes at 18 Mid-Block Locations for Tenth Level Refinements: Random Seed 42	123
Table 6.20a	Driving Behaviour Characteristic (Car Following) Assigned	123
Table 6.20b	Comparison of Actual and Simulated Traffic Volumes at 18 Mid-Block Locations for Eleventh Level Refinements: Random Seed 42	124
Table 6.21	Driving Behaviour (Lateral) Characteristic Assigned	124
Table 6.22	Comparison of Actual and Simulated Traffic Volumes at 18 Mid-Block Locations for Twelfth Level Refinements: Random Seed 42	125
Table 6.23a	Driving Behaviour (Lateral) Characteristic Assigned	125
Table 6.23b	Comparison of Actual and Simulated Traffic Volumes at 18 Mid-Block Locations for Thirteenth Level Refinements: Random Seed 42	126
Table 6.24a	Driving Behaviour (Lateral) Characteristic Assigned	126
Table 6.24b	Comparison of Actual and Simulated Traffic Volumes at 18 Mid-Block Locations for Fourteenth Level Refinements: Random Seed 42	127
Table 6.25	Validation Results for Volume at 18 Mid-block Sections after the Fourteenth Level of Calibration: Random Seed 42	130
Table 6.26	Lower and Upper Bound Values for Vehicle and Driver Characteristics Adopted in the Simulation Trials in VISSIM	131
Table 6.27	Normalized Datasets Used for Training the ANN Model (Partial Listing)	132



Table 6.28	Details on Tests Performed for Identifying the Ideal ANN Configuration	133
Table 6.29	Values of the Relative Importance of Vehicle and Driver Characteristics Computed Based on the Proposed Alternative Approach	138
Table 6.30a	Refined Value of Driving Behavior Characteristic (Car Following) Assigned	139
Table 6.30b	Comparison of Actual and Simulated Traffic Volumes at 18 Mid-Block Locations for the First Level of Extended Multi-level Simulation	139
Table 6.31a	Driving Behavior Characteristic (Car Following) Assigned	140
Table 6.31b	Comparison of Actual and Simulated Traffic Volumes at 18 Mid-Block Locations for the Second Level of Extended Calibration	141
Table 6.32a	Driving Behavior Characteristic (Car Following) Assigned	141
Table 6.32b	Comparison of Actual and Simulated Traffic Volumes at 18 Mid-Block Locations for the Third Level of Extended Calibration	142
Table 6.33a	Driving Behavior Characteristic (Car Following) Assigned	143
Table 6.33b	Comparison of Actual and Simulated Traffic Volumes at 18 Mid-Block Locations for the Fourth Level of Extended Calibration	143
Table 6.34	Comparison of Actual and Simulated Traffic Volumes at 18 Mid-Block Locations for the Fifth Level of Extended Calibration	144
Table 6.35a	Driving Behavior Characteristic (Car Following) Assigned	144
Table 6.35b	Comparison of Actual and Simulated Traffic Volumes at 18 Mid-Block Locations for the Sixth Level of Extended Calibration	145
Table 6.36	Extended Validation Results for Volume at 18 Mid-block Sections after Extended Calibration: Random Seed 42	147
Table 7.1a	Lane-Width Measured Before and After Minor Road Widening Near Bunt's Hostel Junction	152
Table 7.1b	Short-Term Improvement Strategy-1: Comparison of Simulated Volumes, Speeds and Stopped Delays for Flows between Karangalpady and Jyothi Junction via Bunt's Hostel Junction	154
Table 7.1c	Short-Term Improvement Strategy-1: Comparison of Simulated Volumes, Speeds and Stopped Delays for Flows between Karangalpady and Kadri Junction via Bunt's Hostel Junction	156
Table 7.2a	Lane-Width Measured Before and After Minor Road Widening Near Bendoorwell Junction	160
Table 7.2b	Short-Term Improvement Strategy-2: Comparison of Simulated Volumes, Speeds and Stopped Delays for Flows between Kankanady and St. Theresa's School Junction	162
Table 7.2c	Short-Term Improvement Strategy-2: Comparison of Simulated Volumes, Speeds and Stopped Delays for Flows between Kankanady and Balmatta Junction	164
Table 7.3a	Long-Term Improvement Strategy-1: Comparison of Simulated Volumes and Speeds for Flows between PVS Junction and Jyothi Junction via Bunt's Hostel Junction	167
Table 7.3b	Long-Term Improvement Strategy-1: Comparison of Simulated Volumes and Speeds for Flows between PVS Junction and Kadri Junction via Bunt's Hostel Junction	169
Table 7.4	Long-Term Improvement Strategy-2: Comparison of Simulated Volumes and Speeds for Flows between Kankanady and St. Theresa's	172

	School Junction via Bendoorwell Junction	
Table 8.1a	Traffic Flow Computations for 3-Phase Signal Using <i>HCM 2000</i> Design Method: PVS Junction	178
Table 8.1b	Details of 3 Phase Signal Timings Computed Based on <i>HCM 2000</i> Design Method: PVS Junction	179
Table 8.1c	Traffic Flow Computations for 3-Phase Signal Using <i>HCM 2000</i> Design Method: Jyothi Junction	182
Table 8.1d	Traffic Flow Computations for 3-Phase Signal Using <i>HCM 2000</i> Design Method: Bunt's Hostel Junction	183
Table 8.1e	Traffic Flow Computations for 3-Phase Signal Using <i>HCM 2000</i> Design Method: St.Theresa's School Junction	183
Table 8.1f	Details of 3 Phase Signal Timings Computed Based on <i>HCM 2000</i> Design Method: Jyothi Junction	184
Table 8.1g	Details of 3 Phase Signal Timings Computed Based on <i>HCM 2000</i> Design Method: Bunt's Hostel Junction	184
Table 8.1h	Details of 3 Phase Signal Timings Computed Based on <i>HCM 2000</i> Design Method: St.Theresa's School Junction	184
Table 8.2	A Hypothetical Sample Solution Set of Binary Strings with Values of Effective Green Times	196
Table 8.3a	Computational Details for the Initial 0 <sup>th</sup> Test Generation Using the <i>GA</i> Approach: PVS Junction	197
Table 8.3b	Computational Details for the 1 <sup>st</sup> Generation of the First Run Using the <i>GA</i> Approach: PVS Junction	205
Table 8.3c	Computational Details for the 30 <sup>th</sup> Generation of the First Run Using the <i>GA</i> Approach: PVS Junction	206
Table 8.3d	Computational Details for the 4 <sup>th</sup> Generation for the 10 <sup>th</sup> Run for the Overall Best String among All the Test Runs Using the <i>GA</i> Approach: PVS Junction	207
Table 8.3e	Details of 3-Phase Signal Timings Computed Based on the <i>GA</i> Approach: PVS Junction	207
Table 8.3f	3-Phase Signal Timings Based on the <i>GA</i> Approach: Jyothi Junction	208
Table 8.3g	3-Phase Signal Timings Based on the <i>GA</i> Approach: Bunt's Hostel Junction	208
Table 8.3h	3-Phase Signal Timings Based on the <i>GA</i> Approach: St.Theresa's School Junction	208
Table 8.4a	Existing Signal Timings for the 4 Selected Junctions in Mangalore City	209
Table 8.4b	Reduction in Delays and Improvement in Traffic Flows across Selected Junctions for Signal Timings Based on <i>HCM 2000</i> Design Method	210
Table 8.4c	Reduction in Delays and Improvement in Traffic Flows across Selected Junctions for Signal Timings Based on the <i>GA</i> Approach	211

# CHAPTER 1

## INTRODUCTION

### 1.1 GENERAL

Urban roads in developing economies have witnessed a steep growth in traffic volume resulting in an ever increasing demand for road space that does not keep pace with the heavy influx of more and more vehicles on roads. In developing economies, congestion and traffic delays have become a characteristic feature of urban road networks. The heterogeneous mix of slow and fast-moving vehicles and vehicles of varied sizes has further contributed to the chaos resulting in roads operating below existing capacities. In view of the above situation, the factors that cause congestion and bottlenecks in urban transport networks need to be investigated thoroughly.

Identification of solutions to traffic delays and congestion in an urban scenario necessitates monitoring of vehicular movement in the road network of the city. It is imperative to have a proper understanding of vehicular characteristics, driver behavior, and road-network characteristics in order to devise strategies for efficient traffic management.

The field of traffic flow modeling has emerged as an important multi-disciplinary area with contributions from traffic-engineers, city-planners, mathematicians, and specialists in the field of computer sciences. Calibration and validation of vehicle and driver characteristics for the given road network plays a major role in ensuring accuracy and reliability of the simulation models.

The study of traffic congestion requires a proper understanding of the relationship between vehicle characteristics (that include vehicle dimensions, speeds, acceleration, and lateral and longitudinal spacing) and driver characteristics (including look-ahead distance, look-back distance, standstill distance, and stopping sight distance) to mimic existing traffic flows on urban streets.

Complex problems that arise due to the chaos caused by the increasing influx of vehicles on limited road infrastructure necessitate the use of modeling techniques to streamline traffic movement on urban roads.

Simulation approaches permit traffic engineers of developing countries to evolve reliable models to investigate the influence of various factors related to roadways, and driver and vehicle characteristics on traffic flow on urban roads characterized by heterogeneous traffic conditions.

Vehicular speeds on urban traffic networks depend upon a number of factors including road widths, road geometrics, road surface conditions, bottlenecks, vehicle densities, and driver behavior. It is observed that an increase in the traffic volume results in the reduction of operating speeds. The study of movement of vehicles over the urban road network and the traffic handling efficiency at junctions and mid-blocks will go a long way in developing reliable simulation models that enable traffic engineers in making informed decisions for traffic management.

Simulation modeling of traffic flow on urban roads can be performed at varying levels of details using microscopic, sub-microscopic, mesoscopic, and macroscopic levels of analyses. Micro-simulation modeling facilitates the simulation of movement of individual vehicles considering the vehicle characteristics and driver behavior.

The present study focuses on development of a reliable simulation model to evolve strategies for efficient traffic management in view of the limitations in available road-space and the ever increasing number of vehicles. The study involves the formulation of an effective framework for performing calibration and validation of vehicle and driver characteristics for existing roads and traffic characteristics of the city. Additionally, it was also considered necessary to perform an *artificial neural network (ANN)* based sensitivity analysis to identify the factors influencing the predictive capability of the simulation model. The study also provides details on evolving *short-term* and *long-term* strategies for reducing congestion at selected road stretches, and also incorporates the application of genetic algorithm (GA) in fine-tuning the signal timings of selected junctions in the city.

As part of this study, it was proposed to perform a comprehensive study on traffic movements at important locations in Mangalore city, an emerging cosmopolitan city in the District of Dakshina Kannada, in the State of Karnataka, India. The city is located at 12.87° N latitude and 74.88° E longitude at an altitude of 22 metres (72 ft.) above mean sea level. It is the administrative headquarters of the Dakshina Kannada district, the largest urban coastal centre of the State of Karnataka and the fourth largest city in the state (**Website: MCC-2016**).

Mangalore city is presently one of the fastest growing Tier-II cities in India, supported by a very strong industrial base. The city has over the decades, emerged as the industrial and commercial hub of Dakshina Kannada District. The population of the city was estimated at 4,99,487 as per 2011 census (**Census 2011**). 60 wards of the city together constitute 132.45 square-km of the municipal corporation area (**Website: MCC-2016**) and is surrounded by 12 upcoming urban agglomerations. The total road length of the city is about 1170 kilometres as on 2015 (**Website: MCC-2015**).

The movement of vehicles at junctions and on road links is influenced by a number of roadway and traffic factors such as the vehicle type, vehicle dimensions, road condition, traffic flow, traffic composition, and driver characteristics. The primary scope of the present study is focused on performing investigations using micro-simulation on understanding the traffic characteristics of Mangalore city characterized by heterogeneous traffic composition using *VISSIM*. A very important traffic circuit of the city connecting Hampankatta Junction, Navbharat Junction, PVS Junction, Bunt's Hostel Junction, and Jyothi Junction was considered for analysis, in addition to other traffic junctions such as Bendoorwell, Balmatta, and St. Theresa's School Junction encompassing a total land area of 3.08 square km.

The video-graphic data with information on traffic volumes and speeds at various junctions mentioned above, and at 18 mid-block sections of the city was collected for the evening peak-hour from 17.00-18.30 hours on a mid-week day in the month of March 2015. From the consolidated video-graphic database of 80-minutes for the peak period, information pertaining to 60-minutes corresponding to 75% of the consolidated database was used in testing and calibration of the *VISSIM*-based micro-

simulation model procedure, while the remaining data for 20 minutes corresponding to 25% of the consolidated database was used in the validation exercise.

The *initial phase* of the study included the creation of a high-resolution base-map of Mangalore city to a scale of 1:5000 by stitching together 104 screenshots captured from *Google-maps* (**Website: Google-Maps**), which was later superimposed on a scaled *AutoCAD* drawing of the road-network of the city.

Further, as part of the *initial phase* of the study, a *preliminary modeling exercise* was performed in *VISSIM* using default values of vehicle and driver characteristics to identify the best *random seed*. The *GEH statistic* was used as an indicator to assess the accuracy of simulated predictions as followed by a number of agencies in UK (**DMRB 1996; Smith and Blewitt 2010**).

In the next phase, a *basic multi-stage calibration* exercise was performed using the best random seed 42 in *VISSIM* by testing of various combinations of the vehicle and driver characteristics. At each stage of calibration exercise, an attempt was made to enhance the prediction accuracy of traffic volumes at 18 mid-blocks sections of Mangalore city road network by verifying the *GEH statistic* and the *mean absolute error (MAE)* as an indicator. This exercise was then followed by the *basic validation exercise*.

Subsequently, in the next phase, in order to investigate the relative sensitivity of various vehicle and driver characteristics, an *ANN-based sensitivity analysis* was performed. The *ANN* approach was adopted in this part of the study since each of the vehicle and driver characteristics were considered to influence the other, and the degree of relationships could not be clearly understood. In this study, a *modified Garson's approach* is demonstrated for the computation of relative sensitivity based on connection weights between the input layer, the three hidden layers, and the output layer for the optimized *ANN* configuration.

In the later phase of the study, the effect of implementing *short-term* strategies such as widening of existing road-widths, and *long-term* improvement strategies such as introduction of flyovers were examined for selected locations of the city.

As an extension to studies on short-term strategies, the advantages of using the *genetic algorithm (GA)* based approach in the design of traffic signal timings was demonstrated for streamlining traffic flows across four important junctions in the city. The objective function in the *GA* module was formulated based on the HCM-2000 delay model (**TRB 2000**).

The overall approach towards performing calibration studies evolved through the present study is expected to provide the basic framework for calibration and fine-tuning of vehicle and driver characteristics in the development of micro-simulation models. The demonstration of the use of an alternative *modified Garson's approach* for performing *ANN*-based sensitivity analyses for neural networks with three hidden layers provides a sound basis for determining the relative importance of vehicle and driver characteristics in simulation models. In this part of the study, the characteristics such as the *average stand still distance*, *minimum look-ahead distance*, *multiplicative part of safety distance*, and the *lower bounds for speed distributions* identified using the *ANN*-based sensitivity analyses reveal that these have a major influence on the accuracy of predictions in micro-simulation modeling using *VISSIM*.

Additionally, investigations on the study of impact of *short-term* improvements (such as widening of road sections) and *long-term* improvements (such as introduction of flyovers) of selected road sections of the traffic network will form the basis for evolving strategies for improving traffic flow for better traffic management. The study revealed that simulation could be used as an effective tool in identifying bottlenecks in the road network, and in reducing traffic delays due to congestion in the urban scenario. The present work also demonstrates the capability of using *GA* based approaches in traffic signal optimization at selected locations in the traffic network. The findings of this study are expected to assist transport planners in developing innovative solutions to urban traffic management, analysis, design, and operation of vehicles on roadways.

## 1.2 PROBLEM SCENARIO AND NEED FOR THE STUDY

The urban road transport sector plays a major role in providing accessibility and mobility to the citizens of the city and has a profound impact on the economic development of the region. The road transport sector in India has undergone many changes over the past decades. According to the Ministry of Road Transport and Highways (MoRTH), the total road length in India increased by about 15 times between 1947 and 2017 from 3,88,000 km to 58,97,671 km. The length of surfaced roads registered an increase from 2,45,374 km to 37,29,687 km during the same period. Presently, the total road network of India includes 1,14,158 km of national highways, 1,75,036 km of state highways, and 52,79,580 km of other roads (**MoRTH 2019**).

Statistics on roadways compiled for the year 2016-17 (**MoRTH 2019**) indicate that in terms of length of total road network, India has 58,97,671 km to its credit and stands second to United States of America with 66,45,709 km. The computations for road density indicate that India has a road density of 179.41 km per 100 square km while the United States provides a road density of 67.58 km per 100 square km.

**Table 1.2c Growth of Vehicles on Indian Roads from 1951 to 2016 (in Thousands)**

Year (As on 31st March)	Two Wheelers	Cars, Jeeps and Taxis	Buses	Goods Vehicles	Others including Auto-rickshaws	Total Vehicles
1951	27	159	34	82	4	306
1956	41	203	47	119	16	426
1961	88	310	57	168	42	665
1966	226	456	73	259	85	1099
1971	576	682	94	343	170	1865
1976	1057	779	115	351	398	2700
1981	2618	1160	162	554	897	5391
1986	6245	1780	227	863	1462	10577
1991	14200	2954	331	1356	2533	21374
1996	23252	4204	449	2031	3850	33786
2001*	38556	7057	633	2948	4017	53211
2006*	64743	11524	762	4274	5818	87121
2011*	101864	19230	1238	7064	8045	137441
2015*	154297	28609	1527	9344	10474	204251
2016*	168975	30241	1384	10516	12048	223164

Source: Website: MoSPI (2016); \*Website: MoSPI (2018)



However, it may be observed that the road length per 1000 persons in India stands at 4.87 km when compared to 6.43 km for UK and 20.55 km for US.

### **1.3 ADDITIONAL PROBLEMS DUE TO HETEROGENEOUS TRAFFIC**

In India, almost on all rural and urban roads, different types of vehicles share the same road space without any segregation. The heterogeneous mix of vehicles includes fast-moving cars to light commercial vehicles (LCVs), buses, motor-cycles, auto-rickshaws, cycle-rickshaws, bicycles, and animal drawn carts. The wide variety of vehicles and the disparity in the sizes, speeds, and acceleration characteristics result in a chaotic situation on existing roads. The presence of various types of vehicles and various mixes of slow and fast vehicles on roads in India compel Indian drivers to adopt various strategies for maneuvering vehicles to reach their destinations.

The urban transport scenario is further rendered complex due to increased dependence on the private vehicles that further result in reduced road spaces and journey-speeds. Moreover, pedestrians are at times compelled to use the carriageway designated for vehicular movement due to encroachment of footpaths by roadside-vendors. Traffic congestion in the Central Business District (CBD), especially during the peak hours result in constant stoppage of vehicle, and frequent accelerations and decelerations that cause severe wear and tear of vehicle components.

Additionally, the improper design of signal-timings is found to further increase the vehicle delays and queue lengths, thereby considerably affecting the *level of service* (LOS) offered by the roadways. The conflict caused by mixed traffic phenomenon results in accidents.

### **1.4 ROLE OF MODELING TECHNIQUES AND MICROSIMULATION IN THE ANALYSIS OF URBAN TRAFFIC SCENARIO**

Traffic engineers are required to closely analyse the movement of vehicles in urban traffic, and develop efficient traffic management strategies to mitigate traffic congestion. As part of this exercise, it is often required to resort to modeling techniques in order to gauge the impact of driver and vehicle characteristics on traffic flow and to evaluate the efficiency of the functioning of the road network in terms of flow, capacity, and density of traffic. A proper understanding of the impact of

vehicular flow on road networks will provide the necessary background for formulating strategies for improvements in traffic facilities and in devising traffic management policies.

Researchers in the field of traffic flow management adopt *microscopic* and *macroscopic* approaches to develop simulation models to describe the relationships between traffic flow, speed, and density on highways. The *microscopic* approach gives importance to details at micro-level focusing on individual vehicular speeds and spacing, while the *macroscopic* approach deals with traffic-stream flows, densities, and average speeds.

Advancements in computation technology and development of tools for computer aided design have provided vast opportunities for further studies on analysing the flow of vehicles on road networks.

## **1.5 TRANSPORTATION SCENARIO IN MANGALORE CITY AND NEED FOR THE PRESENT STUDY**

One of the earliest references to Mangalore city was made by the Pandyan King Chettian, who called the city as Mangalapuram in 715 AD. The 11<sup>th</sup> century Arabian traveller and historian, Ibn Battuta too refers to Mangalore as Manjarur in his chronicles (**Website: Virtual-Mangalore**). Later developments including the establishment of New Mangalore Port Trust (NMPT), Mangalore Airport, Mangalore Chemicals and Fertilizers (MCF), Mangalore Refineries and Petrochemicals Ltd. (MRPL), BASF, HPCL, and Kudremukh Iron Ore Company Ltd. have triggered large-scale industrial development in the area (**Dalal Consultant and Engineers Ltd. 2003**).

The National and State Highways of Karnataka provide accessibility and mobility for the transportation of goods and people. Four National Highways pass through Mangalore city. NH-66 (previously known as NH-17 until April 2011), which runs from Panvel (in Maharashtra) to Edappally Junction in Kerala, passes through Mangalore. NH-48 (renamed as NH-75) that runs eastward from Mangalore to Bangalore via Hassan, and NH-13 (renamed as NH-169) that runs north-east from Mangalore to Shivamogga via Karkala, and NH-73 that connects Mangalore to

Tumkur via Bantwal, Belthangadi, and Belur provide connectivity to the surrounding region and the neighbouring states. The total road length in Mangalore is about 527.38 km, of which 108 km of road constitute National Highways, 78.5 km of roads constitute State Highways, and 340.88 km of roads constitute Major District roads (GoK 2017).

The industrial development of the region depends to a large extent on the accessibility and mobility provided by the National and State Highways of Karnataka, and the close proximity to the sea-port, air-port, and road and rail terminals ensured the rapid growth of the region. In Mangalore city, 8.47% of land is used for industrial purposes, and 4.33% of the land is used for commercial purposes, while 48.14% of the land is used for residential purposes (Website: MCC-2016). Table 1.3b provides details on the same.

**Table 1.3a Important Software's used in Macro and Micro Simulation**

<b>Software</b>	<b>Developer/ Distributor</b>	<b>Application</b>
<b>ARCADY/ PICADY</b>	Transport Research Laboratory, Crowthorne, UK	Study of delays, and accidents at roundabouts/ study of non-signalized priority junctions, queue analysis, delays, and accidents at isolated junctions
<b>OSCADY</b>	Transport Research Laboratory, Crowthorne, UK	Optimization of signals, signal design, and intersection design
<b>SCOOT</b>	Transport Research Laboratory, Crowthorne, UK	Software for optimizing split cycle offset optimization
<b>SYNCHRO</b>	Trafficware, Sugarland, Texas	Macro-simulation software for optimization of traffic signal
<b>TRANSYT</b>	Transport Research Laboratory, Crowthorne, UK	Macroscopic simulation software for signal timing optimization using genetic algorithm, platoon dispersion, network flow, and optimization
<b>AIMSUN</b>	Universitat Politècnica de Catalunya, Barcelona, Spain	Micro-simulation of car-following, lane-changing, coordinated signal control, traffic management, and analysis of ITS Strategies
<b>ARTEMIS</b>	University of New South Wales, School of Civil Engineering, Australia	Evaluation of various traffic scenarios, identification of solutions to traffic problems, and study of impact of ITS strategies, and congestion management.
<b>CORSIM</b>	Federal Highway Administration, USA	Micro-simulation software for design of runways and freeways, Grade separated expressways, and interstate freeways, evaluation of transit operations
<b>DRACULA</b>	Institute for Transport Studies, University of Leeds, UK	Micro-simulation software for dynamic route assignment and study of impact of real-time

		management strategies
<b>HETEROSIM</b>	Department of Civil Engineering, Indian Institute of Technology, Madras.	C++ and Java based micro-simulation software for discrete event simulation of heterogeneous traffic
<b>PARAMICS</b>	The Edinburgh Parallel Computing Centre and Quadstone Ltd, UK	Micro-simulation software for study of freeways, traffic engineering, ramps, loop detectors, roundabouts, ITS, Toll Plazas, public transport, emission study, and pedestrian modeling
<b>SimTraffic</b>	Trafficware, Sugarland, Texas	Micro-simulation software for analysis of complex traffic networks, roundabouts, and study of impact of LRT
<b>SISTM</b>	Transport Research Laboratory, Crowthorne, UK	Micro-simulation of traffic on motorways in congested areas
<b>VISSIM VISUM</b>	PTV Planuransport Verkehr AG, Karlsruhe, Germany	Micro-simulation software for traffic engineering, urban planning, signal timing, public transport/ traffic analysis and forecast

**Table 1.3b Details on Land Usage (%) in Mangalore**

Vac- ant	Resid- ential	Comm- ercial	Ind- ustr- ial	Transport and Communi- cation	Public Utili- ties	Public and Semi Public uses	Open Spaces	Agricu- ltural Land	Others	Total
NA	48.14	4.33	8.47	20.55	0.34	6.13	8.14	19.91	12.76	<b>128.77</b>

Source: Website: MCC-2016

## 1.6 SCOPE AND OBJECTIVES OF THE WORK

The calibration of vehicle and driver characteristics as part of development of micro-simulation models plays a major role in ensuring the accuracy of prediction of traffic flows in the road network. It is also imperative to determine the relative importance of these characteristics in order to develop a reliable simulation model. The primary scope of the present work involves the development of a framework for performing the calibration of vehicle and driver characteristics, followed by the formulation of an alternative *modified Garson's* approach for determining the relative importance of vehicle and driver characteristics in order to develop more reliable simulation models. The present study also demonstrates the application of micro-

simulation models in assessing the impact of *short-term* and *long-term* strategies for effective management of traffic flow on the road network of Mangalore city characterized by a heterogeneous traffic composition.

The major objectives of this study include the following:

- i. Performing the *basic multi-stage calibration* and *validation* of vehicle and driver characteristics for the development of a *VISSIM-based* micro-simulation model that can simulate traffic flow in the city with reasonably good accuracy.
- ii. Performing studies on an alternative *modified Garson's approach* for *ANN-based sensitivity analysis* of vehicle and driver characteristics (based on connection weights between the input layer, the three hidden layers, and the output layer of the *ANN*) for the computation of relative sensitivity since each of the vehicle and driver characteristics were considered to influence one another mutually.
- iii. Exploring the capabilities of the *VISSIM* model in evaluating the impact of *short-term* and *long-term* strategies for improvement of the road network.
- iv. Exploring the application of *genetic algorithm (GA)* in the design of traffic signal timings based on the HCM delay model and to look for further improvements in traffic flow for selected locations in the city using the calibrated *VISSIM* model.

The present work is organized into a *the initial phase* with preliminary modeling followed by a *basic multi-stage calibration* exercise, *ANN-based* sensitivity analysis, and an analysis on the impact of short-term and long-term improvement strategies on the traffic network. The details of various steps involved are provided below:

- a) In the initial phase of the study, a high resolution digital base-map of the study area was prepared to a scale of 1:5000 using *Gimp* (a high-end image processing software) by stitching together 104 screenshots captured from *Google-maps* (**Website: Google-Maps**), which was later

superimposed on a scaled *AutoCAD* drawing of the road-network of the city. The superimposed image was then used as a template in *VISSIM* to draw the links and connectors.

- b) A *basic multi-stage calibration* exercise was then performed using the best random seed 42 in *VISSIM* starting with the default values of vehicle and driver characteristics, followed by testing of various combinations of the same. The 60-minute video-graphics data corresponding to 75% of the consolidated database was used for this purpose.
- c) In the next stage, an *ANN-based sensitivity analysis* was performed to study the relative sensitivity of various vehicle and driver characteristics. Since various vehicle and driver characteristics are known to influence one another, it was considered ideal to perform this investigation using the *ANN* approach.
- d) The impact of implementation of various *short-term* strategies such as widening of existing road-widths, and *long-term* improvement strategies such as introduction of flyovers were examined for selected locations of the city using the calibrated micro-simulation model.
- e) As part of the studies on *short-term* strategies, a *genetic algorithm (GA)* based approach was employed in the design of traffic signal timings for selected junctions of the city.

## **1.7 ORGANIZATION OF THE REPORT**

Chapter 1 provides an introduction to the topic of study, and the role of simulation studies in urban traffic modeling. Additionally, a brief discussion is provided on the problem scenario and need for further studies due to heterogeneous traffic conditions with details on traffic scenario in Mangalore city. Discussions on modeling techniques with details on software used in simulation studies are also provided along with details on the scope and objectives of the study.

Chapter 2 provides an overview of the literature review performed on research areas related to the application of simulation techniques in traffic flow modeling with

special emphasis on micro simulation applications in *VISSIM*, in addition to applications of *genetic Algorithm (GA)*. This chapter also provides details on literature review related to *artificial neural network (ANN)* applications in traffic flow modeling, and sensitivity analysis in addition to selected studies on the design of isolated traffic signals and computation of delays. The review of literature assisted in the formulation of the objectives of the present study, and the methodology to be adopted.

A theoretical background related to various aspects of simulation based techniques for traffic flow modeling, and the fundamental aspects of macro-measures such as speed-density, speed-flow, and flow-density are discussed in Chapter 3.

Chapter 4 provides a detailed explanation on the methodology adopted in this study, and the stage-wise approach to the investigations performed. The details of the study area, data collection approach, creation of a high resolution *base-map*, interfacing of the *AutoCAD* drawing of the links and junctions, and the creation of a template to be interfaced to *VISSIM* were discussed in Chapter 5.

Chapter 6 provides details on the results and discussions on testing, calibration and validation of the *VISSIM* model for the existing traffic flow scenario. This chapter also includes details on the ANN-based sensitivity analysis performed, and details on further fine-tuning of vehicle and driver characteristics as part of the extended multi-level calibration, in addition to the results on the final validation performed.

Chapter 7 provides details on the results and discussions on *short term* and *long term* improvement proposed as part of this study, with special focus on improving traffic flows at selected junctions in the city. Chapter 8 provides details on the results of the application of the *GA* approach in minimizing 3-phase traffic signal delays computed using the *HCM average delay model* and comparisons with the *HCM 2000 Design Method*.

The conclusions of various phases of the present work, the major contributions of the study, and the limitations are discussed in Chapter 9.

## CHAPTER 2

### LITERATURE REVIEW

#### 2.1 GENERAL

Traffic engineers analyse vehicular movements in the road network to derive a clear understanding of the existing situation that can assist in evolving strategies to streamline traffic movement. Ensuring safe and efficient movement of traffic involves the study of a number of parameters related to vehicle, driver, and road characteristics. The behavior of drivers of various vehicle-types needs to be understood in addition to vehicular dynamics at different operating speeds in order to formulate effective strategies to enable smooth vehicular movement.

It is commonly believed that slower speeds in the traffic network ensure safer vehicular movement. However although this approach tends to reduce the severity of accidents, it does not ensure safety in road-traffic. According to ADOT, the chances of drivers becoming involved in accidents is the lowest when vehicular speeds are closer to the average speed of traffic (**Website: ADOT**).

Effective traffic management policies to ensure safe and efficient movement of vehicles on the existing travel network can be formulated based on studies on vehicular movements and driver behavior. A proper understanding of vehicle, driver, and roadway characteristics, and the influence of lane-change manoeuvres will assist traffic engineers in finding solutions to traffic delays and congestion. Investigations focused on these aspects are considered to generate effective plans for improvements in the road network to ensure smoother flow of traffic.

Micro and macro simulation approaches can be effectively employed in the analysis of traffic delays and congestion. Effective modeling of vehicle and driver characteristics, in addition to roadway geometrics plays a major role in ensuring the accuracy of predictions in simulation models. **Table 2.1a** provides details on the important aspects considered in micro-simulation and macro-simulation approaches.



**Table 2.1a Framework for Fundamental Characteristics of Traffic Flow**

<b>Traffic Characteristics</b>	<b>Microscopic Units Measured</b>	<b>Macroscopic Units Measured</b>
Flow	Time-headways	Flow Rates
Speed	Individual Speeds	Average Speeds
Density	Distance-headways	Density Rates

This chapter provides a brief overview of literature related to microscopic simulation models for speed-flow studies, applications of simulation techniques and *VISSIM* software on various related aspects of traffic and transportation, studies on the application of *Artificial Neural Networks (ANN)* in traffic engineering, design of an *isolated traffic signal* and delays, and applications of *Genetic Algorithm (GA)*. The literature review also provides details on the research gaps identified in the present study.

## **2.2 REVIEW OF EARLIER MICRO-SIMULATION MODELS FOR SPEED-FLOW STUDIES**

The following sections provide details on important studies performed in the area of micro-simulation in traffic and transportation engineering.

**Ahmed (1999)** performed investigations on micro-simulation models using statistically rigorous methods and microscopic data collected on Interstate 93 at the Central Artery, Boston, USA. The *acceleration model* developed considered two aspects of traffic flow: the *car following regime* and the *free-flow regime*. In the car following regime, the drivers were assumed to follow the leader, while in the free flow regime, drivers were assumed to attain their desired speeds within a short span of time. A probabilistic model based on *time-headway thresholds* was used to determine the regime that the driver followed. The model captured the heterogeneity of various types of drivers based on the *headway thresholds* and the *reaction time distributions*.

**Hoseini et al. (2004)** developed a micro-simulation model for driving behavior based on the assumption that drivers tend to optimize the speed while simultaneously avoiding collisions. A basic freeway segment in Iran was divided into smaller cells and vehicles were assumed to occupy the cells ahead based on the speed at each time step. The model also demonstrated the car-following model. Data on vehicle-trajectory obtained from digital images was used in this study.

**Toledo et al. (2005)** developed lane-change models assuming that drivers tend to compare the driving environment in the current and adjacent lanes before making decisions on lane-change considering the utility derived from these lanes. The choice of the target lane was modeled based on a number of factors perceived to be important by the driver. Vehicle trajectory data obtained from section of I-80, Berkeley, USA was used in the simulation study.

**Dogan et al. (2008)** formulated a model to predict the *driver's intentions* during a *lane-change* manoeuvre. The studies were performed at the test facility of the Institute of Neuro-informatik, using the traffic simulator NISYS\_TRS\_1. The behavior of ten drivers was assessed over 150 experiments on lane change manoeuvres. The lane-offset, distance to the front car, and the end time of eye contact, were recorded and analysed in this study.

### **2.3 STUDIES ON APPLICATIONS OF VISSIM IN TRAFFIC AND TRANSPORTATION**

*VISSIM* software possesses the capability to perform microscopic simulations on traffic flows in urban and inter-urban motorways. It is employed as an effective tool in analysing traffic flow characteristics in the travel network, and in evolving optimal and effective signal-control strategies. The software also capable of performing simulations related to testing of various configurations of intersection layouts, design and location of bus-bays and transit-stops, testing of the functioning of toll plazas, and the design of merging and diverging zones on motorways. A number of studies have been performed using micro-simulation techniques in modeling urban traffic.

**Fellendorf and Vortisch (2001)** calibrated and validated the *VISSIM* model for freeways in Germany and US by modeling driver behavior where the traffic regulations were very much different. Here, the driver characteristics were assigned to the model based on inputs from a probe vehicle. The main focus of this study was to investigate the longitudinal movement of cars as part of the car-following model by simulating various types of driver behavior. The study was performed considering traffic conditions with flows up to 2400 vehicles/h/lane characterized mainly by the movement of cars that follow a strict lane-discipline for freeways. The investigations

proved that *VISSIM* was capable of modeling various real-world situations more realistically as it uses a psycho-physical car-following approach.

**Park and Schneeberger (2003)** suggested a nine-step procedure for testing, calibration, and validation of a *VISSIM* model for the design of a coordinated signal based on studies conducted on Lee Jackson Memorial Highway, Fairfax, Virginia. The testing and calibration procedures were performed iteratively using a regression model. Five random seeds were tested in this study. The nine steps involved in calibration include selection of the index for effectiveness, data collection, and identification of the calibration parameter, design of the experiment, performing simulation runs, evaluation, and validation.

**Mosseri et al. (2004)** performed studies on evaluating traffic management strategies at the 2.5 mile long Lincoln tunnel corridor in New Jersey. The study focused on traffic movement on high-occupancy lanes, exclusive bus lanes, and toll lanes using *VISSIM*, where road-geometrics and operational issues were evaluated.

**Velez et al. (2006)** used statistical analysis method, namely the *student's t-test*, to show that the results obtained from a micro-simulated model and the field data for the same road network in Puerto Rico were comparable. **Gallelli and Vaiana (2008)** studied various types of roundabouts by simulating *VISSIM* models, and observed that the software possessed the necessary flexibility to incorporate details of the actual field conditions.

**Mathew and Radhakrishnan (2010)** devised an approach to test and calibrate models simulating heterogeneous flows at road junctions. The study considered the static and dynamic characteristics of vehicles, and the traffic composition. The vehicle and driver characteristics to be calibrated were identified using a sensitivity analysis and the values of these were further optimized using *genetic algorithm (GA)* to ensure lesser prediction errors. Data collected from two intersections in Trivandrum City and one intersection from Jaipur City was used for this purpose. of the Wiedemann 99 model were found to be sensitive in the sensitivity analysis.

**Habtemichael (2012)** performed a sensitivity analysis on 21 parameters

including driver-behavior and lane-change parameters in *VISSIM*. It was found that headway-time and car-following variations were most crucial in predicting car-following behavior on three-lane motorway stretches.

**Bains et al. (2013)** evaluated the influence of posted speed limits on speed-limit compliance, and road capacity using *VISSIM* and observed that there was an increase in the roadway capacity as more drivers complied with the posted speed limits on Mumbai-Pune Expressway.

**Siddharth and Ramadurai (2013)** performed investigations on ANOVA-based sensitivity analysis and derived the optimal values of characteristics using GA while calibrating a *VISSIM* model for heterogeneous traffic conditions at Tidal Park Intersection in IT Corridor, Chennai.

**Durrani et al. (2016)** performed studies on analysing the vehicle following behavior for cars, motor cycles, and heavy vehicles for a 640m long road section of US-101 highway in Los Angeles. It was found that the drivers of heavy vehicles had a tendency to adopt longer safety distances and that these drivers decelerated slowly when following other vehicles. Also, the car-drivers following heavy vehicles also maintained larger safety distances based on the size of the vehicle and the acceleration and deceleration rates.

**Jain et al. (2016)** observed that the traffic flows on the middle lane and the first lane are quite higher when compared to the traffic flow on lane closer to the shoulders. Cars tend to ply on these two lanes while two-wheelers are seen to operate on the middle and outer most lanes of 6-lane divided highways in India. **Lu et al. (2016)** adopted a video-based method for data collection in order to perform calibration of the car-following parameters in *VISSIM* for studies performed in Waterloo, Canada.

**Karakikes et al. (2017)** developed a *VISSIM* model to analyse a motorway network of 500 links and 113 nodes in Bavaria in Germany based on a three-hour simulation study where travel-time determined using Bluetooth detectors were used for calibration and validation. The model developed was found to provide reliable predictions on the flow of cars and heavy vehicles with an accuracy of 96.5%.

**Tian and Zhang (2017)** performed studies in Hefei city of China on the use of an adaptive signal control system based on the field data and also based on simulations performed in *VISSIM* and *TRANSYT*. In this study, the optimal signal timings were determined and the adaptive signal timings were computed using *VISSIM* and *VS-PLUS*.

**Nyame-Baafi et al. (2018)** analysed road networks in Ghana with a special focus on signalized intersections with left-turn lanes. The traffic flow, delay, and the average and maximum queue lengths for testing and calibration were obtained from video-graphs for the morning peak-period.

**Srikanth et al. (2020)** conducted studies on lane-change behavior for the four-lane divided National Highway (NH) NH 163 connecting Warangal and Hyderabad in India using *VISSIM*. Here, it was observed that the number of lane-changes depend mainly on the traffic volume and the number of lanes along the direction of travel.

#### **2.4 STUDIES ON APPLICATIONS OF ANN ON TRAFFIC FLOW MODELING AND DISCUSSIONS ON ANN APPLICATIONS IN SENSITIVITY ANALYSIS**

In the present study, the *ANN*-based approach was considered for the analysis of sensitivity as *ANNs* are capable of capturing the underlying relationships more effectively when compared to other approaches (**Lippman 1987; Scarborough and Somers 2006; Dreiseitla and Ohno-Machadob 2002; Website: WISC\_CS**). **Scarborough and Somers (2006)**, and **Dreiseitla and Ohno-Machadob (2002)** recommend the use of *ANN*-based methods for the analysis of relative importance of input variables for enhanced accuracy in modeled predictions. This sub-section provides details on the same.

**Zhang et al. (1997)** demonstrated the application of a *three-layer feed-forward ANN* model to analyse the freeway traffic flow model as part of real-time predictive control strategies for dynamic traffic control systems.

**Amin et al. (1998)** performed studies on developing macro-level traffic control modules and micro-level modules for vehicle path planning and steering

control in addition to the development of optimization modules for urban traffic management.

**Chen and Wang (2006)** applied the time-series analysis approach to obtain a trend series on traffic flow volumes in road networks in Suzhou city, China. Each hierarchy of time series data was then analysed further using ANN to predict the traffic flow volumes for studies performed.

**Pamula (2011)** demonstrated the use of ANNs in the prediction of short-term traffic intensity and queue length for traffic control and management systems for Katowice in Poland. The results of the analysis were later used in developing traffic flow models in *VISSIM* and *Delphi* software.

**Otkovic et al. (2013a)** demonstrated the application of ANN in the prediction of results related to travel time, queue-length, and traffic flows at two urban roundabouts (Vinkovacka–Drinska Roundabout and Kirova–Opatijska Roundabout) in Croatia in simulation experiments using *VISSIM*. **Otkovic et al. (2013b)** performed studies using ANN for predicting travel time and queue length in car-following models for a one-lane roundabout in Osijek, Croatia using improved value ranges for *VISSIM*.

**Zhu et al. (2014)** demonstrated the application of a new approach based on *radial basis function neural networks (RBFNNs)* to predict short-term traffic volumes at adjacent intersections with good accuracy in Baotou City, China. This approach was found to be more adaptable to situations where missing data need to be handled.

**Özkan and Inal (2014)** observe that ANNs, especially back-propagation-based ANNs designed based on supervised-learning are capable of providing higher prediction accuracy when compared to statistical regression techniques and ANOVA.

**Zhou et al. (2017)** conducted studies using conventional ANN approach on simulating traffic flow oscillations for congested traffic flow conditions in Emeryville, California. The study indicated that such ANN models are not capable of predicting the behavior of drivers in the above mentioned traffic conditions.

**Sharma et al. (2018)** also observe that the application of back-propagation-based ANNs can be of great advantage in traffic flow modelling especially for mixed traffic conditions.

**Zhang and Kamel (2018)** provide details on *ANN*-based mobility model that is considered to be more accurate than the conventional car-following model. The results of the *ANN* were used in the *SUMO (Simulation of Urban MObilities)* simulator, an open-source portable microscopic traffic simulation package similar to *VISSIM*.

#### **2.4.1 Additional Studies on the Applications of ANN in Sensitivity Analysis in the Field of Transportation Engineering**

**Subba-Rao et al. (1998)** adopted an *ANN*-based approach for assessing sensitivity of various input variables in mode-choice modeling of trip-makers, where the weight-partition method as explained by **Garson (1991)** was used. Here, it was observed that the results obtained were almost similar to those determined using the multi-nomial logit model (*MNL*) approach.

**Kalteh (2008)** adopted a similar approach in the study of relative importance of variables that contributed to the prediction of rainfall runoff using *ANN*. **Feng et al. (2011)** too observed that the Garson's algorithm could be used in identifying the variables that influenced route-choice selection that resulted in predictions close to 97.4% accuracy.

### **2.5 GENETIC ALGORITHM (GA) APPLICATIONS IN TRAFFIC AND TRANSPORTATION**

**Foy et al. (1992)** were the first to apply *genetic algorithms (GA)* to signal timing determination for deriving the optimal or near-optimal traffic-signal timings to ensure the least average delay. The phase sequences and the green time splits were optimized in a network of four intersections for a fixed traffic scenario.

**Park et al. (1999)** proposed a *genetic algorithm (GA)* optimization program for oversaturated traffic flow conditions. The solutions found were seen to be slightly better when compared to signal timings obtained based on simulation trials with *TRANSYT-7F 8.1* version.

**Ceylan and Bell (2004)** adopted the use of *genetic algorithm (GA)* in solving network problems formulated using Allsop's and Charlesworth's methods (**Allsop**

**and Charlesworth 1977**). This approach demonstrated an overall improvement of 34%.

**Park et al. (2004)** investigated the application of a GA-based program for the design of a coordinated signal systems. The results obtained were found to be reasonably better than simulation-based approaches using *TRANSYT-7F* or *SYNCHRO*, and were superior to solutions derived using heuristic design approaches.

**Stevanovic et al. (2007)** developed VISGAOST, a GA-based application for signal timing optimization and coordinated signal design to be used in traffic network simulated using *VISSIM* micro-simulation software. The experiments were performed for an arterial road with 12 signalized intersections in Park City, Utah, and a traffic corridor in Albany, New York. A single-objective optimization approach was adopted in this study.

**Yang (2010)** adopted the use of GA to derive near optimal traffic signal timings considering minimization of pedestrian and vehicular delays at intersections. **Dezani et al. (2014)** conducted theoretical investigations on application of the GA approach in optimization of urban traffic flows for various routes based on the timings of the traffic lights in real time. The optimization procedure uses a genetic algorithm considering a Petri net urban traffic flow model assuming a minimum intersection spacing of 100m.

**Eriskin et al. (2017)** adopted the Genetic Algorithm (GA) method to arrive at optimal signal timing and green times. The elimination pairing system (EPS) was adopted in this research. **Jamal et al. (2020)** developed meta-heuristic methods for intelligent traffic control at isolated signalized intersections to handle congested flow conditions in Dhahran, Saudi Arabia.

## **2.6 SELECTED STUDIES ON ISOLATED SIGNAL DESIGN AND DELAYS**

A number of early studies on traffic delays were related to the design of traffic signals and control schemes using fixed-time signal timings. **Webster (1958)** performed pioneering studies on devising methods to arrive at optimized signal timings for pre-timed isolated two-phased signals functioning at under-saturated operating conditions. The basic approach was focused on apportioning the green time



for the two approaches to the junctions such that the degree of saturation is almost the same.

**Miller (1963)** derived the expression for computing average delays caused at intersections controlled by fixed-time signals. In this study, the predicted delays were found to be close to the observed values even for oversaturated operating conditions.

**Webster and Cobbe (1966)** performed investigations on delays due to *uniform arrival* of vehicles at junctions and on delays due to *random arrival* of vehicles during the green period for under-saturated operating conditions.

**Mcshane and Roess (1998)** identified the limitations of the Webster's model and its applications in handling saturated and over-saturated flow conditions. **Akcelik (1988)** provided modifications to the Webster's delay models in order to handle oversaturated flow conditions at non-peak, peak, and post-peak saturation conditions. **HCM 2000 (TRB, 2000)** summarized the findings of previous studies performed on the estimation of delays with discussions on delays computed by **Webster (1958)** and **Webster and Cobbe (1966)**, and other researchers. **Dion et al. (2004)** summarized the details on *time-dependent stochastic delay models* with discussions on the contributions made by **Robertson (1979)** and **Kimber and Hollis (1979)**.

**Liu (2009)**, **Zhao et al. (2013)**, and **Tong et al. (2015)** performed investigations on the development of a *two-stage stochastic programming* (SP) model for arriving at signal timing plan for oversaturated intersections. The model minimized the expected vehicular delays considering uncertainties in inflows and outflows. The model was found to be capable of handling inflows rates close to saturated flow conditions.

**Ma et al. (2016)** performed studies on *multi-stage stochastic programming* by introducing phase clearance reliability so as to incorporate coordinated signal operations. The *adaptive control mechanism* was activated to cater to minor changes in vehicle arrivals. The study performed at signalized intersections at Shanghai indicated that the results were similar to those obtained using the Allsop's method (**Allsop 1971**) and the Webster's method (**Webster 1958**).

**Preethi et al. (2016)** suggested a modification to Webster's delay model for

computing delays at signalized intersections for heterogeneous traffic flow conditions. An adjusted term, the value of which was modeled using *ANN* was applied along with the Webster's model.

Several new approaches based on evolutionary computing and artificial intelligence were proposed for the design and implementation of adaptive signal control systems (**Gartner 1983; Lin and Cooke 1986; Lin and Vijayakumar 1988; Kronborg and Davidson 1993**).

## 2.7 SUMMARY

The above sections provide details on studies related to application of microscopic simulation techniques in speed-flow analysis with special emphasis on the use of *VISSIM* software in traffic and transportation, in addition to investigations on sensitivity analysis based on *Artificial Neural Networks (ANN)*, short-term and long-term improvement strategies, capacity estimation, and isolated signal design using *Genetic Algorithm (GA)* approach based on Webster's and HCM delay model. The above studies are expected to provide the basis for formulating the theoretical background and the development of the methodology for the research work undertaken. **Table 2.1b** provides a brief review of literature on applications of *VISSIM* and soft computing related to micro-simulation modeling of traffic flow.

Earlier studies on micro-simulation modelling of vehicular movement were based on probabilistic time-headway based models that indicated the regime followed by vehicle drivers (**Ahmed 1999**).

The later years witnessed the wide-spread use of sophisticated software such as *CORSIM* (**Bloomberg and Dale 2000**), *VISSIM* (**Fellendorf and Vortisch 2001; Trueblood and Dale 2003**), and so on.

**Fellendorf and Vortisch (2001)** recommend that driver and vehicle characteristics need to be calibrated to suit local traffic conditions and driving styles for modeling urban traffic scenario. In order to improve the predictive capabilities of *VISSIM*, a number of researchers suggested various approaches for calibration of

vehicle and driver characteristics (**Park and Schneeberger 2003; Park and Qi 2005; Lownes and Machemehl 2010**).

A number of approaches were seen to be developed to fine-tune vehicle and driver characteristics in for micro-simulation exercises performed in *VISSIM* (**Subba-Rao et al. 1998; Kalyoncuoglu and Tigdemir 2004; Kalteh 2008; Otkovic et al. 2013a; Otkovic et al. 2013b**). **Park and Schneeberger (2003)** adopted one of the earliest systematic approaches involving a nine-step procedure for testing, calibration, and validation of a *VISSIM* model.

The present study was focused on the development of a *VISSIM*-based micro-simulation model for heterogeneous traffic flow conditions in Mangalore city with 423 links by adopting a stepwise calibration approach involving fine-tuning of vehicle and driver characteristics. It was proposed to adopt a novel approach to perform sensitivity analysis by implementing a modified form of the Garson's algorithm (**Garson 1991**) where the relative importance of input variables can be more precisely computed for *ANN* structures with *multiple-hidden layers*.

The present study incorporates analyses related to car-following model characteristics such as the *minimum collision time-gain*, *time-between direction changes*, *minimum longitudinal speed*, *additive part of desired safety distance*, *multiplicative part of desired safety distance*, *minimum look-ahead distance*, *minimum look-back distance*, *minimum lateral clearance*, and driver behavior, that are not easily measured in field, but are required to be calibrated to ensure better prediction of traffic flows on the road network.

The studies reviewed as part of this chapter provided the necessary basis for performing calibrations of 8 driver-based characteristics and 6 vehicle-based characteristics under Wiedemann-74 (**PTV 2014**) car-following model. The micro-simulation exercises were performed with inputs based on video-graphic surveys conducted at various locations including 18-mid-block sections of the city for the evening peak period.

Based on a review of studies related to the application of the GA approach in the design of signal timings by a number of researchers (**Foy and Benekohal et al.**

1992; Park et al. 1999; Stevanovic et al. 2008; Braun and Weichenmeier 2008) it was proposed to develop a GA-based algorithm that could minimize vehicular delays for selected intersection in Mangalore city.

As part of this study, it was also proposed to adopt the use of *measures of effectiveness* such as the *GEH statistic* value, the *mean absolute errors (MAE)*, and the *RNSE* values in order to indicate the accuracy of simulations based on observed and measured volumes of vehicles passing through 18 mid-block sections of the road network.

**Table 2.1b A Brief Review of Literature on Applications of VISSIM and Soft Computing in Micro-Simulation Modeling of Traffic Flow**

Previous Studies	Details of the Study	Traffic Conditions	Method Adopted	Outcomes of the Study	Remarks/ Research Gap	Present Study
<b>Fellendorf and Vortisch (2001)</b>	The <i>VISSIM</i> model was calibrated and validated for freeways in the U.S. and Germany by modeling vehicle and driver behavior	Homogeneous traffic flow conditions on freeways in US considering the movement of cars following lane-discipline was studied	Microsimulation Modeling in <i>VISSIM</i>	<i>VISSIM</i> found to be capable of modeling real-world traffic more realistically as it uses a psycho-physical car-following approach	Heterogeneous traffic composition was not modeled for urban road conditions.	<i>VISSIM</i> is used to model urban motorized traffic conditions.
<b>Trueblood and Dale (2003)</b>	Studies using <i>VISSIM</i> was performed for six proposed two-lane roundabouts along Missouri Avenue, Missouri, U.S.A	Heterogeneous traffic conditions considering the movement of various vehicle types at roundabouts were studied.	Microsimulation Modeling in <i>VISSIM</i>	<i>VISSIM</i> was found to be flexible in permitting fine-tuning of driver behavior through lane choice and travel speeds	<i>VISSIM</i> was used to model driver behavior for intersections and linking-roads between intersections	<i>VISSIM</i> was used to model the traffic flows on the entire road network considering flows at 8 major intersections.
<b>Park and Qi (2005)</b>	The <i>VISSIM</i> model was calibrated and validated for a set of twenty-one parameters for studies performed in Virginia	Heterogeneous traffic flow conditions for the intersection located at the junction of U.S. Route 15 and U.S. Route 250 in Virginia was analysed.	Macrosimulation Modeling in <i>VISSIM</i>	The calibrated parameters obtained by the proposed procedure provided a more accurate picture of the actual traffic flow.	The predictions obtained using default vehicle and driver parameters were much inferior compared to calibrated model.	33 vehicle and driver parameters were calibrated in order to increase the prediction accuracy to meet the field observed conditions.

<b>Stanek and Milam (2005)</b>	Compared the use of macro-simulation software such as <i>RODEL</i> and <i>SIDRA</i> against microsimulation software such as <i>VISSIM</i> and <i>PARAMICS</i> for high capacity roundabouts.	Heterogeneous traffic flow conditions for roundabouts in Chico and in Placerville, California were studied.	Macrosimulation Modeling in <i>RODEL</i> and <i>SIDRA</i> and Microsimulation Modeling in <i>VISSIM</i> and <i>PARAMICS</i>	<i>VISSIM</i> was found to be more suited for modeling individual driving behavior and permitted easier calibration of field traffic conditions.	<i>VISSIM</i> was used for the calibration of vehicle and driver characteristics for high-capacity roundabouts	<i>VISSIM</i> was used to model the traffic flows on the entire road network considering flows at 8 major intersections.
<b>Gallelli and Vaiana (2008)</b>	Studied the use of <i>VISSIM</i> in modeling various types of roundabouts.	Homogeneous traffic flow conditions considering the movement of motorcars was analysed.	Microsimulation Modeling in <i>VISSIM</i>	Stopping delays were evaluated for various traffic scenarios for roundabouts.	Stopping delays were studied for homogeneous traffic conditions at intersections.	The delays at selected intersections were studied for heterogeneous flow conditions.
<b>Mathew and Radhakrishnan (2010)</b>	An approach to calibrate vehicle and driver characteristics was developed.	Heterogeneous traffic conditions for the two intersections in Trivandrum City and one intersection in Jaipur City.	Microsimulation Modeling in <i>VISSIM</i> was performed along with a <i>GA</i> based sensitivity analysis of car-following parameters.	The car-following parameters such as the average standstill distance, additive part of desired safety distance, and multiplicative part of desired safety distance were found to be highly sensitive.	The study was restricted to investigations at intersections in 2 Indian cities	The present study was focused on simulating the traffic flows for the entire road network spread across 3.08 square km of Mangalore city.
<b>Manjunatha et al. (2013)</b>	Proposed a methodology for calibrating a microsimulation model at two intersections in Mumbai	Heterogeneous traffic conditions were analysed for urban intersections at Mumbai.	Microsimulation Modeling in <i>VISSIM</i> was performed along with a <i>GA</i> based sensitivity analysis of car-following parameters in addition to a multi-parameter sensitivity analysis using <i>ANOVA</i>	The calibration parameters of Wiedemann 99 car-following model such as standstill distance, headway time, car-following variation, oscillation acceleration, and standstill acceleration were found to be highly sensitive	The study was confined to analyses at intersections.	In the present study, a multi-parameter sensitivity analysis was performed to identify highly sensitive parameters of Wiedemann 74 car-following model using the <i>ANN</i> approach.

<b>Durrani et al. (2016)</b>	Wiedemann 99 car-following model for driver behavior was studied for cars, motor cycles, and heavy vehicles	Heterogeneous traffic conditions for a 640-m segment of US-101 in Los Angeles, California were analysed.	Microsimulation Modeling in <i>VISSIM</i>	The study concluded that various combinations of driver behavior parameters must be studied for various vehicle types	The studies were performed only for highway segments in USA.	In the present study, various combinations of vehicle and driver parameters were studied for Wiedemann 74 model for urban roads.
<b>Srikanth et al. (2020)</b>	Studies on calibrating and validating a <i>VISSIM</i> model based on lane-change behavior was performed for highways sections.	Heterogeneous traffic conditions at two locations on National Highway-163 (Warangal to Hyderabad) were considered.	Microsimulation Modeling in <i>VISSIM</i>	It was identified that random seed 40 provided better prediction accuracy when compared to 41, 42, 43, and 44	The studies were performed for highways in India	Out of a number of random seeds analysed, random seed 42 was found to be the best.

Based on the review of literature, the following important observations and gaps in research were made.

**Bloomberg and Dale (2000)** recommended *VISSIM* for modelling heterogeneous traffic flow on urban road networks.

Investigation performed by **Mathew and Radhakrishnan (2010)**, **Siddharth and Ramadurai (2013)**, **Durrani et al. (2016)**, **Srikanth et al. (2020)** focused on calibration and validation of *VISSIM* for simulations performed along selected traffic-corridors, shorter highway sections, and a few intersections whereas, studies related to calibration of vehicle and driver characteristics considering traffic flow in a road-network for a city for heterogeneous traffic flow conditions involving slow and fast vehicles have not been reported. The present study considers the traffic flow of the road network in Mangalore city spread across an area of 3.08 square km.

**Manjunatha et al. (2013)** performed calibration of vehicle and driver parameters including standstill distance, headway time, car-following variation, oscillation acceleration, and standstill acceleration for Wiedemann 99 car-following model, while **Habtemichael (2012)** performed similar studies on calibrating 21 Wiedemann 74 driver behavior parameters. The present study proposed to incorporate

a comprehensive investigation on the calibration of 33 vehicle and driver parameters. Six vehicle characteristics and eight driver characteristics of the Wiedemann 74 car-following model were proposed to be analysed for each of the five vehicle types (such as cars, motor-cycles, LCVs, buses, and auto-rickshaw).

It was also observed that **Mathew and Radhakrishnan (2010)** adopted the use of genetic algorithm to perform sensitivity analysis on various vehicle and driver characteristic, while **Manjunatha et al. (2013)**, and **Siddharth and Ramadurai (2013)** relied on the use of ANOVA method for the same. The present study on the other hand, proposed to focus on the application of ANN in performing sensitivity analysis based on a modified form of Garson's approach adapted for ANNs with more than one hidden layers.

Additionally, the present study also proposes to utilize the capability of the GA approach in the design of signals at selected locations of the city.

## CHAPTER 3

### THEORETICAL BACKGROUND

#### 3.1 GENERAL

Simulation-based techniques have gained popularity in the analysis of traffic flow characteristics for road networks. In this regard, macro-measures that deal with speed-density, speed-flow, and flow-density relationships can be employed in the study of the overall impact of strategies adopted for road network improvement. These measures also assist in the estimation of roadway capacities.

Micro-simulation approaches provide details on vehicular conflicts that occur while vehicles move through bottlenecks, the spot speeds and space-mean speeds of vehicles, the flow of vehicles over a given road section, the impact of various signalization strategies adopted, and the impact of long-term and short term improvements for formulating policies for efficient vehicular movement in cities. The various sub-sections of this chapter provide details on simulation-based approaches to traffic flow modeling.

The later section of this chapter also provides details on the theoretical aspects of *GA* operations. This chapter also provides details on the fundamental aspects of performing a sensitivity analysis using the *ANN* approach for identifying the important vehicle and driver characteristics that influence the accuracy of prediction of *VISSIM*-based micro-simulation models.



### 3.2 IMPORTANCE OF SIMULATION-BASED TRAFFIC FLOW MODELING AND TYPES OF SIMULATION MODELING APPROACHES

In the past few decades, simulation-based approaches have gained popularity considering the complexity involved in formulating analytical models due to vehicle, driver, road-user, and road-geometric related factors, and the high costs involved in the development of the same. Simulation-based analysis of traffic flow characteristics in an urban street system can be performed at varying levels of details using microscopic, sub-microscopic, mesoscopic and macroscopic levels of analyses.

Development of simulation models to simulate the traffic flows in urban road networks involves intensive data collection, data processing, calibration, and validation. Calibration involves the development of the model based on actual data on traffic flows at various mid-blocks of the road network, and the road characteristics, and the assigning of vehicle characteristics, and driver-behavior characteristics. A simulation model is said to be calibrated only when it is capable of replicating the actual traffic flow conditions to a reasonable degree of accuracy. Once the calibration studies are found to provide predictions of traffic flows close to observed values, a validation exercise is performed using a different set of field data for the study area. The simulation model is considered to be reliable when the accuracy of prediction of traffic flows in the calibration and validation studies are minimal and acceptable.

The *GEH* statistic originally proposed in the 1970s by Geoffrey E. Havers, a London-based transport planner, is found to be widely used in determining the forecasting capabilities of simulation models by the United Kingdom Highway Agency as explained in the Design Manual for Roads and Bridges (**DMRB 1996**), Wisconsin Micro-simulation Modeling Guidelines (**Website: Wisconsin**), and Transport for London: Traffic Modeling Guidelines Version 3.0 (**Smith and Blewitt 2010**).

It is used as a measure of effectiveness in predicting traffic volumes and vehicular speeds of traffic models. The *GEH* statistic is expressed as (**Columbia River Crossing 2006; WSP Management Services Ltd. 2011**):

$$GEH = [2 (M - C)^2 / (M + C)]^{0.5} \quad \text{Eq.3.1a}$$

where,  $M$  is the hourly traffic volume over a certain speed range, predicted or simulated by the traffic model, and  $C$  is the observed hourly traffic count for the speed range.

Alternatively, the statistic  $RNSE$  (root normalized squared error), a modified form of the  $GEH$  statistic is also used by various agencies including **Wisconsin DoT (2002)**. The  $RNSE$  statistic is expressed as,

$$RNSE = [(M - C)^2 / C]^{0.5} \quad \text{Eq.3.1b}$$

### **3.2.1 Microscopic Simulation Models**

A microscopic simulation model tends to represent the real-life system comprising the entities such as vehicles and drivers, and the space-time interactions among them at a high level of detail. In micro-simulation study, it is possible to analyse the movement of each vehicle in the traffic stream including lane-change behavior, overtaking manoeuvres, and the effect of changes in driver and vehicle parameters on the system in greater detail.

Micro-simulation approaches can estimate speed-flow, and density relationships more accurately especially in heterogeneous traffic flow conditions. These models need to be developed based on video-graphic data on traffic flow at mid-block sections and intersections of the traffic network or based on other reliable data collection methods.

### **3.2.2 Sub-Microscopic Simulation Models**

Sub-microscopic simulation models describe the characteristics of individual vehicles in the traffic stream with greater detail. Thus, in addition to the detailed description of driving behavior, details on vehicle control are also incorporated. These models also include details on the functioning of specific sub-components (*sub-units*) of the vehicle and the system.

### **3.2.3 Mesoscopic Models**

Mesoscopic models do not attempt to provide details on individual vehicles, while the behavior of road-users can be modeled based on probabilities. For example,

the probability of undertaking a lane change operation can be modeled based on relative lane densities, and speed differentials.

### 3.2.4 Macroscopic Models

Macroscopic models describe traffic behavior at the aggregate level. For example, the traffic stream can be represented using speed, density, and traffic flow instead of analysing details of each and every vehicle or driver.

## 3.3 BASIC ASPECTS ON THE DESIGN OF ISOLATED TRAFFIC SIGNALS USING THE HCM 2000 DESIGN METHOD

This section provides details on the fundamental aspects of the design of isolated traffic signals using the HCM 2000 design method (TRB, 2000) along with explanations on common terms used in signal design, and limits for cycle time and green time according to specifications laid by Indian Roads Congress (IRC) and HCM 2000.

In the design of isolated traffic signals, the effective green time ( $g_i$ ) of phase  $i$  can be assumed to lie between the upper and lower limits  $g_{max}$ , and  $g_{min}$ , and can be expressed as,

$$g_{min} \leq g_i \leq g_{max} \quad \text{Eq.3.2c}$$

where  $g_{max}$  = the maximum effective green time; and  $g_{min}$  = the minimum green time (assumed as 7 sec as per IRC 93-1985). The maximum effective green time for signal phase  $i$  refers to the total time duration over which the vehicles cross a junction.

The above expression can be written in the standard form  $g(x) \geq 0$  for a minimization problem as,

$$g_i - g_{min} \geq 0, \text{ and} \quad \text{Eq.3.2d}$$

$$g_{max} - g_i \geq 0 \quad \text{Eq.3.2e}$$

The above expression can also be written as,

$$C = g_{max} + \left\{ \sum_{j=1, n} (g_{min})_j + \left[ \sum_{i=1, n} L_i + \sum_{i=1, n} (I_i - a_i) \right] \right\} \quad \text{Eq.3.2i}$$

Usually,  $L_i$  is assumed as 2 seconds for each phase, and  $I_i$  is assumed as 4 seconds for each phase according to **IRC 93-1985**. Thus, the total time lost can be computed from **Eq.3.2g** as,

$$\begin{aligned} L &= \sum_{i=1, n} L_i + \sum_{i=1, n} (I_i - a_i) \\ &= (2+2) + [(4-2) + (4-2)] = 8 \text{ seconds} \end{aligned}$$

The above expression can be written in the standard form  $g(x) \geq 0$  for a minimization problem as,

$$C - C_{min} \geq 0, \text{ and} \tag{Eq.3.2k}$$

$$C_{max} - C \geq 0 \tag{Eq.3.2l}$$

Based on **Eq.3.2f**, the expression for the minimum cycle length can be expressed as,

$$C_{min} = g_{max} + [\sum_{j=1, n} g_{j min} + L]$$

Here, while computing the minimum cycle length, the term  $g_{max}$  may be ignored. Also, in the design of an isolated signal for a junction,  $j$  can be assumed as unity. Hence, the above expression reduces to,

$$C_{min} = g_{min} + L \tag{Eq.3.2m}$$

### 3.3.1 Theoretical Considerations in the Design of Pre-timed Isolated Signals for 2 or More Phases Using the HCM 2000 Design Method (TRB, 2000)

The details on computations for cycle lengths and green times for a pre-timed isolated traffic signal based on HCM 2000 (**TRB 2000**) for two or more phases are described in this section.

In the first step, it is required to compute the *total lost-time per cycle* ( $L$ ) based on lost-time ( $t_L$ ) for each lane group  $L$  using the following expression:

$$L = \sum_{L=1, n} t_L \tag{Eq.3.3a}$$

Here, it may be observed that the *volume/capacity ratio* ( $X_i$ ) for lane group  $i$  or phase  $i$  is given as,

$$X_i = q_i \cdot C / s_i \cdot g_i \tag{Eq.3.3b}$$

$$= (q_i / s_i) (C / g_i) = q_i / (\lambda_i s_i)$$

where,  $q_i$  = *flow-rate* (vehicles/h) for lane group  $i$  for which the signal phase timing has to be computed;  $s_i$  = *saturation flow rate* (vehicles/h) for lane group  $i$  assumed based on design standards;  $C$  = given or trial cycle length (s);  $g_i$  = effective green time (s) for lane group  $i$ ; and  $\lambda_i = g_i / C$  = proportion of effective green time.

In the second step, it is required to determine the *minimum cycle length* ( $C_{min}$ ) to avoid over-saturation. This is computed by assuming a *critical volume/ capacity ratio* equal to 1.0. Thus, the above expression can be rewritten as,

$$\begin{aligned} C_{min} &= L / [1.0 - \sum_i (q_i / s_i)_c] && \text{Eq.3.3e} \\ &= L / [1.0 - \sum_i y_{ci}] \\ &= L / [1.0 - (y_{c1} + y_{c2} + y_{c3})] \text{ for a pre-timed isolated 3-Phase signal} \end{aligned}$$

It is now required to cross-check using **Eq.3.3d** whether the *cycle length* ( $C$ ) based on the *total lost-time per cycle* ( $L$ ), the sum of the *critical volume/ capacity ratios* ( $X_c$ ), and the sum of the *critical flow ratios* in each lane group  $i$  ( $y_{ci}$ ) are within practical limits. If not, it is required to further increase the cycle length in increments of 5 seconds (for cycle lengths between 30-90 seconds) or 10 seconds (for cycle lengths greater than 90 seconds) in order to perform the next cycle of computations. Furthermore, the actual *degree of saturation* or the actual *volume/ capacity ratio* for critical movements ( $X_c$ ) can be verified for the revised cycle-length using **Eq.3.3c**.

In **Eq.3.3f**, it is required to compute  $g_i$  using  $X_i$ . But according to **Eq.3.3b**,  $X_i$  can be computed based on  $g_i$ . This recursive nature of the solution approach suggests that the green times need to be computed based on an iterative search process. Alternatively, the *HCM 2000 design method* (**TRB 2000**) explained in Chapter 16 page 100 of the TRB Manual suggests that the green times can be allocated such that the *volume/ capacity ratio* ( $X_c$ ) for critical movements in each phase are equal. Thus, the green times in *HCM 2000 design method* are computed based on the following expression:

$$g_i = q_i \cdot C / (s_i X_c) = (q_i / s_i)_c \cdot (C / X_c) \quad \text{Eq.3.3g}$$

### 3.4 THEORETICAL ASPECTS ON TRAFFIC DELAYS, BASIC ASPECTS OF WEBSTER'S APPROACH, AND HCM2000 AVERAGE DELAY MODEL

A number of investigations have been made on the delays experienced by drivers at road junctions. The modeling of delays that occur on roads characterized by lower traffic intensities is much different than that for congested conditions. The study of delays experienced at intersections can be classified into the following:

- (a) *Steady state stochastic delay models*
- (b) *Deterministic or uniform delay models*
- (c) *Time-dependent delay models*

**Webster (1958)**, **Tanner (1962)**, and **Miller (1968)** performed pioneering studies on stochastic/ random delays, while **May and Keller (1967)**, **Neuberger (1971)**, and **Pignataro et al. (1978)** provide the basic theoretical foundations for *deterministic or uniform delay models* for un-signalized road sections. **Catling (1977)** provided an expression for delay at signalized intersections based on the *deterministic flow model* for under-saturated and over-saturated flows. Pioneering studies on *time-dependent delay models* such concepts were initiated by Whitling in his unpublished works (**Robertson and Gower 1977**). These were further revised and compiled as part of HCM 2000 (**TRB, 2000**).

#### 3.4.1 Steady State Stochastic Delay Model (Webster's Delay Equation)

Stochastic delay models are developed based on the assumption that the occurrence of delays is a random/ stochastic phenomenon. This assumption is true for operating conditions where the average actual arrival of vehicles at intersections is lesser than the *capacity flow* of the junction. **Webster (1958)**, **Tanner (1962)**, and **Miller (1968)** performed pioneering studies on random delays. The Webster's expression for delay is given as (**Webster 1958**),

$$d_i = d_{uniform} + d_{random} - \text{empirical correction factor}$$

That is,

$$d_i = \{ [C(1-\lambda)^2] / [2(1-\lambda x_i)] + (x_i^2 / [2q_i(1-x_i)]) - (0.65(C/q_i^2)^{(1/3)} x_i^{(2+5\lambda)}) \} \quad \text{Eq.3.4a}$$

where,  $d_i$  = average delay per vehicle for a particular phase  $i$  (or approach) of the

intersection;  $C$  = cycle time;  $\lambda$  = proportion of the cycle time which is effectively green for the phase under consideration =  $g_i / C$ ;  $g_i$  = effective green time for approach  $i$ ;  $q_i$  = flow (vehicles/s) for approach  $i$ ;  $s_i$  = saturation flow for approach  $i$ ; and  $x_i$  = the degree of saturation or ratio of the actual flow to the maximum possible flow under a given signal condition for approach  $i = q_i / \lambda \cdot s_i$ .

*Uniform delay* represented by the first term in the Webster's expression as in **Eq.3.4a** refers to the delay due to the uniform arrival of vehicles when the signal is green, while *random delay* represented by the second term in the Webster's expression refers to additional delays caused due to random arrival of vehicles when the signal is red. The third term is an empirical correction term. According to **Courage and Papapanou (1977)**, this correction term approximately results in a 10% reduction in the total delay predicted by the Webster's delay model. This observation was further corroborated later by **Dion et al. (2004)** where it was found that the simulated values of delays were found to lie within an error ranging between 5-15%.

In the expression derived for computing stochastic delays as in **Eq.3.4c**, when the degree of saturation  $x_i$  approaches unity, the delay computed approaches infinity. **Akcelik (1988)**; **McShane and Roess (1998)**; and **Fambro and Roupail (1997)** considered this as major drawback in the Webster's model.

### 3.4.2 Deterministic Delay Models (for Under-saturated and Over-saturated Flows)

At lower degrees of saturation and at steady state flow conditions (where  $x < 1$ ), the delays can be computed using the expression **Eq.3.4a**. Here, the steady state delay model closely follows the uniform delay model as shown by the part of the curve OA in **Fig.3.8a**. The line OB represents the deterministic uniform delay due to uniform arrival of vehicles even when the signal is red.

In the case of vehicular flows at higher degrees of saturation (where  $x > 1$ ), **Catling (1977)** provides an expression for delay based on the *deterministic flow model* for under-saturated and over-saturated flows as follows:

$$D = d_l + (T(x - 1))/2 \tag{Eq.3.4e}$$

where,  $D$  is the delay (average delay per vehicle) experienced at very low traffic intensity;  $T$  = the period over which flows are analysed;  $x$  = the degree of saturation or ratio of the actual flow to the maximum possible flow; and  $d_l$  = uniform delay at under-saturated conditions.

There are two major assumptions based on which the deterministic delay models are derived. These are listed as follows:

- (a) No initial queue exists at the beginning of the interval  $[0, T]$
- (b) Traffic intensity is constant over the interval  $[0, T]$ .

### **3.4.3 Time-dependent Stochastic Delay Models (for Under-saturated and Over-saturated Flows)**

One of the defects of the deterministic delay models is that it assumes that the initial queue length at the beginning of the interval is zero. This need not be true. The time dependent models overcome this defect by combining the advantages of steady-state stochastic models and deterministic models

In over-saturated conditions, the number of vehicles reaching the intersections will be more than the number of vehicles dispatched by the traffic signals. This results in increasing residual queue lengths. The limitation of the Webster's model was addressed by the *time-dependent delay model* originally conceived by P.D. Whiting while formulating an expression for random delays (**Robertson and Gower 1977**). This model was later investigated by **Robertson (1979)**, and further modified by **Kimber and Hollis (1979)**.

The *time dependent delay* model was formulated to overcome the deficiencies in the formulation of the *stochastic* and *deterministic delay* models. **Burrow (1989)**, **Catling (1977)**, **Brilon and Wu (1990)**, **Akcelik (1980; 1988; 1994)**, and **Teply (1995)** performed investigations on delays at saturation and congested flow conditions. The models suggested in HCM 2000 (**TRB 2000**) incorporate the necessary corrections to the overall formulation of delays.

#### **3.4.3.1 HCM Average Delay Model (TRB, 2000)**

The *average delay* model according to HCM 2000 (**TRB, 2000**) for one of the approaches to a junction is expressed as,



$$d = d_1.PF + d_2 + d_3 \quad \text{Eq.3.4h}$$

where,  $d$  = average delay per vehicle, s/veh;  $d_1$  = uniform delay assuming uniform vehicle arrivals, s/veh;  $PF$  = uniform delay progression adjustment factor which accounts for the effects of signal progression which is approximately equal to 1.0 for uncoordinated signals and not greater than 1.0 according to HCM 2000;  $d_2$  = incremental delay (s/vehicle) to account for random vehicle arrivals and over saturated queues for the period of analysis;  $d_3$  = supplemental delay (s/vehicle) to account for over saturation queues that might have existed just before the analysis period ( $T$ ), which may be ignored if such situations do not exist.

The expression for *uniform delay* according to HCM 2000 is given as,

$$d_1 = C. (1-g/C)^2 / \{ 2 [1 - (\text{Min}(1, X) . g/C)] \} \quad \text{Eq.3.4i}$$

where,  $d_1$  = uniform delay (s/vehicle) assuming uniform vehicle arrivals;  $C$  = cycle length (s) used in pre-timed signal control, or average cycle length (s) for actuated control;  $g$  = effective green time (s) for the lane group for pre-timed signal controls, or average lane group effective green time (s) for actuated signal controls;  $X$  = volume/capacity ratio or degree of saturation for the lane group.

The *calibration term* ( $K$ ) is included to adjust for the type of traffic controller used. For pre-timed signals, a value of  $K = 0.50$  is used, which is based on a queuing process with random arrivals and uniform service time equivalent to the lane-group capacity. The *incremental delay adjustment factor* ( $I$ ) incorporates the effect of arrivals from upstream signals. For a signal analysis of an isolated intersection, a value of 1.0 is used for  $I$ .

### 3.5 GENERAL THEORETICAL ASPECTS OF GA OPERATIONS

The *genetic algorithm* ( $GA$ ) approach is an evolutionary optimization technique, formulated on the basis of the mechanics of natural-selection and evolution. In this approach, the solution to a problem situation evolves based on traditional stochastic operations of *selection*, *crossover* and *mutation*. The search for the *optima* is performed over a space represented by means of binary-bit descriptions of the input signals.

A GA has the capability to perform a search for the *global-optima* over a wider solution space, reducing the possibility of being trapped in *local-optima* (**Goldberg 2002**). The GA approach functions in a manner similar to the simulation technique, and does not require the use of complex mathematical relationships, and their derivatives for arriving at the *optima*. Additionally, the GA is capable of handling optimization problems with *disconnected search spaces* (**Goldberg 2002**). In contrast, the simulation technique is most effectively used to arrive at *optima* from an existing feasible solution.

### 3.5.1 Functioning of Genetic Algorithm Applications

Genetic algorithms differ from the conventional search procedures in the following manner (**Goldberg 1989**):

- Genetic algorithms work with a coding of the parameter set, not the parameters themselves.
- Genetic algorithms search from a population of points (in the solution space), not from a single point.

Although there are no distinct guidelines for choosing of an algorithm for solving a given problem, **Rao (2003)** proposes that the following factors need to be considered while selecting the optimization approach:

- the type of problem to be solved (linear, non-linear, or other types);
- the important variables and parameters that influence the objective function;
- the overall efficiency and dependability of the optimization approach in handling the type of problem;

### 3.5.2 Fundamental Genetic Operations

- The GA utilizes the principle of *survival-of-the-fittest* by transferring the characteristics of the best chromosome to the next generation of strings and by combining the characteristics of a set of strings to explore new search points (**Goldberg 2002**). The main genetic operations performed include *reproduction, crossover, and mutation*.

- The operation of genetic algorithm begins with the generation of a population of random binary strings representing the solution set for the decision variables.
- The strings of the new population are further evaluated and the fitness indices are again computed. If the values of the best solution strings do not satisfy a convergence-criteria, the next generation of strings are again produced using genetic operations, and the procedure is continued iteratively. In GA terminology, one cycle of such genetic operations and the subsequent evaluation procedure is known as a *generation* (**Goldberg 2002**).
- Reproduction, crossover, and mutation are simple and straightforward genetic operations that can be performed on a group of strings or chromosomes. The reproduction operator selects the best strings that can form the next generation of population.
- *Elitism* is the name of the approach in which the characteristics of the best strings of the chromosomes are retained while creating the next generation (**Deb 2000**). Elitism can very rapidly increase the performance of a GA, since it prevents the loss of the best solution found so far.

## CHAPTER 4

### METHODOLOGY OF THE STUDY

#### 4.1 INTRODUCTION

Micro-simulation techniques are effectively used in the study of vehicular movements on urban road networks. These techniques provide the necessary basis for investigating bottlenecks and congestion at mid-blocks and road junctions. Simulation-based approaches are considered to be cost-effective in modeling vehicular flows, performing detailed analyses on the existing traffic scenario, and in the study of impact of short-term and long-term improvements in the road network.

In order to develop a simulation model representing traffic flow conditions in a city, it was required to collect important details on classified traffic flow at important locations of the travel network and turning movements at junctions. It was also required to obtain details on vehicular speeds and delays at these locations. Prior to performing a full-fledged micro-simulation modeling in *VISSIM*, details on characteristics of various types of vehicles, in addition to driver and roadway characteristics that would be useful in performing the *basic multi-stage calibration* exercises were compiled. The *basic validation* exercise was then performed on a different set of data.

It was also required to perform a sensitivity analysis to ascertain the influence of various vehicle and driver characteristics for ensuring a higher accuracy in simulation exercises. In the next phase, considering the complex inter-relationships between various vehicle and driver characteristics, it was proposed to perform an *ANN-based sensitivity analysis*.

As part of the study, the capabilities of the *VISSIM*-based micro-simulation model developed was demonstrated by performing studies on short term and long term improvements to selected road sections in addition to investigations on the application of the *genetic algorithm (GA)* based approach in the design of traffic signal timings.

The following sections in this chapter provide details on the methodology adopted in this study, the stage-wise approach to investigations, and the basic aspects of model development in *VISSIM*.

#### 4.2 OVERALL METHODOLOGY ADOPTED IN THE STUDY

The investigations performed as part of this study deal with the development of a micro-simulation based approach using *VISSIM* for understanding the traffic-flow characteristics of Mangalore city characterized by heterogeneous traffic conditions. Based on a preliminary study of traffic flow in Mangalore city, Hampankatta Junction, Navabharat Junction, PVS Junction, Bunt's Hostel Junction, and Jyothi Junction, were considered to be of importance in addition to Bendoorwell Junction, Balmatta junction, and St. Theresa's School junction spread over the core-city area of 3.08 square km.

The important steps in the methodology adopted for the development of a *VISSIM* based model for simulation of traffic flows for the urban road network in Mangalore, along with brief details on analyses performed at each stage of the present study are provided in **Fig.4.1**, and a description of the same given below:

- i. In the *initial phase* of the study, a map study of the city was performed for the identification of the important roads and junctions, followed by creation of an *AutoCAD* drawing of the road network with exact dimensions of road junctions and links, creation of a high-resolution digital *base-map* of the city, and interfacing of the digital *base-map* to the *AutoCAD* drawing.

An *AutoCAD* drawing with details on the road geometrics, width of the road links, and details on dimensions at the junctions was prepared based on measurements made at various locations in the city. For the road-stretches of the city that remained unchanged for the past decade, the information contained in drawings prepared previously by **Dalal Consultants and Engineers Ltd. (2007)** were used to update the *AutoCAD* drawing.

- ii. As part of the *initial phase* of the study, a data collection exercise was performed to obtain classified vehicle volumes and turning movements at

important road junctions, and the vehicular flows and speeds at 18 important mid-block sections for 90 minutes.

- iii. Additionally, as part of the *initial phase* of the study, a *preliminary modeling exercise* was performed in VISSIM using default values of vehicle and driver characteristics to identify the best *random seed* based on the *GEH* statistic.
- iv. In the next phase, a *basic multi-stage calibration* of vehicle and driver characteristics was performed using the best random seed 42 for the development of a VISSIM-based micro-simulation model that could simulate traffic flow in the city with a reasonably good accuracy.
  - Stage 1: Assigning *minimum lateral clearances* between vehicles for various vehicle types.
  - Stage 2a: Assigning acceptable *desired acceleration distributions* for various vehicle types.
  - Stage 2b: Assigning acceptable *maximum acceleration* distributions for various vehicle types.
  - Stage 2c: Assigning acceptable *deceleration distributions* for various vehicle types.
  - Stage 7a: Assigning the *lower bounds* for *desired speeds* for *speed distributions* of each vehicle type.
  - Stage 7b: Assigning the *upper bounds* for *desired speeds* for *speed distributions* of each vehicle type.
  - Stage 8: Assigning *minimum look-back distances* as part of car-following characteristics for various vehicle types.
  - Stage 13: Refining the value of *minimum longitudinal speed* as part of lane change behavior for various vehicle types.
  - Stage 14: Refinement of *minimum collision time-gain* as part of lateral driving behavior for various vehicle types.
- v. After performing the basic calibration and validation exercises, an *ANN-based sensitivity analysis* was performed to identify the set of highly sensitive vehicle and driver characteristics that influenced the predictive capability of the VISSIM model.
- vi. The refined VISSIM model developed for the city was then used to evaluate the impact of *short-term* and *long-term* strategies for improvement of selected critical locations in the road network.

As part of the studies on evaluating the impact of *short-term* improvement strategies, it was proposed to study the effect of minor widening of selected road sections at Bendoorwell Junction, and the road section between Karangalpady Junction and Bunt's Hostel Junction.

As part of the studies on evaluating the impact of *long-term* improvement strategies, it was considered ideal to suggest the use of a fly-over close to Bunt's Hostel Junction to cater to traffic arriving from PVS Junction, moving towards Jyothi Junction and Kadri Junction. A similar exercise was also performed close to Bendoorwell Junction to cater to traffic arriving from Kankanady Junction, moving towards St. Theresa's School Junction.

- vii. In the later part of this study, the application of a *genetic algorithm (GA)* based approach was investigated for the design of signal timings at four selected locations in the city.

The results of the studies performed above are expected to provide transport engineers with the required background information to understand the influence of *vehicle, driver, lane-change, and roadway* characteristics on modeling traffic for heterogeneous traffic conditions.

#### **4.3 AN OVERVIEW OF VISSIM 7.0**

There are a number of software used in performing micro and macro-level simulations on urban road networks. These include *VISSIM/ VISUM, TRANSYT, PARAMICS, HETROSIM, CORSIM, SimTraffic, SCOOT, Aimsun, SYNCHRO, OSCADY, ARCADY, PICADY, SISTM*, and so on.

*VISSIM*, the software used in this study, is developed by PTV AG, Germany (PTV 2011). It is a micro-simulation based software tool that can simulate traffic movement of cars, trucks, buses, pedestrians, bicyclists, and heavy rail and light rail transit in urban areas. *VISUM*, a macro-simulation module developed by PTV is often bundled with *VISSIM* in order to assist in performing detailed analyses related to public transport and multi-modal transportation.

The software also permits the use of traffic control options such as yield-signs, stop-signs and pre-timed or actuated traffic signal controls. It incorporates user-defined internal logic in the use of *pre-timed trafficsignal controls*.

The earlier versions of *VISSIM* were not developed to model Indian driving behavior. The lane occupancy setting had to be adjusted to model the high vehicle densities in India. But in *VISSIM5.40*, a provision for *space-sharing* is introduced where the vehicles utilize the entire road-width available.

*VISSIM* can provide outputs in the form of tables, as well as graphic representations, and animations. Animation can be performed by specifying either 2D or 3D option.

The major inputs for the simulation model are classified into *roadway geometry, traffic composition and traffic control, vehicle characteristics, driver characteristics, and lane-change characteristics*.

- *Roadway geometry* details that are required to be given as input include information on the spatial location, width, type of road, and the number of lanes of the road.
- *Traffic composition* characteristics include data on vehicle volume, routing proportion (turning movements at junctions), and the proportion of each type of vehicle.
- *Traffic control* provides information on the type of traffic control such as signalized, pre-timed or actuated signalized control.

A *VISSIM* model can provide output on details such as the travel-time, travel-distance, average-speed of each vehicle, and traffic flow for the link (trap-length) considered for the study. The software is also capable of providing output on details such as traffic flows, queue lengths, delays, speeds and densities at specific locations and at intersections. *VISSIM* is the most popular software used in microscopic traffic simulation based on a study performed by **Brackstone et al. (2012)**.

*VISSIM* performs simulations for vehicular movements on urban arterial roads based on *Wiedemann 74* driver characteristics based on studies performed on the German Autobahn by **Wiedemann (1974)**, and incorporates updates based on



**Wiedemann and Reiter (1992).** The *Wiedemann 99* driver characteristics incorporated in *VISSIM* was based on unpublished research work on driver behaviour on freeways.

#### **4.4 BASIC STEPS FOR MODEL DEVELOPMENT IN VISSIM**

As part of the preliminary preparations for commencement of the modeling exercise, it is necessary to perform the following basic steps in order to develop a micro-simulation model within a smaller span of time:

- The characteristics of each vehicle type used in the modeling exercise must be clearly defined with details on the *dynamic characteristics* including details on the speed, acceleration, and the deceleration distributions. The upper and lower limits for the distributions need to be provided, and the shape of the distribution curves must be specified. Additionally, details on lateral clearances too must be provided for each vehicle-type.
- The *composition of vehicles* with details on the proportions of various vehicle-types needs to be provided as input to the simulation model for every traffic generation point, in addition to similar details at all turning movements at the junctions.
- The development of a micro simulation model in *VISSIM* requires a high-resolution scaled map of about 1:5000 to be used as the template in the background, preferably in combination with *AutoCAD* based images showing detailed designs of road junctions in order to develop the *links* and *connectors* in *VISSIM* more effectively.
- The road network can then be developed in *VISSIM* using *links and connectors* with the image in the background. *Connectors* can be used to streamline the vehicular flows along the desired directions.
- The *routing* of vehicles is then performed based on the traffic flow pattern for the city. A route is a fixed sequence of links and connectors from a particular *routing decision point* to at least one *destination point*. For this purpose, it is necessary to observe the routes followed by vehicles in the system while allocating the *routing decision* for each vehicle type.

- It is required to study the turning movement of vehicles at the junctions in order to specify the *priority rules* such that the simulated vehicles move without much of conflicts in a manner similar to the actual traffic movement where drivers take care to avoid accidents. *Priority rules* can be applied in *conflict areas* where two or more links or connectors meet such that the right of way can be given to any one of the turning movements.
- The output files obtained from *VISSIM* will include details on *link evaluations*, details on classified vehicle flows, speeds, lane-changes, and delays (*vehicle records*), and details on the signal plans. The required output can also be specified by the user.

### Initial Phase: Performing a Map Study for Mangalore City

#### Creation of a Composite .dwg file using an AutoCAD Drawing and a High-Resolution Base Map

A map study of the city was performed for the identification of the important roads and junctions, followed by creation of an *AutoCAD* drawing of the road network with exact dimensions of road junctions and links, creation of a high-resolution digital *base-map* of the city, and interfacing of the digital *base-map* to the *AutoCAD* drawing.

- An *AutoCAD* drawing with details on the road geometrics, widths of the road links, and dimensions at the junctions was prepared based on measurements made at various locations.
- The *AutoCAD* drawing prepared in the previous step was then overlaid on the digitized base-map in *AutoCAD* environment, and the *AutoCAD* drawing was re-aligned to ensure a perfect match. The *.jpgbase-map* along with the *re-alignedAutoCAD* drawing was then saved as a composite *.dwg* image.

#### Performing Data Collection

A data collection exercise was performed to obtain classified vehicle volumes and turning movements at important road junctions, and the vehicular flows and speeds at 18 important mid-block sections for 90 minutes.

- Data on vehicular flows and speeds were collected at 18 important mid-block sections of the road network.
- A 60-minute data corresponding to 75% of the data collected was used for testing and calibration of the *VISSIM* model, while the remaining 25% of the data corresponding to 20 minutes of video-graphic data was used for validation.

#### Preliminary Modeling Exercise to Determine the Best Random Seed

A *preliminary modeling exercise* was performed in *VISSIM* using default values of vehicle and driver characteristics to identify the best *random seed* based on the *GEH* statistic.

- A preliminary micro-simulation model in *VISSIM* was developed comprising 8 major junctions and 18 mid-block sections of the city.
- The vehicle and driver characteristics set to default values.

To Basic Multi-stage Calibration and Validation Exercises

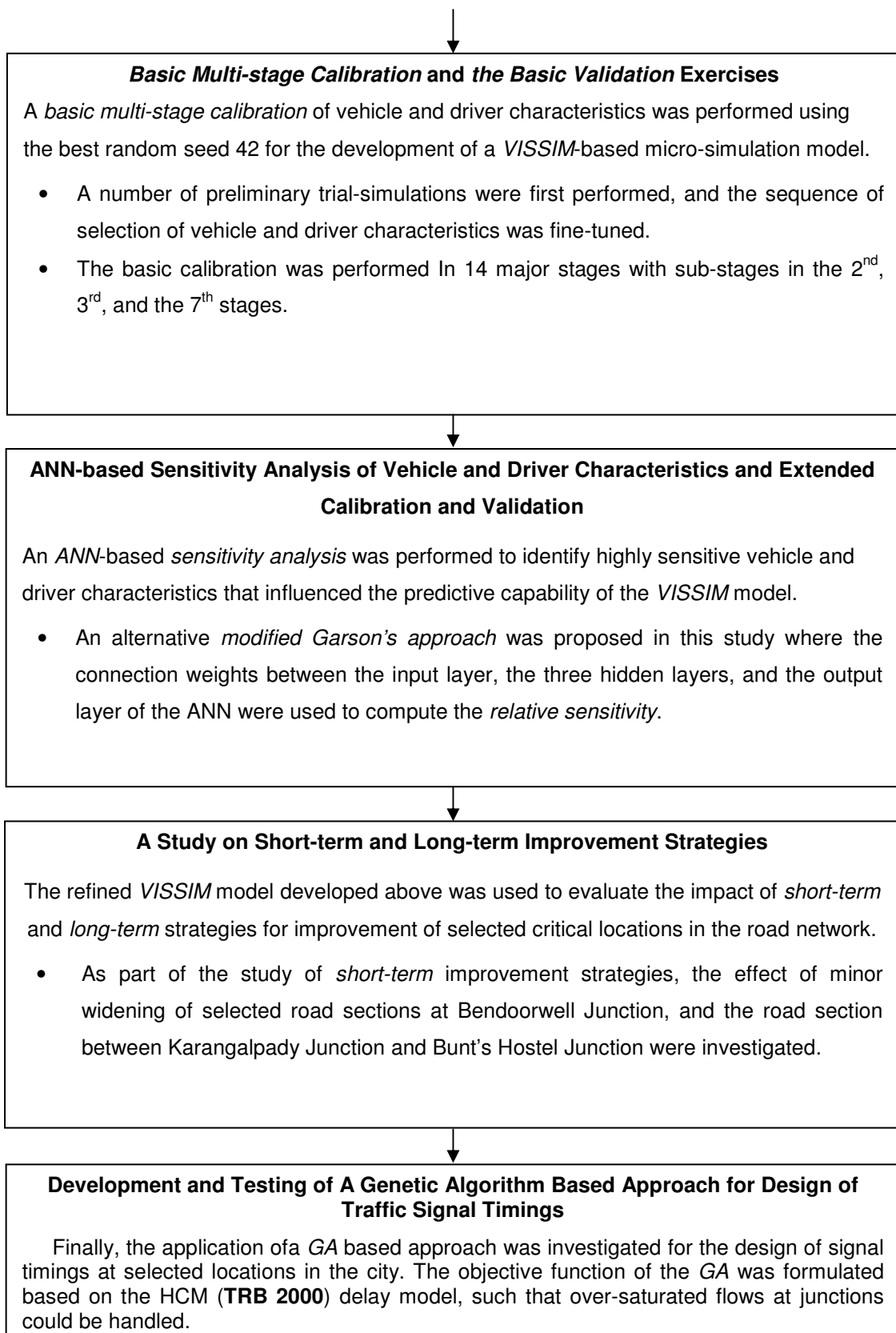


**Fig.4.1 A Schematic Diagram on Various Steps in the Methodology Adopted**

## CHAPTER 5

### DETAILS OF THE STUDY AREA, DATA COLLECTION APPROACH, AND CREATION OF A TEMPLATE TO BE INTERFACED TO *VISSIM*

#### 5.1 INTRODUCTION

The methodology adopted in this study, and the basic aspects related to the development of the *VISSIM* model for simulation were discussed in the previous chapter. The following sections of this chapter provide details on the characteristics of the study area, existing traffic scenario, the identification of important road links and junctions of the city, and the creation of a template to be interfaced to *VISSIM*.

#### 5.2 STUDY AREA CHARACTERISTICS

In order to create a simulation model representing the traffic movements on the road network for Mangalore city, data on classified traffic volume, turning movements at intersections, dimensions of road links, and layout of intersections were required to be used. The details on level of congestion on major road sections, and the bottlenecks at various locations were noted so that future improvements could be made. The following sub-sections provide details on the study area, and data collection.

##### 5.2.1 Details of the Study Area

Mangalore is an upcoming beautiful scenic city with all-round greenery in the southern part of the State of Karnataka, India. It is an emerging city located at 12.87° N latitude and 74.88° E longitude at an altitude of 22 metres (72 ft.) above mean sea level, and is well-connected by air, rail and road. Mangalore City Corporation (MCC) witnessed an increase in population from 1,95,000 in 1971 to 4,88,968 in 2011 (**Census 2011**) presently spread over 60 urban wards covering an area of about 132.45 square km (**Website: MCC-2016**). The road network for the city has a total length of approximately 1170 kilometres (**Website: MCC-2015**) to serve an estimated current population of about 601,173 (**GoK 2013**).

Mangalore was declared as a Municipal Town on 23<sup>rd</sup> May 1866 under the provisions of the Madras Town Improvement Act of 1866. The city was part of the erstwhile Mysore State during 1948-56, and became part of Karnataka State from 1956 onwards. In 1965, it became a Municipal City under the Karnataka Municipal Act 1964 (**Website: MCC-2015**).

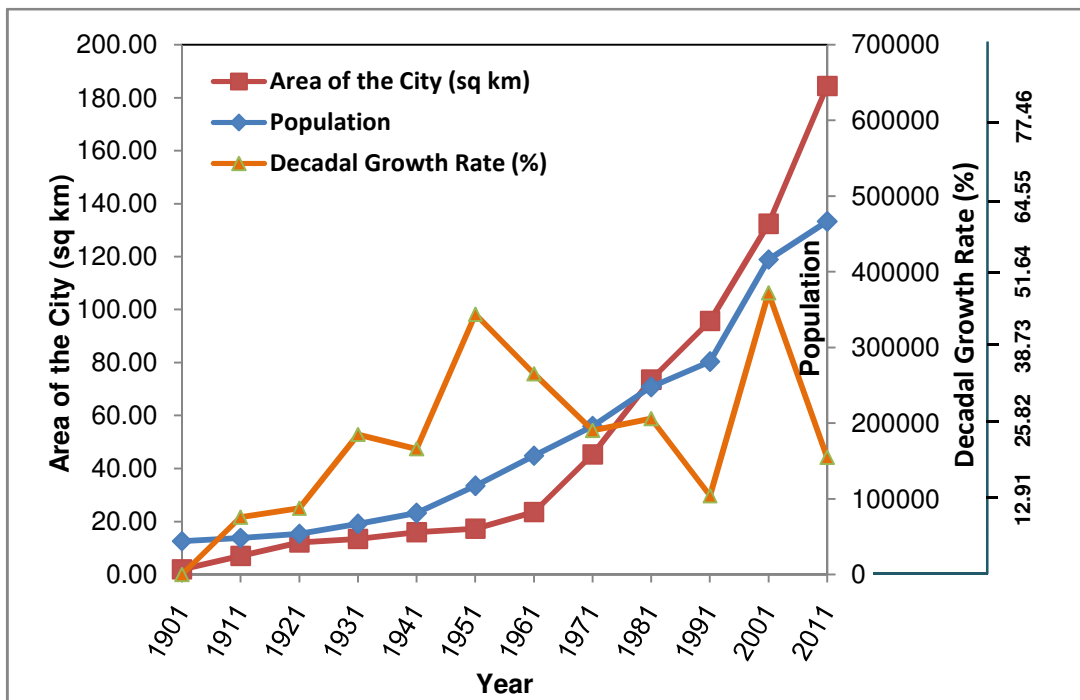


**Fig.5.1a Graphical Representation of Growth of Mangalore City**

The heterogeneous mix of vehicles in the city includes fast-moving cars, light commercial vehicles (LCVs), buses, auto-rickshaws, motorcycles, and other vehicles. The average annual increase in the total vehicles from 2012-2019 was about 9.44% constituting a total of 863,440 vehicles as in March 2019. Presently, the percentage of cars, motorized two-wheelers, auto-rickshaws, LCVs, buses, trucks, and other vehicle types comprise 20%, 66%, 4%, 2%, 1%, 3%, and 4%. (**GoK 2019**). **Table 5.2a** provides details on registered motor-vehicles in Mangalore District. **Fig.5.2a** provides a graphical representation of the same.

**Table 5.2a Details on Vehicle Registrations: 2012-2019**

Vehicle Category	For the Year 2012 to 2019								Average Growth Rate (%)
	2012	2013	2014	2015	2016	2017	2018	2019	
Cars	94381	105825	116459	128331	139391	152272	163941	176211	8.87
Two-wheelers	285725	311556	343608	385772	427796	477515	519885	565728	9.43
Auto-rickshaw	14370	16822	18733	21270	24096	27480	30342	32834	11.60
LCVs	7636	9269	10627	11891	13474	14969	16788	18254	11.57
Buses	9287	10052	10322	10605	10891	11516	11849	11988	4.22
Trucks	21657	22481	23270	24350	25465	26176	26647	27348	3.35
Other Vehicles	26949	27213	27569	27783	29142	29573	30211	31077	1.50
<b>Total Vehicles</b>	<b>460005</b>	<b>503218</b>	<b>550588</b>	<b>610002</b>	<b>670255</b>	<b>739501</b>	<b>799663</b>	<b>863440</b>	<b>8.77</b>

Source: GoK (2019)

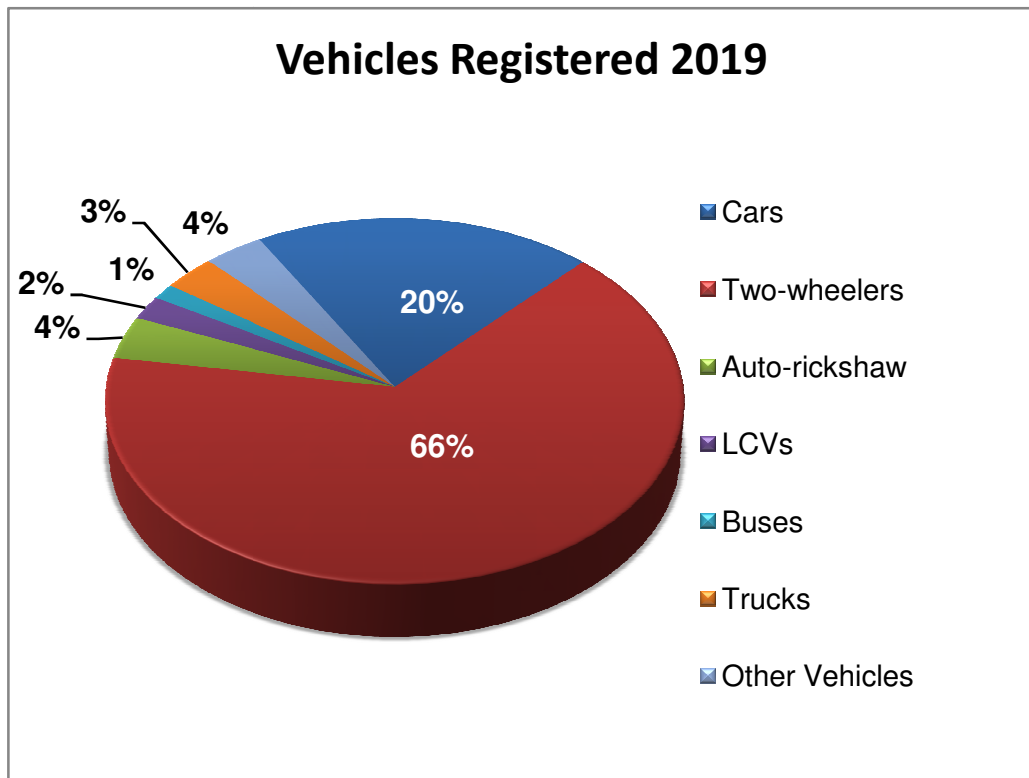


**Fig.5.2a Percentage of Registered Vehicles in 2019**

### **5.2.2 Important Roads and Intersections in the City**

Three National Highways viz, NH-17 coming from Kanyakumari in Tamil Nadu in the south going North along the west coast linking the Mangalore Urban agglomeration to all the coastal towns and finally to the Goa state and Bombay, NH-48 linking Mangalore and Bangalore and NH-13 linking Mangalore and Solapur pass through the city. A domestic airport is located at Bajpe, which is 15 km from the city connecting it to Bangalore and Mumbai. By rail, a broad gauge railway line connects it to Southern parts of India and Konkan railway connects it to Bombay. The horizontal link between Bangalore, Hassan and Mangalore is presently being upgraded and once completed will provide also a good link to the rest of Karnataka. Mangalore also has a Port. The old Mangalore Port at Bunder and the New Port at Panambur are functional with the latter being the only major port of the state of Karnataka. Mangalore city, initially located between Nethravathi river and the Gurupura river, has today grown beyond Gurupur river up to Surathkal in the North.

### **5.2.3 Existing Scenario of Traffic and Transportation in Mangalore**

Until 2007, other than a few major roads, all other roads and streets of the city were very narrow. It was proposed to widen certain important roads in the built-up area under the Comprehensive Traffic and Transport Planning for Mangalore. New roads were proposed to meet the future requirement considering the rapid growth of Traffic volume.

In the previous master plan or C.D.P (Comprehensive Development Plan) approved in 2003, it was proposed to realign and widen the existing congested roads especially in the downtown areas to reduce the difficulties in finding parking spaces. As part of the master plan, a number of drawings were prepared on important junctions of the city by M/s Dalal Consultants, Mangalore (**Dalal Consultant and Engineers Ltd. 2003**). These were widely referred and updated in later stages of this study.



**a) Traffic:**

As in other cities of India, the roads in Mangalore city are characterized by heterogeneous traffic conditions with a mix of fast and slow moving vehicles. There are no animal drawn vehicles, and cycle-rickshaws as the topography is not conducive for the use of such modes. The road traffic consists mainly of cars, light and medium sized vans, light commercial vehicles, jeeps, taxis, scooters and motor cycles, light commercial vehicles, buses, auto-rickshaws, and trucks. Pedestrian traffic is found to be very heavy in the CBD areas of the city due to the intense concentration of commercial activities.

**b) Speed**

Due to the intermix of various slow and fast vehicle types, the journey-speeds on roads are considerably lesser, affecting the capacity of roads adversely. Severe congestion and traffic-problems are observed in the CBD area, especially during the peak hours.

**c) Delays**

The drive on city-roads is characterized by frequent stoppages, acceleration, deceleration, and movement in lower gears resulting in higher operational costs, and wear and tear of vehicles. The conflict, confusion and chaos due to mixed traffic conditions lead to bottlenecks in traffic movement. The road-network has remained almost the same for the past many years although a number of road links have been widened to a reasonable extent. However, the influx of new vehicles on road due to the increase in the population has added to the chaotic situation in the city.

**d) Pedestrian Traffic**

Although pedestrian traffic has increased over the past many years, footpaths of sufficient width are lacking in many parts of the city. Pedestrian movements are comparatively higher in the downtown areas close to Hampankatta Junction, Jyothi Junction, Balmatta Junction, Bunt's Hostel Junction, and PVS Junction. The encroachment of footpaths by shopkeepers and roadside vendors has further worsened the scenario.

## e) Signals

The following Junctions in Mangalore City are signalized:

- a) Bunt's Hostel Junction
- b) Hampankatta Junction
- c) Bendoorwell Junction
- d) Jyothi Junction
- e) PVS Junction
- f) St. Theresa's School Junction
- g) Balmatta Junction
- h) Karavali Junction or Kankanady Bye-pass Road Junction
- i) Lalbagh Junction (Mangalore City Corporation)

However, it is felt that traffic signal timings need to be designed scientifically. The improper design of signal-timings is found to increase the vehicle delay and queue length, thereby considerably affecting the level of service offered by these signals. In order to reduce the cost due to delays, and stoppages, and to increase the journey-speeds, it is better to adopt the use of coordinated signals.

### **5.3 CREATION AND UPDATING OF *AutoCAD* DRAWINGS OF ROADS, JUNCTIONS, AND DEVELOPMENT OF A COMPOSITE HIGH-RESOLUTION BASE MAP**

The present study included 423 links of the road network spanning over 3.08 square km of Mangalore city connecting the major junctions at Hampankatta, Navbharat, PVS, Bunt's Hostel, Jyothi, Bendoorwell, Balmatta, and St. Theresa's School. A few of these junctions are provided by fixed time traffic signals with manual override option to handle peak-hour traffic, while a majority of the junctions are manually controlled.

An *AutoCAD* drawing with details on the road geometrics, the width of road links, and the dimensions of the junctions was prepared based on measurements made at site in March 2015. . Additionally, *AutoCAD* drawings on road junctions in the CBD area prepared by M/s Dalal Consultants, Mangalore (**Dalal Consultant and Engineers Ltd. 2003**) which were submitted to Karnataka Urban Development and Costal Environmental Projects, Govt. of Karnataka as part of Traffic Management

Report for Mangalore Town were updated with the latest dimensions and incorporated in this study.

Subsequently, a digitized high resolution *.jpg* base-map (of 6284 x 6726-pixel size and 3.43MB size) of the city was developed at a scale of 1:5000. This map was created by stitching together 104 high-resolution snapshots obtained from *Google maps* with 10% overlaps using a powerful image processing software such as *Gimp*. **Fig.5.4** provides a detailed view of the high-resolution map thus created.

The *.jpg* image file of the digitized base-map was first imported to *AutoCAD*. Based on the known distances between important far-away junctions as seen on *www.google.map*, the digitized base-map was rescaled, and refitted in *AutoCAD* environment. The updated *AutoCAD* drawing prepared earlier was then overlaid on the digitized base-map, and re-aligned to ensure a perfect match. Minor corrections in the road and junction alignments were made with the *.jpg* base-map in the background. The *.jpg* base-map, along with the re-aligned *AutoCAD* drawing was then saved as a composite *.dwg* file as shown in **Fig.5.5**. This composite image was later used as a template in VISSIM to develop the *links* and *connectors* of the road network.

The composite *.dwg* image file created in the previous step was then imported by VISSIM using the *background* option, and the image was used as a template for drawing the '*Links*' and '*Connectors*' of the road network using the VISSIM network window. The distances between the junctions were re-checked and the background image was further scaled if required. The final image of the road network after superimposing the VISSIM network over the *AutoCAD* drawing, and the high resolution map created in *Gimp*, and after incorporating the *links* and *connectors* is shown in **Fig 5.6**.

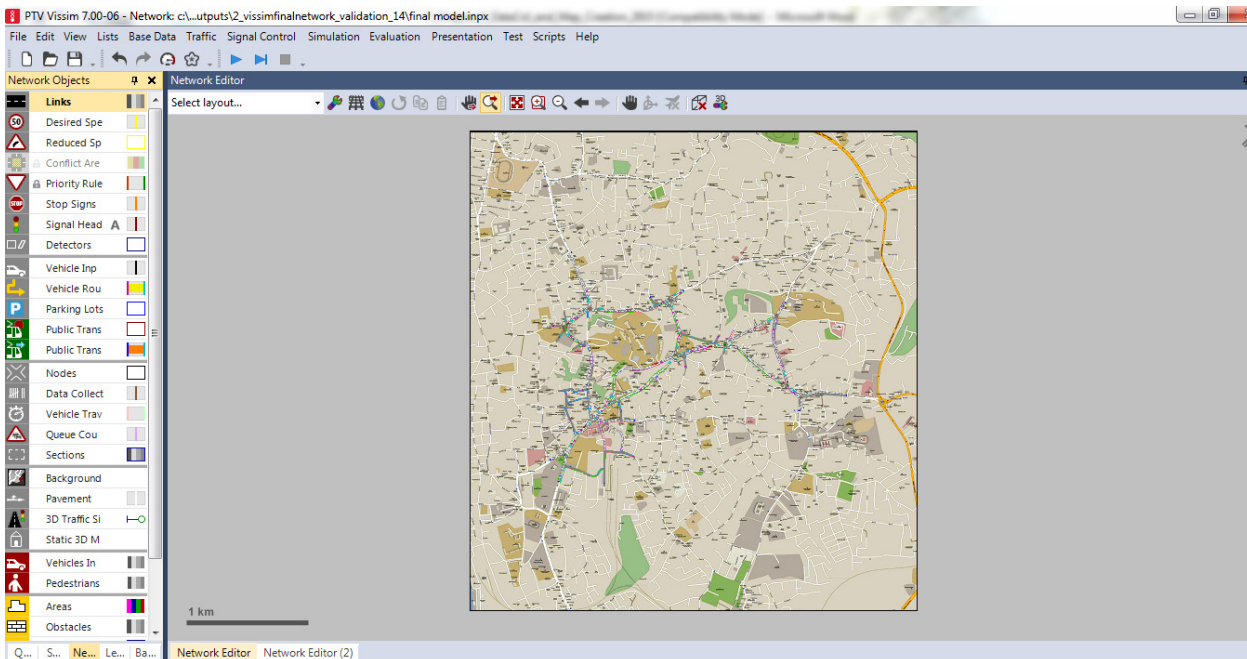


**Fig.5.6 Links and Connectors for the City Road Network Drawn on the Template (comprising AutoCAD Drawing Superimposed on Stitched GIMP Image)**

#### **5.4 TRAFFIC DATA COLLECTION AT SELECTED MID-BLOCKS AND JUNCTIONS**

The traffic circuit that connects the busiest activity centres of Mangalore, such as Hampankatta Junction, Navabharat Junction, PVS Junction, Bunt's Hostel Junction, Jyothi Junction, Balmatta Junction, St. Theresa's School Junction, and Bendoorwell Junction is considered to be the CBD of the city that boasts of the most important shopping centres, malls, banks, cinema theatres, hospitals, education-centres, railway station, bus terminus, and offices located in close proximity to each other. Data on turning movements at the junctions, classified vehicular flows, and existing signal timings were collected in March 2015. Additionally, details on classified volume counts and speeds were obtained for important mid-block sections listed in **Table 5.3a** using video-graphic methods.

Video-graphic data on vehicular movements at eight major traffic junctions of the city, and at 18 important mid-block sections of the road network were recorded for the peak period between 17:00-18:30 hours on Tuesday 10<sup>th</sup> March 2015. Out of 90 minutes data collected for the peak period, a total of 80 minutes data was considered for the development of the VISSIM model. Video-graphic data pertaining to 60-

minutes duration that constitutes 75% of the whole data was used for testing and calibration of the *VISSIM* model, while the remaining 20 minute video-graphic data that constitutes 25% of the whole data was used for validation of the *VISSIM* model.

**Table 5.3a Important Mid-Block Sections Considered for Volume and Speed Studies**

Sl. No.	From	To
1	Jyothi Junction	Hampankatta Junction
2	Hampankatta Junction	Jyothi Junction
3	PVS Junction	Bunts Hostel Junction
4	Bunts Hostel Junction	PVS Junction
5	Navabharat Junction	PVS Junction
6	PVS Junction	Navabharat Junction
7	Hampankatta Junction	Navabharat Junction
8	Navabharat Junction	Hampankatta Junction
9	Jyothi Junction	Bunts Hostel Junction
10	Bunts Hostel Junction	Jyothi Junction
11	Jyothi Junction	Balmatta Junction
12	Balmatta Junction	Jyothi Junction
13	Balmatta Junction	St. Theresa School Junction
14	St. Theresa School Junction	Balmatta Junction
15	Bendoorwell Junction	Balmatta Junction
16	Balmatta Junction	Bendoorwell Junction
17	Bendoorwell Junction	St. Theresa School Junction
18	St. Theresa School Junction	Bendoorwell Junction

The peak period was identified to lie between 17:00 and 19:00 hours based on traffic-flow surveys conducted between 7:00 to 21:00 hours at five critical sections of urban roads of Mangalore city on 3<sup>rd</sup> March 2015. The evening peak was expected due to traffic generated from educational institutions, schools, government and corporate offices, business centers, malls, bus-stations, and the railway stations. Similar findings were made by **Dalal Consultants (2003)**, and **Hemanth (2009)**. Details on traffic-flow volumes observed at important critical mid-block sections of the city are provided in **Table 5.3b**. **Fig.5.7** provides a graphical representation of the total traffic flows observed at the selected critical mid-block sections for each of the two-hour periods surveyed.

A description on some of the most important junctions considered for the study is also provided below.

### ***Hampankatta Junction***

Hampankatta Junction is deemed to be the heart of Mangalore city. It is the main hub of public utilities such as Mangalore Central Railway Station, Service Bus Stand, Central Market, City Central Library, KMC Hospital, St. Aloysius College, and the City Centre Mall. This junction is also considered to be one of the busiest and congested areas that have undergone ad hoc changes at various points in time. But these minor changes, often lead to chaos in other parts of the city.

One of the approaches to this junction leads to the railway Station, Wenlock Hospital and Milagres Church, while the second one leads to the Service Bus Stand. The third leg leads to City Centre Mall and the fourth one leads to St Aloysius Church and Kasturba Medical College, ending up at Jyothi Junction.

### ***Navabharat Junction***

This intersection connects PVS Junction and Hampankatta Junction via City Point Centre, Karnataka Bank, St. Aloysius PU College, and the Old Bus Stand. Bus service through this intersection is found to be lesser when compared to the rest of the intersections under study. One of the main legs leads to PVS Junction, while another leg leads to City Centre back to Hampankatta Junction. Another important leg connects Canara Girls High School, while another connects Anie Besant Theosophical Society. This junction is also known popularly as the City Point Junction.

### ***PVS Junction***

One of the approaches to this T-intersection connects Navabharat Junction while the other connects Bunts Hostel Junction. The third leg leads to Lalbagh, and KSRTC Bus Station, that also leads to Edapally-Panvel highway, NH 17.

### ***Bunt's Hostel Junction***

This too, is a T-junction with one leg leading to Jyothi Junction, another leg leading to PVS Junction, and the third leg leading to Kadri and Nanthoor Junctions. The Shri Ramakrishna Degree College is located close to Bunt's Hostel Junction.

### ***Jyothi Junction***

This intersection connects to Bunts Hostel Junction and Balmatta through two legs. The third and fourth legs are one way roads leading to and from Hampankatta. KMC Hospital, Jyothi Talkies and Vijaya Bank Regional office are some of the main institutions at the intersection.

### ***Balmatta Junction, Bendoorwell Junction and St. Theresa's School Junction***

Traffic entering the downtown area of the city enter through Nanthoor Junction reach Jyothi Junction via Kadri, St. Theresa's School junction, Bendoorwell Junction and Balmatta Junction. Similarly, traffic entering the city from Pumpwell Junction reaches Jyothi Junction via Kankanady Bye-pass Junction, Bendoorwell, and Balmatta Junction. Additionally, traffic from the other parts of the city, such as from Falnir Road, and KMC Attavar also reach Jyothi Junction via Bendoorwell Junction and Balmatta Junction. Due to this reason, Balmatta Junction and Bendoorwell Junction are mostly congested especially during peak periods.

## CHAPTER 6

### RESULTS AND DISCUSSIONS ON TESTING, CALIBRATION AND VALIDATION OF VISSIM MODEL FOR EXISTING SCENARIO

#### 6.1 INTRODUCTION

The initial part of this study dealt with the collection of data related to physical measurements of junction spaces, vehicle-classified turning-movements, creation of a high-resolution map of the city using *Gimp*, creation of an *AutoCAD* drawing representing the layout of the junctions, interfacing of the high resolution map to the *AutoCAD* drawing, and interfacing of the composite *.dwg* file to *VISSIM 7.0* for creation of the *network file*. These were discussed in detail in the previous chapter.

The next part of the study is related to the selection of the random seed that can ensure lesser errors in simulation, the development of model through testing and calibration, and performing validation of the model using a different set of field-data for the city. The initial simulation-trials for identification of the best random seed were performed using default values of vehicle and driver characteristics defined in *VISSIM*. In this exercise, the *GEH statistic* was used as a basis to finalize the best *random seed* for the preliminary calibration of the model based on the traffic flow volumes at 18 mid-block sections.

After identification of the best random seed, the testing and calibration exercise was performed for various combinations of vehicle and driver characteristics using a trial-and-error approach. Here too, the *GEH statistic* was used as a basis to compare the actual and predicted traffic flows across 18 mid-block sections in the city.

In the later stages, it was proposed to perform an ANN-based sensitivity analysis, followed by *short-term and long-term improvements to the existing road network*, in addition to analysing the use of genetic algorithm (GA) based signal timing at selected locations in the city.



## 6.2 RESULTS AND DISCUSSIONS ON TESTING, CALIBRATION, AND *GEH* STATISTICS

The *testing and calibration* procedure was required to be performed in the development stage of the model, to ensure that the output generated conformed to the actual field conditions with a reasonable level of accuracy. 75% of the actual data collected that corresponds to a 60-minute video-graphic data was used for identification of the *best random seed* and for the testing and calibration exercises. The validation exercise was subsequently performed using the remaining 25% of the actual data collected during the peak period.

The detailed flow chart describing the procedure adopted in the calibration process is provided in **Fig.6.1**. The important stages in the testing and calibration procedure adopted are listed below, and are explained in the following sections of this chapter.

- **Providing the *AutoCAD* Drawing, Base Map, and the Input data to *VISSIM***
  - Creation of an *AutoCAD* drawing of the city with details on road-geometrics, and appending of junction details using an updated existing *AutoCAD* drawing.
  - Creation of a high resolution 1:5000 scale Google base-map of the city using *Gimp*.
  - Superimposing the *AutoCAD* drawing on the high resolution map, realigning of the *AutoCAD* drawing, and creation of a composite *.dwg* file.
  - Importing the composite *.dwg* file to *VISSIM* for creating a *Network Map* with *links* and *connectors*.
  - Assigning traffic-volume generation points, at entry points to the city network and assigning turning movements for vehicle classes based on actual data.
  
- **Selection of the Best Random Seed**
  - Assigning default settings for *vehicle characteristics*, and *driving behavior* based on *Wiedemann 74* (**Wiedemann 1974**) driver characteristics for urban traffic with merging. It may be observed that in the case of freeway traffic with straight roads with no merging, *Wiedemann 99* driver characteristics are adopted.
  - Performing a search for the best random seed from 1-50 and comparisons of performances for selected random seeds 25, 28, 42, and 50.

- Identification of the best random seed based on *GEH* statistics by comparing simulated volumes with observed volumes at 18 mid-blocks of the city.
- **Fine-tuning of Vehicle and Driver Characteristics to Match Volume Measurements at 18 Mid-Block Locations as part of the Testing and Calibration Exercise**
  - First Level of Refinement of Characteristics for Calibration using Random Seed 42 (Assigning *minimum lateral clearances*).
  - Second Level of Refinement of Characteristics for Calibration using Random Seed 42 (Assigning acceptable *acceleration* and *deceleration* distributions for vehicle types).
  - Third Level of Refinement of Characteristics for Calibration using Random Seed 42 (Further refinements in *desired* and *maximum accelerations*).
  - Fourth Level of Refinement of Characteristics for Calibration using Random Seed 42 (Assigning *minimum look-ahead distances* for each vehicle type as part of *car following behavior*).
  - Fifth Level of Refinement of Characteristics for Calibration using Random Seed 42 (Further refinements in *maximum accelerations*).
  - *Sixth Level of Refinement of Parameters for Calibration using Random Seed 42* (Further refinements in *desired accelerations*).
  - Seventh Level of Refinement of Characteristics for Calibration using Random Seed 42 (Assigning the *speed distributions* for each vehicle type).
  - Eighth Level of Refinement of Characteristics for Calibration using Random Seed 42 (Assigning *minimum look-back distances* for each vehicle type as part of *car following behavior*).
  - Ninth Level of Refinement of Characteristics for Calibration using Random Seed 42 (Assigning the *average standstill distances* as part of *car following behavior*).
  - Tenth Level of Refinement of Characteristics for Calibration using Random Seed 42 (Refining the values for *additive part of desired safety distances* as part of *car following behavior*).
  - Eleventh Level of Refinement of Characteristics for Calibration using Random Seed 42 (Refining the values for *multiplicative part of desired safety distances* as part of *car following behavior*).
  - Twelfth Level of Refinement of Characteristics for Calibration using Random Seed 42 (Assigning the values for *time-lag between lane/ direction change procedures* as part of *lateral driving behavior*).
  - Thirteenth Level of Refinement of Characteristics for Calibration using Random Seed 42 (Refinement of the *minimum longitudinal speeds* as part of *lateral driving behavior*).

- Final Level of Refinement of Characteristics for Calibration using Random Seed 42 (Refinement of *minimum collision time-gain* as part of *lateral driving behavior* or the minimum value of *minimum collision time-gain* for the next vehicle or signal head, which must be reached so that a change of the lateral position on the lane is worthwhile and will be performed).
- Verification of Speeds at 18 Mid-Block Locations for the Calibration Procedure
  - Study of Mid-Block Speeds for Calibrations as in Section 6.2.1.2 (Default settings)
  - Study of Mid-Block Speeds for Calibrations as in Section 6.2.8: Seventh Level of Refinement (Vehicle and driver characteristics related to desired speed distribution)
  - Study of Mid-Block Speeds for Calibrations as in Section 6.2.15: Final Level of Refinements
- Verification of Turning Movements at Junctions for the Volume-based Calibrated Model as in Section 6.2.16: Final Level of Refinements
- Validation of the Calibrated Model
  - Validation of Vehicular Volumes for Model Calibrated Based on Vehicular Flows as in Section 6.3.1.
  - Validation of Vehicular Speeds for Model Calibrated Based on Vehicular Flows as in Section 6.3.2.
  - Validation of Junction Turning Movements at Major Intersections for Model Calibrated Based on Vehicular Flows as in Section 6.3.3.

### **6.2.1 Interfacing the Composite .dwg File, and Field Data to Create a Network Map in VISSIM, Initial Default Settings, and Selection of the Best Random Seed**

In the preliminary stages of model development, it was required to create an *AutoCAD* drawing of the city with details on road-geometrics. Details of road junctions that had not changed over the years were appended from previously existing *AutoCAD* drawings prepared by **Dalal Consultants and Engineers Ltd. (2007)**. Also, details on the development of a high-resolution .jpg digitized *base-map* of 3.08 sq. km of the city at a scale of 1:5000, was discussed in the previous chapter. It may be observed that the composite .dwg file obtained by superimposing the *AutoCAD* drawing on the digitized base-map, and realigning the *AutoCAD* drawing was used as a template in *VISSIM* to draw the *links* and *connectors* for the network using the *network editor* option.

After representing the road network of the city in *VISSIM* in the form of approximately 423 *links* and *connectors*, 19 traffic generation points were identified. The traffic-volumes generated at these traffic entry points for each vehicle-type were assigned at various locations of the city based on actual data used for calibration. The proportions of turning movements for each vehicle-type at the junctions were then assigned using the *vehicle routing* option.

In the initial part of the calibration procedure, the *vehicle characteristics* such as speed distribution, acceleration and deceleration, and the *driving behaviour characteristics* (with details on vehicle-following, lane-change, lateral-distance, and signal-control) were set to default settings. Initial trial runs were performed in *VISSIM* using random seeds varying from 1-50. Later, the performance of a smaller set of random seeds comprising 42, 25, 28, and 50 that provided better predictions of traffic flows was studied. The observed and simulated traffic volumes were compared for 18 mid-block sections of the city, and the *GEH statistic* was used to evaluate the suitability of the *random seed* adopted for simulation. The best random seed was then selected.

The assigning of driving behaviour characteristics was performed based on *Wiedemann 74* (**Wiedemann 1974**) driver characteristics for urban traffic with merging. Driver characteristics deal with circumstances involving free driving, approaching manoeuvres, car-following, and braking. The default values of vehicle characteristics in *VISSIM* were used in the initial trials.

#### **6.2.1.1 Setting of the Default Values for Vehicle and Driving Characteristics**

The default speed assumed in the initial stages of simulation studies was 50kmph for all vehicle types in the road network. The lateral clearances for standing and driving conditions were set to 1m.

The driving behaviour characteristics for car-following, lane-change, and lateral movements were assumed as suggested by *VISSIM*. The default values assigned for various vehicle and driver characteristics in the initial trial runs are summarized in **Table 6.1**.

### 6.2.1.2 Selection of the best Random Seed using Default Settings

It is possible to perform simulations in VISSIM by assigning a particular random seed. This ensures uniformity in output for a given input data. Simulation runs can be performed using various random seeds. The random seed that ensures a better fit between the observed and the simulated values can be considered as the best random seed.

In the present study, initial trial runs for random numbers from 1 to 50 were performed with default values of vehicle and driver characteristics using the data set apart for calibration. Based on the test runs performed, it was found that the random seeds, 25, 28, 42, and 50 performed better in predicting the traffic flows across 18 mid-block sections. **Fig.6.2a** provides details on the location of the mid-block sections in the city. The *GEH statistic* was used to compare the difference between the observed and the simulated values. The theoretical details on the same were provided in **Chapter 3**.

**Table 6.2a** provides details on computations related to the *GEH* calibration procedure for 18 mid-block locations in the city for simulations performed using random seed 25 where comparisons between the observed and simulated volumes are made. Similarly, **Table 6.2b**, **Table 6.2c**, and **Table 6.2d** provide details on computations for simulations performed using random seeds 28, 42, and 50. **Fig.6.2b** provides a comparison between the observed and simulated traffic volumes at the 18 mid-block sections, for studies performed using random seeds 25, 28, 42, and 50.

**Table 6.2a *GEH* Calibration for Volumes at 18 Mid-Blocks for Default Settings: Random Seed 25**

Direction		Simulated	Observed	Observed-Simulated	Error (%)	Abs. Error (%)	GEH STATISTIC
From	To						
Jyothi	Hampankatta	1680	2580	900	34.9	34.9	19.50
Hampankatta	Jyothi	1600	2320	720	31.0	31.0	16.26
Jyothi	Balmatta	1200	1830	630	34.4	34.4	16.19
Balmatta	Jyothi	1565	2585	1020	39.5	39.5	22.39
Balmatta	St. Theresa	460	710	250	35.2	35.2	10.34
St. Theresa	Balmatta	640	805	165	20.5	20.5	6.14
Bendoorwell	Balmatta	1050	1455	405	27.8	27.8	11.44
Balmatta	Bendoorwell	1040	1680	640	38.1	38.1	17.35
Bendoorwell	St. Theresa	935	1205	270	22.4	22.4	8.25
St. Theresa	Bendoorwell	755	1100	345	31.4	31.4	11.33
<b>Average</b>					<b>33.4%</b>	<b>33.4%</b>	<b>15.69</b>

**Table 6.2b *GEH* Calibration for Volumes at 18 Mid-Blocks for Default Settings: Random Seed 28**

Direction		Simulated	Observed	Observed-Simulated	Error (%)	Abs. Error (%)	<i>GEH</i> STATISTIC
From	To						
Jyothi	Hampankatta	1735	2580	845	32.8	32.8	18.19
Hampankatta	Jyothi	1635	2320	685	29.5	29.5	15.40
PVS	Bunts	895	1465	570	38.9	38.9	16.59
Bunts	PVS	1055	1505	450	29.9	29.9	12.58
Navabharat	PVS	1460	2510	1050	41.8	41.8	23.57
PVS	Navabharat	1745	2370	625	26.4	26.4	13.78
Hampankatta	Navabharat	1070	2225	1155	51.9	51.9	28.46
Navabharat	Hampankatta	1355	2100	745	35.5	35.5	17.92
Jyothi	Bunts	1225	2020	795	39.4	39.4	19.74
Bunts	Jyothi	1420	1970	550	27.9	27.9	13.36
Jyothi	Balmatta	1150	1830	680	37.2	37.2	17.62
Balmatta	Jyothi	1740	2585	845	32.7	32.7	18.17
St. Theresa	Bendoorwell	690	1100	410	37.3	37.3	13.70
<b>Average</b>					<b>34.3%</b>	<b>34.3%</b>	<b>16.10</b>

**Table 6.2c *GEH* Calibration for Volumes at 18 Mid-Blocks for Default Settings: Random Seed 42**

Direction		Simulated	Observed	Observed-Simulated	Error (%)	Abs. Error (%)	<i>GEH</i> STATISTIC
From	To						
Jyothi	Hampankatta	1715	2580	865	33.5	33.5	18.67
Navabharat	Hampankatta	1320	2100	780	37.1	37.1	18.86
Jyothi	Bunts	1290	2020	730	36.1	36.1	17.94
Bunts	Jyothi	1480	1970	490	24.9	24.9	11.80
Jyothi	Balmatta	1080	1830	750	41.0	41.0	19.66
Balmatta	Jyothi	1610	2585	975	37.7	37.7	21.29
Balmatta	St. Theresa	535	710	175	24.6	24.6	7.01
St. Theresa	Balmatta	665	805	140	17.4	17.4	5.16
Bendoorwell	Balmatta	990	1455	465	32.0	32.0	13.30
Balmatta	Bendoorwell	1000	1680	680	40.5	40.5	18.58
Bendoorwell	St. Theresa	915	1205	290	24.1	24.1	8.91
St. Theresa	Bendoorwell	740	1100	360	32.7	32.7	11.87
<b>Average</b>					<b>33.4%</b>	<b>33.4%</b>	<b>15.79</b>

**Table 6.2d *GEH* Calibration for Volumes at 18 Mid-Blocks for Default Settings: Random Seed 50**

Direction		Simulated	Observed	Observed-Simulated	Error (%)	Abs. Error (%)	<i>GEH</i> STATISTIC
From	To						
Jyothi	Hampankatta	1680	2580	900	34.	34.9	19.50
Hampankatta	Navabharat	975	2225	1250	56.2	56.2	31.25
Navabharat	Hampankatta	1305	2100	795	37.9	37.9	19.27
Jyothi	Bunts	1305	2020	715	35.4	35.4	17.54
Bunts	Jyothi	1415	1970	555	28.2	28.2	13.49
Jyothi	Balmatta	1145	1830	685	37.4	37.4	17.76
St. Theresa	Bendoorwell	610	1100	490	44.5	44.5	16.76
<b>Average</b>					<b>35.1%</b>	<b>35.1%</b>	<b>16.56</b>

## 6.2.2 First Level of Refinement of Vehicle and Driver Characteristics for Calibrations Using Random Seed 42

As part of the first level of refinements, the values for *minimum lateral clearances* for standing and moving vehicles were assigned, and the calibration was performed.

### *Setting of lateral clearances*

The values for lateral clearances adopted in this study for each vehicle-type with respect to the other vehicle-types are shown in **Table 6.3a**. These values were arrived at based on field observations and also based on values adapted and modified from **Arasan and Krishnamurthy (2008)** provided in **Table 6.3b** for the arterial roads of Chennai city. The lateral clearances at 0 kmph and for speed ranges between 50-60 kmph were observed for Mangalore city, and the values were found to tally approximately with observations made by **Arasan and Krishnamurthy (2008)**.

**Table 6.3b Maximum and Minimum Lateral Clearances: Arasan and Krishnamurthy (2008)**

Vehicle Type	Lateral Clearance Share (m)	
	At zero speed (Standing Vehicle)	At a speed of 60 km/h (Moving Vehicle)
Buses	0.3	0.6
Trucks	0.3	0.6
LCV	0.3	0.5
Cars	0.3	0.5
Motorized Three-Wheelers	0.2	0.4
Motorized Two-Wheelers	0.1	0.3
Bicycles	0.1	0.3*
Tricycles	0.1	0.3*

\* Maximum speed of these vehicles is assumed as 20 km/h

Source: Arasan and Krishnamurthy (2008)

### *Results of micro-simulations in VISSIM*

**Table 6.3c** provides details on lateral clearances for standing and moving vehicles as adopted by **Manjunatha et al. (2013)** for simulation studies performed on signalized intersections in Mumbai, while **Table 6.3d** gives details on the same for studies performed by **Bains et al. (2013)** on expressways connecting Mumbai and Pune.

In the study of literature related to calibration using *VISSIM*, it is observed that some studies consider the average of the predictions made based on a set of random seeds. Studies made by **Gomes, et al. (2004)**, and **Asman et al. (2019)** belong to this category. However, studies by **Halcrow (2013)**, and **Karakaikes et al. (2017)**, do not recommend taking of average of the predictions made based on calibrations using various suitable random seeds. This ensured that the variations in traffic flows reported depended on changes in vehicle and driver characteristics, and were not masked by variations due to seed selection. **VDOT (2020)** also advocates the use of a consistent set of random seeds identified based on default values of vehicle and driver characteristics.

In the present study too, simulations were performed using the best random seed 42, after assigning the above mentioned values to *lateral clearances* (standing and driving) for various vehicle-types. **Table 6.4** provides details on computations related to comparisons between the observed and simulated traffic volumes for 18 mid-block locations in the city.

However, it may be observed that the assigned values of lateral-clearances are closer to the observed vehicular flows when compared to the default values of 1.0 m suggested by *VISSIM*. The result indicated that there were other characteristics that needed to be fine-tuned.

**Table 6.4 Comparison of Actual and Simulated Traffic Volumes at 18 Mid-Block Locations for First Level Refinements: Random Seed 42**

Direction		Simulated	Observed	Observed-Simulated	Error (%)	Abs. Error (%)	GEH STATISTIC
From	To						
Jyothi	Hampankatta	1715	2580	865	33.5	33.5	18.67
Hampankatta	Jyothi	1700	2320	620	26.7	26.7	13.83
PVS	Bunts	890	1465	575	39.2	39.2	16.76
Bunts	PVS	1025	1505	480	31.9	31.9	13.50
Navabharat	PVS	1345	2510	1165	46.4	46.4	26.54
St. Theresa	Balmatta	665	805	140	17.4	17.4	5.16
Bendoorwell	Balmatta	990	1455	465	32.0	32.0	13.30
Balmatta	Bendoorwell	1000	1680	680	40.5	40.5	18.58
Bendoorwell	St. Theresa	915	1205	290	24.1	24.1	8.91
St. Theresa	Bendoorwell	740	1100	360	32.7	32.7	11.87
<b>Average</b>					<b>33.4%</b>	<b>33.4%</b>	<b>15.79</b>



### 6.2.3 Second Level of Refinement of Vehicle and Driver Characteristics for Calibrations Using Random Seed 42

In the first level of calibration performed above, all vehicle types including Indian vehicles such as auto-rickshaws and LCVs that constitute approximately 17% and 2.2% of the total vehicles, were assigned with default values of acceleration and deceleration. As part of the second level of calibrations, values for the *desired acceleration*, *maximum acceleration*, and *desired decelerations* for each vehicle type were planned to be further fine-tuned.

#### *Setting of distributions for acceleration*

The values for the *desired acceleration*, and the *maximum acceleration* were assigned in this level of calibration based on a trial and error approach as in **Table 6.5a**, and **Table 6.5b** and also based on observations made by **Arasan and Krishnamurthy (2008)** as given in **Table 6.5c-1**. Additionally, **Table 6.5c-2** provides details on the maximum acceleration rates as specified by various vehicle manufacturers in India.

**Table 6.5c-2 Acceleration Rates for Various Vehicle Types as Specified by Vehicle Manufacturers**

Vehicle Name	Max. Acceleration	Max. Acceleration (m/s <sup>2</sup> )
Bajaj Discover	0-60 kmph in 5.94 sec	2.8
Hero CD-Dawn	0-60 kmph in 5.0 sec	3.3
Hero CD-Deluxe	0-60 kmph in 5.0 sec	3.3
Hero Splendor NXG	0-60 kmph in 8.7 sec	1.9
Bajaj Pulsar 135 LS	0-60 kmph in 5.1 sec	3.3
Hero CBZ Xtream	0-60 kmph in 5.0 sec	3.3
Volkswagen Polo 1.0 TSI	0-100 in 9.97 sec	2.8
Skoda Rapid 1.0 TSI	0-100 in 10.09 sec	2.8
Volkswagen Vento 1.0 TSI	0-100 in 10.42 sec	2.7
BMW 6 Series GT 2.0 Petrol AT	0-100 in 6.53 sec	4.3
Jaguar XJ50 3.0 Diesel AT	0-100 in 6.64 sec	4.2
Audi A6 2.0 Petrol AT	0-100 in 7.04 sec	3.9
Volkswagen Passat 2.0 Diesel AT	0-100 in 8.65 sec	3.2
Kia Seltos 1.4 Turbo Petrol MT	0-100 in 9.36 sec	3.0
<i>Sources: Website: BikeDekho; Website: Zigwheels; Website: Autocar India</i>		

### *Setting of distributions for deceleration*

Considering the turning movements at intersections in the city, a design speed of 30-40 kmph was assumed which tallied with the design speeds for rotaries according to IRC 65 (IRC 1976). Similarly, a stopping distance of 30-40m was assumed based on IRC 86 (IRC 1983). A stopping distance of around 60m was assumed for approach speeds of 60kmph. The corresponding *desired deceleration* rates for various vehicle-types were computed as in **Table 6.5d**.

### *Results of micro-simulations in VISSIM*

Simulations were performed after assigning the above mentioned values to the *desired acceleration* and the *deceleration distributions* for various vehicle-types. **Table 6.6** provides details on computations related to comparisons between the observed and simulated traffic volumes. In the present simulation run, it can be seen that the *mean absolute error (MAE)* between the observed and simulated volumes remained almost the same at around 33.4%, and the *GEH statistic* also remained unchanged at around 15.79.

The default values suggested by VISSIM for accelerations at 30kmph for light vehicles (such as cars, two-wheelers, auto-rickshaws and LCVs) are  $2.5\text{m/s}^2$ , while for heavier vehicles (such as for buses and trucks), a value of  $1.2\text{m/s}^2$  was suggested. These default values were found to be highly generalized and not vehicle-specific. Similarly, the default value suggested by VISSIM for decelerations at 30kmph for light vehicles was  $-2.8\text{m/s}^2$  and for heavier vehicles was  $-0.8\text{m/s}^2$ . Although the refined values suggested in this level of calibration were more realistic, the changes in values did not seem to affect the accuracy significantly.

**Table 6.6 Comparison of Actual and Simulated Traffic Volumes at 18 Mid-Block Locations for Second Level Refinements: Random Seed 42**

Direction		Simulated	Observed	Observed-Simulated	Error (%)	Abs. Error (%)	GEH STATISTIC
From	To						
Navabharat	PVS	1345	2510	1165	46.4	46.4	26.54
PVS	Navabharat	1710	2370	660	27.8	27.8	14.61
Bendoorwell	Balmatta	990	1455	465	32.0	32.0	13.30
Balmatta	Bendoorwell	1000	1680	680	40.5	40.5	18.58
Bendoorwell	St. Theresa	915	1205	290	24.1	24.1	8.91
St. Theresa	Bendoorwell	740	1100	360	32.7	32.7	11.87
<b>Average</b>					<b>33.4%</b>	<b>33.4%</b>	<b>15.79</b>

#### **6.2.4 Third Level of Refinement of Vehicle and Driver Characteristics for Calibration Using Random Seed 42**

Since the changes to the *desired* and *maximum acceleration* distributions performed in the second level of calibrations did not improve upon the predictions, it was proposed to assign the same values for the *desired accelerations* and the *maximum accelerations* for various vehicle-types.

##### ***Refining of distributions for desired acceleration***

In the third level of calibration, the values for the distributions for the *desired accelerations* and the maximum accelerations were kept the same for various vehicle-types and refined as shown in **Table 6.7a** using a trial and error approach.

##### ***Results of micro-simulations in VISSIM***

Simulations were performed after assigning the above mentioned values to the *desired* and *maximum acceleration* distributions for various vehicle-types. **Table 6.8** provides details on computations related to comparisons between the observed and simulated traffic volumes for 18 mid-block locations in the city.

#### **6.2.5 Fourth Level of Refinement of Vehicle and Driver Characteristics for Calibration Using Random Seed 42**

In this step, the driving behavior characteristics such as the *minimum look-ahead distance* considered under *car following situations* were modified. **Siddharth and Ramadurai (2013)** suggested a range of 10-30 m for both *minimum look-ahead distance* and *minimum look back distance*. Based on a trial and error approach, the refined values for driving behavior characteristic as suggested in **Table 6.9** were arrived at in this study.

##### ***Results of micro-simulations in VISSIM***

The results of the simulation performed after fine-tuning the *minimum look-ahead distance* are given in **Table 6.10**.

Here, it can be seen that the *mean absolute error (MAE)* reduced from 32.9% to 29.5%, and that the *GEH* statistic reduced from 15.52 to 13.74 indicating that the assigned values resulted in lesser prediction errors. This trial also indicated that the *minimum look-ahead distances* are moderately sensitive in influencing the accuracy of prediction of the simulation model.

### 6.2.6 Fifth Level of Refinement of Vehicle and Driver Characteristics for Calibration Using Random Seed 42

In the fifth calibration level, it was proposed to increase the assigned values for *maximum accelerations* by approximately 10% based on a trial and error approach as shown in **Table 6.11** when compared to the values assigned at the third level of simulation.

#### *Results of micro-simulations in VISSIM*

The results for the present simulation run are given in the **Table 6.12**. Here, it can be seen that the *mean absolute error (MAE)* reduced from 29.5% to 27.5%, and the *GEH* statistic reduced from 13.74 to 13.01 indicating that the assigned values resulted in improved model predictions. In this level of calibration, the *maximum accelerations* are found to have a less moderate sensitivity in influencing the accuracy of prediction of the simulation model.

**Table 6.11 Maximum Acceleration Rates Assigned for Different Vehicle Types**

Maximum Accelerations (m/s <sup>2</sup> )			
Vehicle Type	0 km/h	30 Km/h	60 Km/h
Car	3.2	2.5	1.9
Auto	1.6	1.2	0.6
Bike	3.2	2.2	1.8
LCV	1.6	1.1	0.9
Buses	1.3	1.3	0.7
Trucks	1.3	1.3	0.7

**Table 6.12 Comparison of Actual and Simulated Traffic Volumes at 18 Mid-Block Locations for Fifth Level Refinements: Random Seed 42**

Direction		Simulated	Observed	Observed-Simulated	Error (%)	Abs. Error (%)	GEH STATISTIC
From	To						
Jyothi	Hampankatta	1725	2580	855	33.1	33.1	18.43
Hampankatta	Jyothi	1750	2320	570	24.6	24.6	12.64
PVS	Bunts	870	1465	595	40.6	40.6	17.41

Bunts	PVS	1060	1505	445	29.6	29.6	12.43
Navabharat	PVS	1750	2510	760	30.3	30.3	16.47
PVS	Navabharat	1770	2370	600	25.3	25.3	13.19
Hampankatta	Navabharat	1330	2225	895	40.2	40.2	21.23
Navabharat	Hampankatta	1435	2100	665	31.7	31.7	15.82
Jyothi	Bunts	1310	2020	710	35.1	35.1	17.40
Bunts	Jyothi	1720	1970	250	12.7	12.7	5.82
Jyothi	Balmatta	1130	1830	700	38.3	38.3	18.20
<b>Average</b>					<b>27.5%</b>	<b>27.5%</b>	<b>13.01</b>

### 6.2.7 Sixth Level of Refinement of Vehicle and Driver Characteristics for Calibration Using Random Seed 42

Compared to the previous step, in this set of trials, the values for the *desired accelerations* were further increased by approximately 10% based on a trial and error approach as shown in **Table 6.13**.

#### *Results of micro-simulations in VISSIM*

The results of the simulation run performed with the above settings are shown in **Table 6.14**. Here, it can be seen that the *mean absolute error (MAE)* remained almost at around 27.2%, and the *GEH statistic* slightly reduced from 13.01 to 12.60 indicating that the assigned values resulted in a less moderate improvement in model predictions. The results based on refinements on the *desired accelerations* and *maximum accelerations* performed at the second, third, fifth, and sixth calibration levels indicate that the *desired accelerations* and also the *maximum accelerations* are less moderately sensitive in influencing the accuracy of prediction of the simulation model.

**Table 6.14 Comparison of Actual and Simulated Traffic Volumes at 18 Mid-Block Locations for Sixth Level Refinements: Random Seed 42**

Direction		Simulated	Observed	Observed-Simulated	Error (%)	Abs. Error (%)	GEH STATISTIC
From	To						
Jyothi	Hampankatta	1765	2580	815	31.6	31.6	17.49
Hampankatta	Jyothi	1770	2320	550	23.7	23.7	12.16
PVS	Bunts	1020	1465	445	30.4	30.4	12.62
Bunts	PVS	1040	1505	465	30.9	30.9	13.04
Navabharat	PVS	1780	2510	730	29.1	29.1	15.76
PVS	Navabharat	1855	2370	515	21.7	21.7	11.20
Balmatta	Bendoorwell	1115	1680	565	33.6	33.6	15.11
Bendoorwell	St. Theresa	935	1205	270	22.4	22.4	8.25
St. Theresa	Bendoorwell	850	1100	250	22.7	22.7	8.01
<b>Average</b>					<b>27.2%</b>	<b>27.2%</b>	<b>12.60</b>

### 6.2.8 Seventh Level of Refinement of Vehicle and Driver Characteristics for Calibration Using Random Seed 42

At this level of calibration, refinements were made to the *desired speed distributions* for various vehicle-types.

**Table 6.16 Comparison of Actual and Simulated Traffic Volumes at 18 Mid-Block Locations for Seventh Level Refinements: Random Seed 42**

Direction		Simulated	Observed	Observed-Simulated	Error (%)	Abs. Error (%)	GEH STATISTIC
From	To						
Jyothi	Hampankatta	1900	2580	680	26.4	26.4	14.37
Hampankatta	Jyothi	1845	2320	475	20.5	20.5	10.41
PVS	Bunts	1000	1465	465	31.7	31.7	13.25
Bunts	PVS	1065	1505	440	29.2	29.2	12.27
Navabharat	PVS	1710	2510	800	31.9	31.9	17.42
PVS	Navabharat	1875	2370	495	20.9	20.9	10.74
Hampankatta	Navabharat	1370	2225	855	38.4	38.4	20.17
Navabharat	Hampankatta	1520	2100	580	27.6	27.6	13.63
Balmatta	Bendoorwell	1160	1680	520	31.0	31.0	13.80
Bendoorwell	St. Theresa	1000	1205	205	17.0	17.0	6.17
St. Theresa	Bendoorwell	900	1100	200	18.2	18.2	6.32
<b>Average</b>					<b>24.5%</b>	<b>24.5%</b>	<b>11.46</b>

#### *Setting of desired speed distributions*

According to IRC 86 (IRC, 1983), the design speeds specified by for urban arterial and sub-arterial roads are 80kmph and 60kmph respectively. In this study, the maximum speed for urban roads is set at 70kmph for cars and around 60kmph for other vehicles. The *speed distributions* adopted in this part of simulation trials were derived as shown in the **Table 6.15a** mainly based on a trial and error approach and also based on speeds specified by Arasan and Krishnamurthy (2008) as shown in the **Table 6.15b**.

#### *Results of micro-simulations in VISSIM*

Further simulations were performed after assigning the *desired speed distributions* for various vehicle types. **Table 6.16** provides details on computations related to the calibration procedure for 18 mid-block locations in the city where comparisons between the observed and simulated volumes are made. Here, it can be seen that in the present simulation, the *mean absolute error (MAE)* reduced from 27.2% to 24.5%, and the *GEH* statistic showed a reduction from 12.60 to 11.46, signifying a moderate improvement in prediction of traffic volumes at the 18 mid-block

sections. This indicates that the *desired speed distributions* are moderately sensitive in influencing the accuracy of prediction of the simulation model.

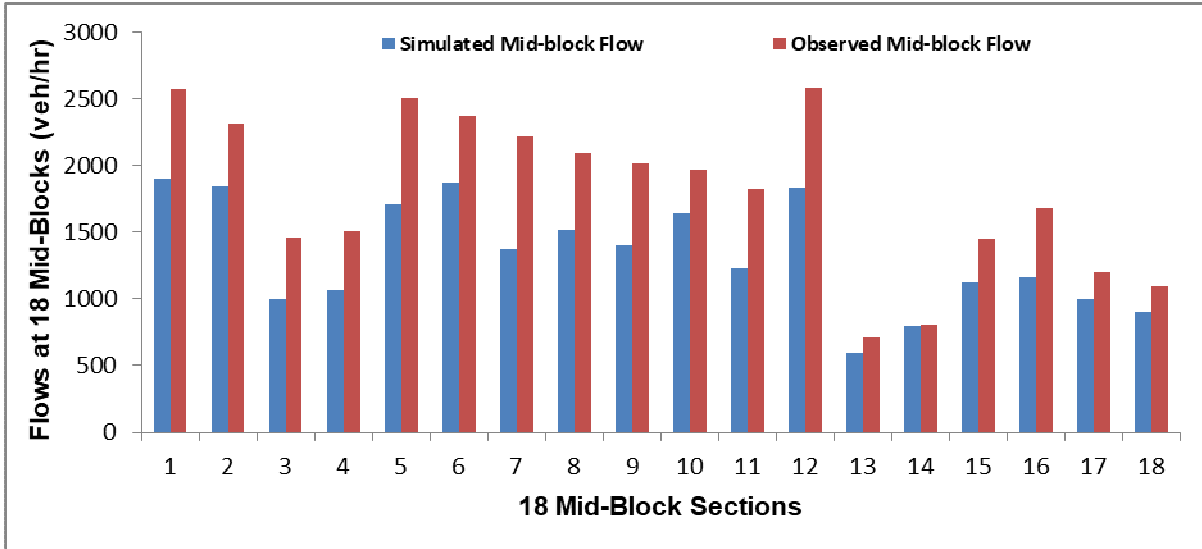


**Fig.6.3 Comparison of Observed and Simulated Flows at 18 Mid-block Locations for the Seventh level of Refinement Using Random Seed 42**

In the above step, it was observed that further changes to vehicle characteristics such as accelerations, decelerations, and speed distributions did not result in improving the accuracy of prediction model, as the *GEH* statistic was found to hover close to around 11.46.

### 6.2.9 Eighth Level of Refinement of Vehicle and Driver Characteristics for Calibration Using Random Seed 42

In this step, the driving behavior characteristics such as the *minimum look-back distances* considered under *car following situations* were modified. **Siddharth and Ramadurai (2013)** suggested a range of 10-30 m for *minimum look-back distances*. Based on a trial and error approach, the refined values for driving behavior characteristic as suggested in **Table 6.17a** were arrived at in this study.

#### ***Results of micro-simulations in VISSIM***

The results of the micro-simulation after fine-tuning the above mentioned characteristics are given in **Table 6.17b**. In the present simulation, the *mean absolute error (MAE)* reduced from 24.5% to 22.4%, and the *GEH* statistic reduced from 11.46

to 10.40 indicating that the *minimum look back distance* is moderately sensitive in influencing the accuracy of prediction of the simulation model.

**Table 6.17b Comparison of Actual and Simulated Traffic Volumes at 18 Mid-Block Locations for Eighth Level Refinements: Random Seed 42**

Direction		Simulated	Observed	Observed-Simulated	Error (%)	Abs. Error (%)	GEH STATISTIC
From	To						
Jyothi	Hampankatta	1930	2580	650	25.2	25.2	13.69
Hampankatta	Jyothi	1785	2320	535	23.1	23.1	11.81
PVS	Bunts	1110	1465	355	24.2	24.2	9.89
Bunts	PVS	1075	1505	430	28.6	28.6	11.97
Navabharat	PVS	1900	2510	610	24.3	24.3	12.99
PVS	Navabharat	1860	2370	510	21.5	21.5	11.09
Hampankatta	Navabharat	1505	2225	720	32.4	32.4	16.67
Navabharat	Hampankatta	1455	2100	645	30.7	30.7	15.30
Jyothi	Bunts	1415	2020	605	30.0	30.0	14.60
Bunts	Jyothi	1790	1970	180	9.1	9.1	4.15
Jyothi	Balmatta	1245	1830	585	32.0	32.0	14.92
Balmatta	Jyothi	1890	2585	695	26.9	26.9	14.69
<b>Average</b>					<b>22.4%</b>	<b>22.4%</b>	<b>10.40</b>

#### 6.2.10 Ninth Level of Refinement of Vehicle and Driver Characteristics for Calibration Using Random Seed 42

In this step, the *driving behavior characteristics* such as the *average standstill distances* considered under *car following* situations were modified. **Siddharth and Ramadurai (2013)** suggested a calibrated value of 1m for the same. Based on a trial and error approach, the refined values for driving behavior characteristic as suggested in **Table 6.18a** were arrived at in the next step of simulation.

**Table 6.18a Driving Behavior Characteristic (Car Following) Assigned**

Driving Behavior Characteristic	Modified value
Average standstill distance	1m

#### *Results of micro-simulations in VISSIM*

The results of the micro-simulation exercise after fine-tuning the above mentioned characteristics are given in **Table 6.18b**. In the current simulation run, the absolute errors reduced from 22.4% to 17.9%, and the *GEH* statistic reduced significantly from 10.4 to 7.84, indicating that the *average standstill distance* is highly sensitive in influencing the accuracy of prediction of the simulation model.



**Table 6.18b Comparison of Actual and Simulated Traffic Volumes at 18 Mid-Block Locations for Ninth Level Refinements: Random Seed 42**

Direction		Simulated	Observed	Observed-Simulated	Error (%)	Abs. Error (%)	GEH STATISTIC
From	To						
Jyothi	Hampankatta	2224	2580	356	13.8	13.8	7.26
Hampankatta	Jyothi	2033	2320	287	12.4	12.4	6.15
Bunts	Jyothi	1706	1970	264	13.4	13.4	6.16
Jyothi	Balmatta	1375	1830	455	24.9	24.9	11.37
Balmatta	Jyothi	2087	2585	498	19.3	19.3	10.30
Balmatta	St. Theresa	564	710	146	20.6	20.6	5.78
St. Theresa	Balmatta	697	805	108	13.4	13.4	3.94
Bendoorwell	Balmatta	1156	1455	299	20.5	20.5	8.28
Balmatta	Bendoorwell	1276	1680	404	24.0	24.0	10.51
Bendoorwell	St. Theresa	975	1205	230	19.1	19.1	6.97
St. Theresa	Bendoorwell	991	1100	109	9.9	9.9	3.37
				<b>Average</b>	<b>17.9%</b>	<b>17.9%</b>	<b>7.84</b>

**6.2.11 Tenth Level of Refinement of Vehicle and Driver Characteristics for Calibration Using Random Seed 42**

In this step, the driving behavior characteristics such as the *additive part of safety distances* considered under *car following situations* was modified. Based on a trial and error approach, the refined values for driving behavior characteristic as suggested in **Table 6.19a** were arrived at in the next step of simulation.

**Table 6.19a Driving Behavior Characteristic (Car Following) Assigned**

Driving Behavior Characteristic	Modified value
Additive part of safety distances	0.40m

**Results of micro-simulations in VISSIM**

The results of the micro-simulation approach after fine-tuning the above mentioned characteristic are given in **Table 6.19b**.

**Table 6.19b Comparison of Actual and Simulated Traffic Volumes at 18 Mid-Block Locations for Tenth Level Refinements: Random Seed 42**

Direction		Simulated	Observed	Observed-Simulated	Error (%)	Abs. Error (%)	GEH STATISTIC
From	To						
Jyothi	Hampankatta	2354	2580	226	8.8	8.8	4.55
Hampankatta	Jyothi	2043	2320	277	11.9	11.9	5.93
PVS	Bunts	1166	1465	299	20.4	20.4	8.24
Bunts	PVS	1330	1505	175	11.6	11.6	4.65
Navabharat	PVS	2131	2510	379	15.1	15.1	7.87
PVS	Navabharat	1997	2370	373	15.7	15.7	7.98
Hampankatta	Navabharat	1965	2225	260	11.7	11.7	5.68
Navabharat	Hampankatta	1585	2100	515	24.5	24.5	12.00

Jyothi	Bunts	1738	2020	282	14.0	14.0	6.51
Bunts	Jyothi	1832	1970	138	7.0	7.0	3.17
Jyothi	Balmatta	1418	1830	412	22.5	22.5	10.22
				<b>Average</b>	<b>13.6%</b>	<b>13.6%</b>	<b>5.98</b>

### 6.2.12 Eleventh Level of Refinement of Vehicle and Driver Characteristics for Calibration Using Random Seed 42

In this step, the driving behavior characteristics such as the *multiplicative part of safety distances* considered under *car following situations* was modified. Based on a trial and error approach, the refined values for driving behavior characteristic as suggested in **Table 6.20a** were arrived at in the next step of simulation.

#### *Results of micro-simulations in VISSIM*

The results of the micro-simulation approach after fine-tuning the above mentioned characteristic are given in **Table 6.20b**. In the current simulation run, the absolute errors reduced from 13.6% to 11.3% and the *GEH* statistic reduced from 5.98 to 5.01. Thus, the *multiplicative part of safety distance* was found to have a moderate influence on improving the accuracy of prediction of the simulation model.

**Table 6.20b Comparison of Actual and Simulated Traffic Volumes at 18 Mid-Block Locations for Eleventh Level Refinements: Random Seed 42**

Direction		Simulated	Observed	Observed-Simulated	Error (%)	Abs. Error (%)	<i>GEH</i> STATISTIC
From	To						
Jyothi	Hampankatta	2451	2580	129	5.0	5.0	2.57
Hampankatta	Jyothi	1964	2320	356	15.3	15.3	7.69
PVS	Bunts	1215	1465	250	17.1	17.1	6.83
Balmatta	St. Theresa	631	710	79	11.1	11.1	3.05
St. Theresa	Balmatta	723	805	82	10.2	10.2	2.97
Bendoorwell	Balmatta	1420	1455	35	2.4	2.4	0.92
Balmatta	Bendoorwell	1414	1680	266	15.8	15.8	6.76
Bendoorwell	St. Theresa	1136	1205	69	5.7	5.7	2.02
St. Theresa	Bendoorwell	1059	1100	41	3.7	3.7	1.25
				<b>Average</b>	<b>11.3%</b>	<b>11.3%</b>	<b>5.01</b>

### 6.2.13 Twelfth Level of Refinement of Vehicle and Driver Characteristics for Calibration Using Random Seed 42

In this step, the driving behavior characteristics such as the *time-lags between lane/ direction change procedures* considered under *lateral movement* of vehicles was modified. Based on a trial and error approach, the refined values for driving behavior characteristic as suggested in **Table 6.21** were arrived at in the next step of simulation.

### Results of micro-simulations in VISSIM

The results of the micro-simulation approach after fine-tuning the above mentioned characteristics are given in **Table 6.22**. The *GEH* statistic was found to reduce from 5.01 to 3.62, and the average absolute error was found to reduce from 11.3% to 8.4%. Thus, the *time-lag between lane/ direction changes* was found to be highly sensitive in reducing prediction errors.

**Table 6.22 Comparison of Actual and Simulated Traffic Volumes at 18 Mid-Block Locations for Twelfth Level Refinements: Random Seed 42**

Direction		Simulated	Observed	Observed-Simulated	Error (%)	Abs. Error (%)	GEH STATISTIC
From	To						
Jyothi	Hampankatta	2513	2580	67	2.6	2.6	1.33
Hampankatta	Jyothi	2136	2320	184	7.9	7.9	3.90
PVS	Bunts	1237	1465	228	15.6	15.6	6.20
Bunts	PVS	1418	1505	87	5.8	5.8	2.28
Navabharat	PVS	2168	2510	342	13.6	13.6	7.07
PVS	Navabharat	2254	2370	116	4.9	4.9	2.41
Hampankatta	Navabharat	2082	2225	143	6.4	6.4	3.08
Navabharat	Hampankatta	1728	2100	372	17.7	17.7	8.50
Jyothi	Bunts	1878	2020	142	7.0	7.0	3.22
Bunts	Jyothi	1864	1970	106	5.4	5.4	2.42
Jyothi	Balmatta	1540	1830	290	15.8	15.8	7.06
Balmatta	Jyothi	2463	2585	122	4.7	4.7	2.43
<b>Average</b>					<b>8.2%</b>	<b>8.4%</b>	<b>3.62</b>

### 6.2.14 Thirteenth Level of Refinement of Vehicle and Driver Characteristics for Calibration Using Random Seed 42

In this step, the driving behavior characteristics such as the *minimum longitudinal speeds* as part of *lane change behavior* were modified. According to **PTV (2011)**, the *minimum longitudinal speed* defined as the minimum longitudinal speed which permits lateral movements. The default value of 1 km/h ensures that vehicles can also move laterally if they have almost come to a halt already. Based on a trial and error approach, the refined values for driving behavior characteristic as suggested in **Table 6.23a** were arrived at in the next step of simulation.

### Results of micro-simulations in VISSIM

The results of the micro-simulation approach after fine-tuning the above mentioned characteristics are given in **Table 6.23b**. The *GEH* statistic was found to reduce from 3.62 to 3.13, and the average absolute error was found to reduce from 8.4%

to 7.3%. Thus, the *minimum longitudinal speeds* (as part of *lane change behavior*), was found to be moderately sensitive in reducing prediction errors.

**Table 6.23b Comparison of Actual and Simulated Traffic Volumes at 18 Mid-Block Locations for Thirteenth Level Refinements: Random Seed 42**

Direction		Simulated	Observed	Observed-Simulated	Error (%)	Abs. Error (%)	GEH STATISTIC
From	To						
Jyothi	Hampankatta	2535	2580	45	1.7	1.7	0.89
Hampankatta	Jyothi	2147	2320	173	7.5	7.5	3.66
PVS	Bunts	1302	1465	163	11.1	11.1	4.38
Bunts	PVS	1422	1505	83	5.5	5.5	2.17
Navabharat	PVS	2276	2510	234	9.3	9.3	4.78
PVS	Navabharat	2276	2370	94	4.0	4.0	1.95
Hampankatta	Navabharat	2081	2225	144	6.5	6.5	3.10
Navabharat	Hampankatta	1758	2100	342	16.3	16.3	7.79
Jyothi	Bunts	1903	2020	117	5.8	5.8	2.64
Bunts	Jyothi	1885	1970	85	4.3	4.3	1.94
Jyothi	Balmatta	1551	1830	279	15.2	15.2	6.79
Balmatta	Jyothi	2479	2585	106	4.1	4.1	2.11
Balmatta	St. Theresa	629	710	81	11.4	11.4	3.13
<b>Average</b>					<b>7.1%</b>	<b>7.3%</b>	<b>3.13</b>

### 6.2.15 Fourteenth or Final Level of Refinement of Vehicle and Driver Characteristics for Calibration Using Random Seed 42

In this step, the driving behavior characteristic such as the *collision time gain* as part of *lateral driving behavior* was modified. According to PTV (2011), the minimum value of *minimum collision time-gain* for the next vehicle or signal head, which must be reached so that a change of the lateral position on the lane is worthwhile and will be performed. Based on a trial and error approach, the refined values for driving behavior characteristic as suggested in Table 6.24a were arrived at in the next step of simulation.

**Table 6.24a Driving Behaviour (Lateral) Characteristic Assigned**

Driving Behavior Characteristic	Modified value
Minimum Collision time-gain	0.57s

#### *Results of micro-simulations in VISSIM*

The results of the micro-simulation approach after fine-tuning the above mentioned characteristics are given in Table 6.24b. The *GEH* statistic was found to reduce from 3.13 to 2.52 and the average absolute error was found to reduce from 7.3% to 5.9%. Thus, the *collision time gain* was found to be moderately sensitive in reducing prediction errors.

**Table 6.24b Comparison of Actual and Simulated Traffic Volumes at 18 Mid-Block Locations for Fourteenth Level Refinements: Random Seed 42**

Direction		Simulated	Observed	Observed-Simulated	Error (%)	Abs. Error (%)	GEH STATISTIC
From	To						
Jyothi	Hampankatta	2548	2580	32	1.2	1.2	0.63
Hampankatta	Jyothi	2158	2320	162	7.0	7.0	3.42
PVS	Bunts	1345	1465	120	8.2	8.2	3.20
Bunts	PVS	1423	1505	82	5.4	5.4	2.14
Navabharat	PVS	2428	2510	82	3.3	3.3	1.65
PVS	Navabharat	2284	2370	86	3.6	3.6	1.78
Bendoorwell	Balmatta	1455	1455	0	0.0	0.0	0.00
Balmatta	Bendoorwell	1454	1680	226	13.5	13.5	5.71
Bendoorwell	St. Theresa	1144	1205	61	5.1	5.1	1.78
St. Theresa	Bendoorwell	1062	1100	38	3.5	3.5	1.16
				<b>Average</b>	<b>5.8%</b>	<b>5.9%</b>	<b>2.52</b>

Here, it can be seen that the overall *GEH* value of 2.52 is lesser than 5 on a network-wide basis, satisfying one of the basic criteria specified by **DMRB (1996)**, **FHA (2004)** and **Wisconsin DOT (2002)** too, provide similar guidelines for simulation studies on freeways. It is also specified that the *GEH* values for 85% of the links must be lesser than 5 to ensure a good match for traffic modeling using hourly volume data for the calibration and validation models. These two criteria were satisfied in the final calibrated model after the 14<sup>th</sup> stage of refinement.

**Table 6.24c** provides micro-level details on the speeds for various classes of vehicles. In this table, it can be seen that the *GEH* statistic values are lesser than 5.0 for more than 85% of the data rows indicating a better fit between the observed scenario and calibrated model. Additionally, **Table 6.24d**, **Table 6.24e**, and **Table 6.24f** provide information on the computations related to delays for various classes of vehicles at PVS Junction, Bunts Hostel Junction, and Jyothi Junction for the final stage of calibration. At these three junctions, too, it can be seen that the simulated delays tally with the observed delays of vehicles entering and leaving the junctions in more than 85% of the turning movements.

**Table 6.24c Comparison of Actual and Simulated Speeds for Each Vehicle Class at 18 Mid-Block Locations for the Final Stage of Calibration: Random Seed 42**

Direction		Simulated Speeds for Each Vehicle Class (a)		Observed Average Speed (b)	(b)-(a)	Error (%)	Absolute Error (%)	GEH Statistic	RNSE
From	To								
Jyothi	Hampankatta	Two-wheelers	41.64	39.89	-1.75	-4.4	4.4	0.27	0.28
		Auto-rickshaws	39.63	37.76	-1.87	-5.0	5.0	0.30	0.30
		Cars	43.38	42.88	-0.50	-1.2	1.2	0.08	0.08
		LCVs	40.47	39.89	-0.58	-1.5	1.5	0.09	0.09
		Buses	41.92	41.47	-0.45	-1.1	1.1	0.07	0.07
		Trucks	0.00	0.00	0.00	0.0	0.0	0.00	0.00
Hampankatta	Jyothi	Two-wheelers	42.48	39.58	-2.90	-7.3	7.3	0.45	0.46
		Auto-rickshaws	40.84	37.74	-3.10	-8.2	8.2	0.49	0.50
		Cars	46.86	44.00	-2.86	-6.5	6.5	0.42	0.43
		LCVs	43.78	40.20	-3.58	-8.9	8.9	0.55	0.56
		Buses	44.44	40.58	-3.86	-9.5	9.5	0.59	0.61
		Trucks	0.00	0.00	0.00	0.0	0.0	0.00	0.00
PVS	Bunts	Two-wheelers	29.65	24.54	-5.11	-20.8	20.8	0.98	1.03
		Auto-rickshaws	27.90	24.56	-3.34	-13.6	13.6	0.65	0.67
		Cars	28.66	24.98	-3.68	-14.7	14.7	0.71	0.74
		LCVs	31.09	28.32	-2.77	-9.8	9.8	0.51	0.52
		Buses	27.37	20.44	-6.93	-33.9	33.9	1.42	1.53
		Trucks	22.57	18.28	-4.29	-23.5	23.5	0.95	1.00
Bunts	PVS	Two-wheelers	41.29	38.41	-2.88	-7.5	7.5	0.46	0.46
		Auto-rickshaws	40.04	37.32	-2.72	-7.3	7.3	0.44	0.45
		Cars	41.99	39.50	-2.49	-6.3	6.3	0.39	0.40
		LCVs	43.20	40.79	-2.41	-5.9	5.9	0.37	0.38
		Buses	45.15	44.09	-1.06	-2.4	2.4	0.16	0.16
		Trucks	39.46	36.34	-3.12	-8.6	8.6	0.51	0.52
Jyothi	Bunts	Two-wheelers	40.40	38.40	-2.00	-5.2	5.2	0.32	0.32
		Auto-rickshaws	38.30	36.04	-2.26	-6.3	6.3	0.37	0.38
		Cars	40.74	38.22	-2.52	-6.6	6.6	0.40	0.41
		LCVs	41.49	39.59	-1.90	-4.8	4.8	0.30	0.30
		Buses	38.37	36.47	-1.90	-5.2	5.2	0.31	0.31
		Trucks	0.00	0.00	0.00	0.0	0.0	0.00	0.00
Bunts	Jyothi	Two-wheelers	37.22	35.17	-2.05	-5.8	5.8	0.34	0.35
		Auto-rickshaws	35.12	34.04	-1.08	-3.2	3.2	0.18	0.19
		Cars	37.44	35.79	-1.65	-4.6	4.6	0.27	0.28
		LCVs	37.29	35.22	-2.07	-5.9	5.9	0.34	0.35
		Buses	35.86	34.05	-1.81	-5.3	5.3	0.31	0.31
		Trucks	38.70	36.75	-1.95	-5.3	5.3	0.32	0.32
Jyothi	Balmatta	Two-wheelers	33.27	28.16	-5.11	-18.1	18.1	0.92	0.96
		Auto-rickshaws	31.35	26.62	-4.73	-17.8	17.8	0.88	0.92
		Cars	33.38	28.75	-4.63	-16.1	16.1	0.83	0.86
		LCVs	33.37	28.82	-4.55	-15.8	15.8	0.82	0.85
		Buses	30.40	26.24	-4.16	-15.9	15.9	0.78	0.81
		Trucks	29.04	23.88	-5.16	-21.6	21.6	1.00	1.06
Balmatta	Jyothi	Two-wheelers	40.21	38.14	-2.07	-5.4	5.4	0.33	0.33
		Auto-rickshaws	38.51	36.42	-2.09	-5.7	5.7	0.34	0.35
		Cars	41.65	39.52	-2.13	-5.4	5.4	0.33	0.34
		LCVs	38.98	37.08	-1.90	-5.1	5.1	0.31	0.31
		Buses	41.49	39.28	-2.21	-5.6	5.6	0.35	0.35
		Trucks	0.00	0.00	0.00	0.0	0.0	0.00	0.00
Balmatta	St. Theresa	Two-wheelers	42.60	39.10	-3.50	-8.9	8.9	0.55	0.56
		Auto-rickshaws	40.44	37.79	-2.65	-7.0	7.0	0.42	0.43
		Cars	46.12	42.43	-3.69	-8.7	8.7	0.55	0.57
		LCVs	43.67	39.63	-4.04	-10.2	10.2	0.63	0.64

		Buses	45.57	42.79	-2.78	-6.5	6.5	0.42	0.43
		Trucks	41.32	37.74	-3.58	-9.5	9.5	0.57	0.58
St. Theresa	Balmatta	Two-wheelers	24.94	24.14	-0.80	-3.3	3.3	0.16	0.16
		Auto-rickshaws	24.98	24.12	-0.86	-3.6	3.6	0.17	0.18
		Cars	24.96	24.32	-0.64	-2.6	2.6	0.13	0.13
		LCVs	25.04	24.49	-0.55	-2.2	2.2	0.11	0.11
		Buses	23.01	21.35	-1.66	-7.8	7.8	0.35	0.36
		Trucks	0.00	0.00	0.00	0.0	0.0	0.00	0.00
Bendorwell	Balmatta	Two-wheelers	20.74	20.39	-0.35	-1.7	1.7	0.08	0.08
		Auto-rickshaws	19.05	18.64	-0.41	-2.2	2.2	0.09	0.10
		Cars	19.93	19.64	-0.29	-1.5	1.5	0.07	0.07
		LCVs	23.86	22.43	-1.43	-6.4	6.4	0.30	0.30
		Buses	20.17	18.45	-1.72	-9.3	9.3	0.39	0.40
		Trucks	0.00	0.00	0.00	0.0	0.0	0.00	0.00
St. Theresa	Bendorwell	Two-wheelers	43.08	41.09	-1.99	-4.9	4.9	0.31	0.31
		Auto-rickshaws	41.36	39.02	-2.34	-6.0	6.0	0.37	0.37
		Cars	47.33	45.15	-2.18	-4.8	4.8	0.32	0.32
		LCVs	46.49	44.16	-2.33	-5.3	5.3	0.35	0.35
		Buses	45.42	43.32	-2.10	-4.8	4.8	0.32	0.32
		Trucks	0.00	0.00	0.00	0.0	0.0	0.00	0.00
					<b>Average</b>	<b>-6.96%</b>	<b>6.96%</b>	<b>0.39</b>	<b>0.40</b>

**Table 6.24d Actual Vs Simulated Delays for Various Vehicle Classes for Turning Movements at PVS Junction for Calibration Data: Random Seed 42**

Direction		Simulated Delays for Each Vehicle Class (a)	Observed Average Delay (b)	(b)-(a)	Error (%)	Absolute Error (%)	GEH Statistic	RNSE	
From	To								
Lalbhad	Navabharat	Two-wheelers	68.73	73.28	4.55	6.2	6.2	0.54	0.53
		Auto-rickshaws	76.05	82.80	6.75	8.2	8.2	0.76	0.74
		Cars	77.02	81.54	4.52	5.5	5.5	0.51	0.50
		LCVs	78.59	82.71	4.12	5.0	5.0	0.46	0.45
		Buses	69.84	74.98	5.14	6.9	6.9	0.60	0.59
		Trucks	96.96	104.06	7.10	6.8	6.8	0.71	0.70
Bunts	Lalbhad	Two-wheelers	78.67	85.01	6.34	7.5	7.5	0.70	0.69
		Auto-rickshaws	84.19	90.83	6.64	7.3	7.3	0.71	0.70
		Cars	99.42	106.26	6.84	6.4	6.4	0.67	0.66
		LCVs	0.00	0.00	0.00	0.0	0.0	0.00	0.00
		Buses	146.58	154.19	7.61	4.9	4.9	0.62	0.61
		Trucks	36.75	40.24	3.49	8.7	8.7	0.56	0.55
Bunts	Navabharat	Two-wheelers	67.61	73.10	5.49	7.5	7.5	0.65	0.64
		Auto-rickshaws	68.02	73.29	5.27	7.2	7.2	0.63	0.62
		Cars	76.16	81.67	5.51	6.7	6.7	0.62	0.61
		LCVs	25.80	29.51	3.71	12.6	12.6	0.71	0.68
		Buses	0.00	0.00	0.00	0.0	0.0	0.00	0.00
		Trucks	0.00	0.00	0.00	0.0	0.0	0.00	0.00
					<b>Average</b>	<b>8.3%</b>	<b>8.3%</b>	<b>0.925</b>	<b>0.887</b>

**Table 6.24e Actual Vs Simulated Delays for Various Vehicle Classes for Turning Movements at Bunt's Hostel Junction for Calibration Data: Random Seed 42**

Direction	Simulated Delays for	Observed	(b)-(a)	Error	Absolute	GEH	RNSE
-----------	----------------------	----------	---------	-------	----------	-----	------

From	To	Each Vehicle Class (a)		Average Delay (b)		(%)	Error (%)	Statistic	
PVS	Jyothi	Two-wheelers	128.43	136.47	8.04	5.9	5.9	0.70	0.69
		Auto-rickshaws	158.57	164.05	5.48	3.3	3.3	0.43	0.43
		Cars	131.65	137.98	6.33	4.6	4.6	0.55	0.54
		LCVs	0.00	0.00	0.00	0.0	0.0	0.00	0.00
		Buses	201.06	212.36	11.30	5.3	5.3	0.79	0.78
		Trucks	329.50	348.83	19.33	5.5	5.5	1.05	1.03
Jyothi	Kadri	Two-wheelers	98.06	104.35	6.29	6.0	6.0	0.63	0.62
		Auto-rickshaws	133.38	139.70	6.32	4.5	4.5	0.54	0.54
		Cars	117.65	123.46	5.81	4.7	4.7	0.53	0.52
		LCVs	63.05	67.91	4.86	7.2	7.2	0.60	0.59
		Buses	115.41	121.80	6.39	5.2	5.2	0.59	0.58
		Trucks	0.00	0.00	0.00	0.0	0.0	0.00	0.00
				<b>Average</b>	<b>9.6%</b>	<b>9.6%</b>	<b>0.706</b>	<b>0.682</b>	

**Table 6.24f Actual Vs Simulated Delays for Various Vehicle Classes for Turning Movements at Jyothi Junction for Calibration Data: Random Seed 42**

Direction		Simulated Delays for Each Vehicle Class (a)		Observed Average Delay (b)	(b)-(a)	Error (%)	Absolute Error (%)	GEH Statistic	RNSE
From	To								
Bunts	Balmatta	Two-wheelers	52.79	65.18	12.39	19.0	19.0	1.61	1.54
		Auto-rickshaws	54.46	66.34	11.88	17.9	17.9	1.53	1.46
		Cars	62.09	74.53	12.44	16.7	16.7	1.50	1.44
		LCVs	62.50	75.65	13.15	17.4	17.4	1.58	1.51
		Buses	0.00	0.00	0.00	0.0	0.0	0.00	0.00
		Trucks	346.83	425.71	78.88	18.5	18.5	4.01	3.82
Bunts	Hampankatta	Two-wheelers	89.93	94.68	4.75	5.0	5.0	0.49	0.49
		Auto-rickshaws	91.76	97.83	6.07	6.2	6.2	0.62	0.61
		Cars	87.51	92.05	4.54	4.9	4.9	0.48	0.47
		LCVs	41.60	44.17	2.57	5.8	5.8	0.39	0.39
		Buses	144.72	154.42	9.70	6.3	6.3	0.79	0.78
		Trucks	0.00	0.00	0.00	0.0	0.0	0.00	0.00
Balmatta	Hampankatta	Two-wheelers	88.45	94.05	5.60	6.0	6.0	0.59	0.58
		Auto-rickshaws	123.74	131.38	7.64	5.8	5.8	0.68	0.67
		Cars	132.84	140.93	8.09	5.7	5.7	0.69	0.68
		LCVs	37.55	39.45	1.90	4.8	4.8	0.31	0.30
		Buses	173.21	182.15	8.94	4.9	4.9	0.67	0.66
		Trucks	0.00	0.00	0.00	0.0	0.0	0.00	0.00
				<b>Average</b>	<b>6.4%</b>	<b>6.4%</b>	<b>0.643</b>	<b>0.626</b>	

### 6.2.16 Comparison of Results of Calibration of Vehicle and Driver Characteristics Using Random Seed 42 and Random Seed 25

Calibration studies were also performed using random seed 25 in the same manner as was done in the case of random seed 42. **Table 6.24g** provides a summary of the same. Here, it can be observed that in calibrations up to Stage 7b, the *GEH* values for random seed 25 were marginally lesser than that of random seed 42. However, from



Stage 8 onwards, it can be seen that the results generated by random seed 42 are more accurate. **Fig.6.5b** provides a graphical representation comparing the performance of random seed 42, and random seed 25 showing the reduction in the *mean absolute prediction errors* over the fourteen stages of the calibration procedure for flows measured across 18 mid-block sections.

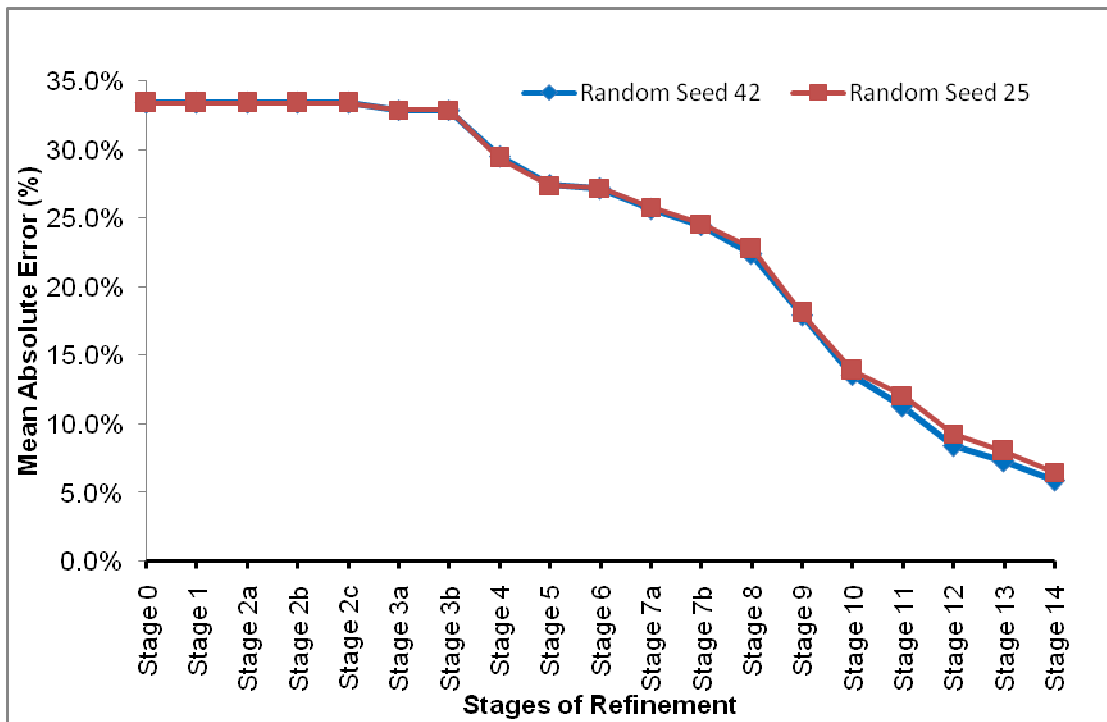


**Fig.6.5b Comparison of Reduction in the Mean Absolute Prediction Errors Over Fourteen Stages of Calibration for Random Seed 42, and Random Seed 25**

The comparative study on the performance of random seed 25 and random seed 42 indicate that the overall errors in prediction on using random sees higher than 25 can result in more refined predictions as observed by **Wang et al. (2012)**. The above results also corroborate the observations made by **Ishaque and Noland (2005)**, **Kamdar (2004)**, and **TJPDC (2007)** that the use of random number 42 provided reliable estimates of the actual values in a wide variety of simulation experiments.

### 6.3 VALIDATION OF VISSIM MODEL AFTER CALIBRATION

The process of verifying the forecasting capability of any calibrated simulation model, for a new set of field-data is called validation. From a consolidated 80-minute video-graphic recording of vehicle movements in Mangalore city, a 20-minute video-graphic data corresponding to 25% of the consolidated data was used for validation.

#### 6.3.1 Validation of Traffic Volumes after the Fourteenth Level of Calibration

The vehicle and driver parameters refined after the fourteenth level of calibration were noted, and the validation exercise was performed using the data set apart for the same. The simulated vehicular volumes were then obtained for the 18 mid-block locations for the validation model. **Table 6.25a** provides details on the computation of the average absolute error between the simulated and observed vehicular volumes at the 18 mid-block sections. In the validation exercise, it was seen that the *mean absolute error (MAE)* 10.8%, while the absolute error after the calibration procedure was found to be 5.9%.

In the validation exercise, it can be seen that the overall *GEH* value of 2.71 is lesser than 5 on a network-wide basis, satisfying one of the basic criteria specified by **DMRB (1996)**, **FHA (2004)**, and **Wisconsin DOT (2002)**. It is also observed that the *GEH* values of 85% of the links considered are lesser than 5, satisfying the second criteria. **Fig 6.6** provides a pictorial representation of the differences between the observed volumes and the simulated volumes for vehicular flows along the 18 mid-block sections for the validation using random seed 42.

**Table 6.25a Validation Results for Volume at 18 Mid-block Sections after the Fourteenth Level of Calibration: Random Seed 42**

Direction		Simulated	Observed	Observed-Simulated	Error (%)	Abs. Error (%)	GEH Statistic
From	To						
Jyothi	Hampankatta	847	765	-82	-10.7	10.7	2.89
Hampankatta	Jyothi	692	835	143	17.1	17.1	5.18
PVS	Bunts	549	475	-74	-15.6	15.6	3.27
Balmatta	Jyothi	947	775	-172	-22.2	22.2	5.86
Balmatta	St. Theresa	263	260	-3	-1.2	1.2	0.19
St. Theresa	Balmatta	240	250	10	4.0	4.0	0.64
Bendoorwell	Balmatta	481	455	-26	-5.7	5.7	1.20
Balmatta	Bendoorwell	557	550	-7	-1.3	1.3	0.30
Bendoorwell	St. Theresa	377	435	58	13.3	13.3	2.88
St. Theresa	Bendoorwell	332	395	63	15.9	15.9	3.30
<b>Average</b>					<b>0.2%</b>	<b>10.8%</b>	<b>2.71</b>

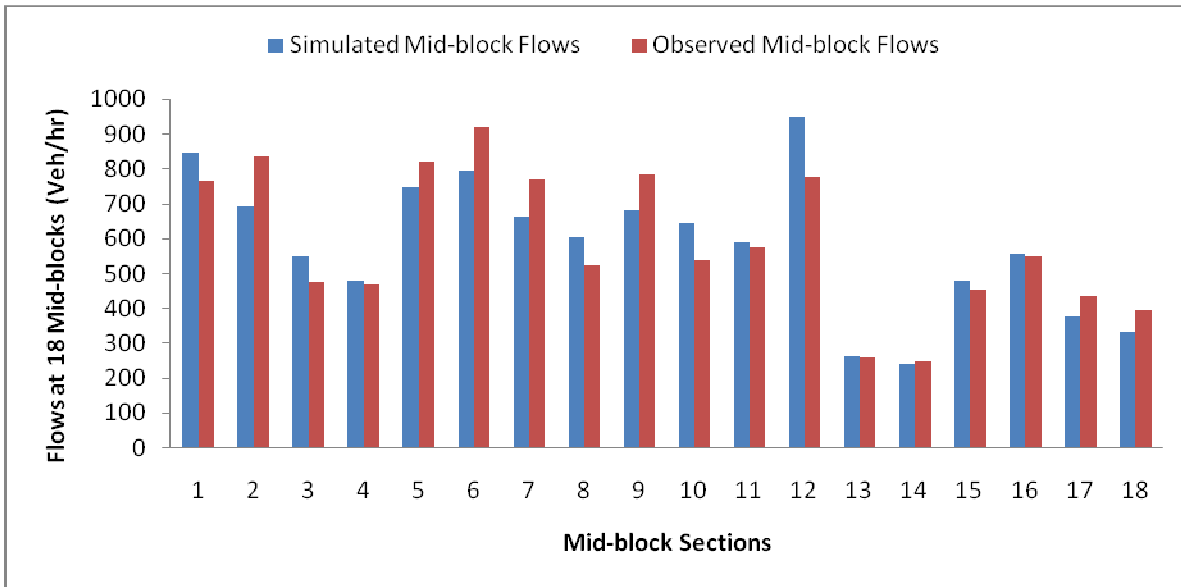


**Fig.6.6 Comparison of Observed and Simulated Flows at 18 Mid-block Locations for Validation after the Fourteenth Level of Calibration Using Random Seed 42**

Table 6.25b provides micro-level details on the speeds for various classes of vehicles. In this table, it can be seen that the *GEH* statistic values are lesser than 5.0 for more than 85% of the data rows indicating a better fit between the observed speeds and the simulated speeds for the validated model.

**Table 6.25b Comparison of Actual and Simulated Speeds for Each Vehicle Class at 18 Mid-Block Locations Using Random Seed 42 for Validation**

Direction		Simulated Speeds for Each Vehicle Class (a)	Observed Average Speed (b)	(b)-(a)	Error (%)	Absolute Error (%)	<i>GEH</i> Statistic	<i>RNSE</i>	
From	To								
Jyothi	Hampankatta	Two-wheelers	42.29	39.53	-2.76	-7.0	7.0	0.43	0.44
		Auto-rickshaws	40.30	37.59	-2.71	-7.2	7.2	0.43	0.44
		Cars	43.63	43.01	-0.62	-1.4	1.4	0.09	0.09
		LCVs	43.36	39.78	-3.58	-9.0	9.0	0.56	0.57
		Buses	43.83	41.52	-2.31	-5.6	5.6	0.35	0.36
		Trucks	0.00	0.00	0.00	0.0	0.0	0.00	0.00
Hampankatta	Jyothi	Two-wheelers	42.96	39.62	-3.34	-8.4	8.4	0.52	0.53
		Auto-rickshaws	40.84	37.89	-2.95	-7.8	7.8	0.47	0.48
		Cars	46.56	44.32	-2.24	-5.1	5.1	0.33	0.34
		LCVs	42.65	40.37	-2.28	-5.6	5.6	0.35	0.36
		Buses	0.00	0.00	0.00	0.0	0.0	0.00	0.00
		Trucks	0.00	0.00	0.00	0.0	0.0	0.00	0.00
PVS	Bunts	Two-wheelers	16.54	16.04	-0.50	-3.1	3.1	0.12	0.12
		Auto-rickshaws	15.62	15.43	-0.19	-1.2	1.2	0.05	0.05
		Cars	17.48	15.32	-2.16	-14.1	14.1	0.53	0.55
		LCVs	25.93	15.22	-10.71	-70.3	70.3	2.36	2.74

		Buses	7.57	10.34	2.77	26.8	26.8	0.92	0.86	
		Trucks	7.69	10.18	2.49	24.4	24.4	0.83	0.78	
Navabharat	Hampankatta	Two-wheelers	42.99	36.67	-6.32	-17.2	17.2	1.00	1.04	
		Auto-rickshaws	40.96	35.67	-5.29	-14.8	14.8	0.85	0.89	
		Cars	44.80	41.35	-3.45	-8.3	8.3	0.53	0.54	
		LCVs	44.08	40.02	-4.06	-10.2	10.2	0.63	0.64	
		Buses	0.00	0.00	0.00	0.0	0.0	0.00	0.00	
		Trucks	46.45	36.54	-9.91	-27.1	27.1	1.54	0.00	
Jyothi	Bunts	Two-wheelers	40.65	38.40	-2.25	-5.9	5.9	0.36	0.36	
		Auto-rickshaws	39.10	35.96	-3.14	-8.7	8.7	0.51	0.52	
		Cars	40.91	38.36	-2.55	-6.7	6.7	0.41	0.41	
		LCVs	37.69	39.62	1.93	4.9	4.9	0.31	0.31	
		Buses	40.99	36.51	-4.48	-12.3	12.3	0.72	0.74	
		Trucks	0.00	0.00	0.00	0.0	0.0	0.00	0.00	
Bunts	Jyothi	Two-wheelers	38.55	35.21	-3.34	-9.5	9.5	0.55	0.56	
		Auto-rickshaws	36.65	33.96	-2.69	-7.9	7.9	0.45	0.46	
		Cars	38.51	35.84	-2.67	-7.4	7.4	0.44	0.45	
		LCVs	33.70	35.17	1.47	4.2	4.2	0.25	0.25	
		Buses	34.53	33.95	-0.58	-1.7	1.7	0.10	0.10	
		Trucks	32.97	36.64	3.67	0.0	0.0	0.62	0.00	
Jyothi	Balmatta	Two-wheelers	18.28	20.90	2.62	12.5	12.5	0.59	0.57	
		Auto-rickshaws	17.16	19.43	2.27	11.7	11.7	0.53	0.52	
		Cars	18.92	18.43	-0.49	-2.7	2.7	0.11	0.12	
		LCVs	17.49	18.34	0.85	4.6	4.6	0.20	0.20	
		Buses	16.21	18.05	1.84	10.2	10.2	0.44	0.43	
		Trucks	15.86	17.12	1.26	7.4	7.4	0.31	0.31	
Balmatta	Jyothi	Two-wheelers	39.19	37.13	-2.06	-5.5	5.5	0.33	0.34	
		Auto-rickshaws	37.97	36.39	-1.58	-4.3	4.3	0.26	0.26	
		Cars	40.78	39.57	-1.21	-3.1	3.1	0.19	0.19	
		LCVs	37.44	36.98	-0.46	-1.2	1.2	0.08	0.08	
		Buses	39.25	39.20	-0.05	-0.1	0.1	0.01	0.01	
		Trucks	0.00	0.00	0.00	0.0	0.0	0.00	0.00	
Balmatta	Bendoorwell	Two-wheelers	41.74	37.15	-4.59	-12.3	12.3	0.73	0.75	
		Auto-rickshaws	40.61	35.98	-4.63	-12.9	12.9	0.75	0.77	
		Cars	44.47	39.13	-5.34	-13.7	13.7	0.83	0.85	
		LCVs	43.91	38.46	-5.45	-14.2	14.2	0.85	0.88	
		Buses	41.95	43.71	1.76	4.0	4.0	0.27	0.27	
		Trucks	0.00	0.00	0.00	0.0	0.0	0.00	0.00	
Bendoorwell	St. Theresa	Two-wheelers	42.10	40.13	-1.97	-4.9	4.9	0.31	0.31	
		Auto-rickshaws	40.53	38.66	-1.87	-4.8	4.8	0.30	0.30	
		Cars	45.96	44.32	-1.64	-3.7	3.7	0.24	0.25	
		LCVs	44.45	41.35	-3.10	-7.5	7.5	0.47	0.48	
		Buses	0.00	0.00	0.00	0.0	0.0	0.00	0.00	
		Trucks	30.00	39.64	9.64	24.3	24.3	1.63	1.53	
St. Theresa	Bendoorwell	Two-wheelers	43.05	40.95	-2.10	-5.1	5.1	0.32	0.33	
		Auto-rickshaws	40.59	38.68	-1.91	-4.9	4.9	0.30	0.31	
		Cars	48.09	45.04	-3.05	-6.8	6.8	0.45	0.46	
		LCVs	46.69	43.80	-2.89	-6.6	6.6	0.43	0.44	
		Buses	0.00	0.00	0.00	0.0	0.0	0.00	0.00	
		Trucks	0.00	0.00	0.00	0.0	0.0	0.00	0.00	
						<b>Average</b>	<b>-7.90</b>	<b>10.53</b>	<b>0.52</b>	<b>0.52</b>

**Table 6.25c Actual Vs Simulated Delays for Various Vehicle Classes for Turning Movements at PVS Junction for Validation Data: Random Seed 42**

Direction		Simulated Delays for Each Vehicle Class (a)		Observed Average Delay (b)	(b)-(a)	Error (%)	Absolute Error (%)	GEH Statistic	RNSE
From	To								
Lalbhadg	Navabharat	Two-wheelers	30.39	32.96	2.57	7.8	7.8	0.46	0.45
		Auto-rickshaws	29.65	32.43	2.78	8.6	8.6	0.50	0.49
		Cars	33.65	36.26	2.61	7.2	7.2	0.44	0.43
		LCVs	16.03	17.71	1.68	9.5	9.5	0.41	0.40
		Buses	0.00	0.00	0.00	0.0	0.0	0.00	0.00
		Trucks	41.63	45.65	4.02	8.8	8.8	0.61	0.59
Bunts	Navabharat	Two-wheelers	84.98	92.56	7.58	8.2	8.2	0.80	0.79
		Auto-rickshaws	97.30	105.34	8.04	7.6	7.6	0.80	0.78
		Cars	98.83	106.09	7.26	6.8	6.8	0.72	0.71
		LCVs	14.76	17.33	2.57	14.8	14.8	0.64	0.62
		Buses	0.00	0.00	0.00	0.0	0.0	0.00	0.00
		Trucks	0.00	0.00	0.00	0.0	0.0	0.00	0.00
					<b>Average</b>	<b>9.6%</b>	<b>9.6%</b>	<b>1.290</b>	<b>1.216</b>

**Table 6.25d Actual Vs Simulated Delays for Various Vehicle Classes for Turning Movements at Bunt's Hostel Junction for Validation Data: Random Seed 42**

Direction		Simulated Delays for Each Vehicle Class (a)		Observed Average Delay (b)	(b)-(a)	Error (%)	Absolute Error (%)	GEH Statistic	RNSE
From	To								
PVS	Jyothi	Two-wheelers	234.59	254.17	19.58	7.7	7.7	1.25	1.23
		Auto-rickshaws	271.23	292.27	21.04	7.2	7.2	1.25	1.23
		Cars	243.05	259.94	16.89	6.5	6.5	1.07	1.05
		LCVs	0.00	0.00	0.00	0.0	0.0	0.00	0.00
		Buses	423.91	452.89	28.98	6.4	6.4	1.38	1.36
		Trucks	447.70	495.78	48.08	9.7	9.7	2.21	2.16
Jyothi	PVS	Two-wheelers	92.72	106.12	13.40	12.6	12.6	1.34	1.30
		Auto-rickshaws	93.85	107.06	13.21	12.3	12.3	1.32	1.28
		Cars	101.57	115.29	13.72	11.9	11.9	1.32	1.28
		LCVs	11.70	13.51	1.81	13.4	13.4	0.51	0.49
		Buses	299.56	337.10	37.54	11.1	11.1	2.10	2.04
		Trucks	0.00	0.00	0.00	0.0	0.0	0.00	0.00
Jyothi	Kadri	Two-wheelers	104.82	116.51	11.69	10.0	10.0	1.11	1.08
		Auto-rickshaws	58.53	66.29	7.76	11.7	11.7	0.98	0.95
		Cars	149.49	169.86	20.37	12.0	12.0	1.61	1.56
		LCVs	64.40	72.40	8.00	11.0	11.0	0.97	0.94
		Buses	277.60	312.83	35.23	11.3	11.3	2.05	1.99
		Trucks	0.00	0.00	0.00	0.0	0.0	0.00	0.00
					<b>Average</b>	<b>10.0%</b>	<b>10.0%</b>	<b>1.000</b>	<b>0.968</b>

**Table 6.25e Actual Vs Simulated Delays for Various Vehicle Classes for Turning Movements at Jyothi Junction for Validation Data: Random Seed 42**

Direction		Simulated Delays for Each Vehicle Class (a)		Observed Average Delay (b)	(b)-(a)	Error (%)	Absolute Error (%)	GEH Statistic	RNSE
From	To								
Balmatta	Bunts	Two-wheelers	110.55	121.52	10.97	9.0	9.0	1.02	1.00
		Auto-rickshaws	103.92	111.73	7.81	7.0	7.0	0.75	0.74
		Cars	124.26	133.91	9.65	7.2	7.2	0.85	0.83
		LCVs	0.00	0.00	0.00	0.0	0.0	0.00	0.00
		Buses	279.88	302.43	22.55	7.5	7.5	1.32	1.30
		Trucks	0.00	0.00	0.00	0.0	0.0	0.00	0.00
Balmatta	Hampankatta	Two-wheelers	107.87	116.75	8.88	7.6	7.6	0.84	0.82
		Auto-rickshaws	104.73	113.18	8.45	7.5	7.5	0.81	0.79
		Cars	124.82	134.36	9.54	7.1	7.1	0.84	0.82
		LCVs	68.06	73.50	5.44	7.4	7.4	0.65	0.63
		Buses	263.57	285.16	21.59	7.6	7.6	1.30	1.28
		Trucks	0.00	0.00	0.00	0.0	0.0	0.00	0.00
					<b>Average</b>	<b>7.2%</b>	<b>7.2%</b>	<b>0.890</b>	<b>0.861</b>

## 6.4 SENSITIVITY ANALYSIS

The following sub-sections provide the details on the preparation of datasets for ANN-based *sensitivity analysis*, determination of ideal configuration of the ANN model, and the approach adopted in the study.

### 6.4.1 Preparation of Datasets for ANN-Based Sensitivity Analysis

A number of simulations were performed in VISSIM to prepare the database comprising 109 rows of datasets to be trained using an ANN. The values of the vehicle and driver characteristics were changed one at a time for approximately 5 to 7 simulation trials for each level of calibration as part of the fourteen-level calibration exercise, and the corresponding changes in the *mean absolute errors* in simulated traffic volumes were tabulated. **Table 6.26** provides details on the lower and upper bound values for vehicle and driver characteristics for calibrations performed in VISSIM.

**Table 6.27 Normalized Datasets Used for Training the ANN Model (Partial Listing)**

Details on Data Set for Sensitivity Analysis for Vehicle and Driver Characteristics															
Calibration Stage Sl. No.	Minimum Lateral Clearance (m)	Desired Acceleration (m/s <sup>2</sup> )	Maximum Acceleration (m/s <sup>2</sup> )	Deceleration Distribution (m/s <sup>2</sup> )	Lower-bound for Speed Distribution (kmph)	Upper-bound for Speed Distribution (kmph)	Minimum Look-ahead Distance (m)	Minimum Look-back Distance (m)	Average Standstill Distance (m)	Additive Part of Safety Distance (m)	Multiplicative Part of Safety Distance (m)	Time Between Direction Changes (s)	Minimum Longitudinal Speed (kmph)	Minimum Collision Time-gain (s)	Mean Absolute Error (MAE) in VISSIM Prediction (%)
0	1.0	0.4	0.4	0.3	1.0	0.7	0.2	0.2	0.7	1.0	1.0	0.1	1.0	1.0	1.0
1	0.5	0.4	0.4	0.3	1.0	0.7	0.2	0.2	0.7	1.0	1.0	0.1	1.0	1.0	1.0
	0.3	0.4	0.4	0.3	1.0	0.7	0.2	0.2	0.7	1.0	1.0	0.1	1.0	1.0	1.0
	0.8	0.4	0.4	0.3	1.0	0.7	0.2	0.2	0.7	1.0	1.0	0.1	1.0	1.0	1.0
	0.7	0.4	0.4	0.3	1.0	0.7	0.2	0.2	0.7	1.0	1.0	0.1	1.0	1.0	1.0
	0.9	0.4	0.4	0.3	1.0	0.7	0.2	0.2	0.7	1.0	1.0	0.1	1.0	1.0	1.0
	0.4	0.4	0.4	0.3	1.0	0.7	0.2	0.2	0.7	1.0	1.0	0.1	1.0	1.0	1.0
2a	0.5	0.2	0.4	0.3	1.0	0.7	0.2	0.2	0.7	1.0	1.0	0.1	1.0	1.0	1.0
	0.5	0.3	0.4	0.3	1.0	0.7	0.2	0.2	0.7	1.0	1.0	0.1	1.0	1.0	1.0
	0.5	0.4	0.4	0.3	1.0	0.7	0.2	0.2	0.7	1.0	1.0	0.1	1.0	1.0	1.0
	0.5	0.5	0.4	0.3	1.0	0.7	0.2	0.2	0.7	1.0	1.0	0.1	1.0	1.0	1.0
	0.5	0.1	0.4	0.3	1.0	0.7	0.2	0.2	0.7	1.0	1.0	0.1	1.0	1.0	1.0
	0.5	0.2	0.4	0.3	1.0	0.7	0.2	0.2	0.7	1.0	1.0	0.1	1.0	1.0	1.0
2b	0.5	0.2	0.3	0.3	1.0	0.7	0.2	0.2	0.7	1.0	1.0	0.1	1.0	1.0	1.0
	0.5	0.2	0.6	0.3	1.0	0.7	0.2	0.2	0.7	1.0	1.0	0.1	1.0	1.0	1.0
	0.5	0.2	0.7	0.3	1.0	0.7	0.2	0.2	0.7	1.0	1.0	0.1	1.0	1.0	1.0
	0.5	0.2	0.7	0.3	1.0	0.7	0.2	0.2	0.7	1.0	1.0	0.1	1.0	1.0	1.0
	0.5	0.2	0.3	0.3	1.0	0.7	0.2	0.2	0.7	1.0	1.0	0.1	1.0	1.0	1.0
	0.5	0.2	0.4	0.3	1.0	0.7	0.2	0.2	0.7	1.0	1.0	0.1	1.0	1.0	1.0
-	-	-	-	-	-	-	-	-	-	-	-	-	-	-	-
13	0.5	0.3	0.3	0.3	0.6	0.9	0.8	0.6	0.3	0.2	0.2	0.5	0.5	1.0	0.2
	0.5	0.3	0.3	0.3	0.6	0.9	0.8	0.6	0.3	0.2	0.2	0.5	0.8	1.0	0.2
	0.5	0.3	0.3	0.3	0.6	0.9	0.8	0.6	0.3	0.2	0.2	0.5	0.7	1.0	0.2
	0.5	0.3	0.3	0.3	0.6	0.9	0.8	0.6	0.3	0.2	0.2	0.5	0.4	1.0	0.2
	0.5	0.3	0.3	0.3	0.6	0.9	0.8	0.6	0.3	0.2	0.2	0.5	0.3	1.0	0.2
	0.5	0.3	0.3	0.3	0.6	0.9	0.8	0.6	0.3	0.2	0.2	0.5	0.9	1.0	0.2
14	0.5	0.3	0.3	0.3	0.6	0.9	0.8	0.6	0.3	0.2	0.2	0.5	0.5	0.3	0.2
	0.5	0.3	0.3	0.3	0.6	0.9	0.8	0.6	0.3	0.2	0.2	0.5	0.5	0.2	0.2
	0.5	0.3	0.3	0.3	0.6	0.9	0.8	0.6	0.3	0.2	0.2	0.5	0.5	0.4	0.2
	0.5	0.3	0.3	0.3	0.6	0.9	0.8	0.6	0.3	0.2	0.2	0.5	0.5	0.8	0.2
	0.5	0.3	0.3	0.3	0.6	0.9	0.8	0.6	0.3	0.2	0.2	0.5	0.5	0.6	0.2
	0.5	0.3	0.3	0.3	0.6	0.9	0.8	0.6	0.3	0.2	0.2	0.5	0.5	0.1	0.2

#### 6.4.2 Determination of Ideal Configuration of ANN Model for Sensitivity Analysis

The 109 datasets listed in **Table 6.27** comprising details on the normalized values of the *vehicle and driver characteristics* used in each simulation run of the calibration exercise, and the corresponding predicted *mean absolute errors* were used to train the ANN model. The *EasyNN-plus* software was used for this purpose. The ANN model was initially configured with 14 neurons in the input layer to represent inputs related to 14 vehicle and driver characteristics, 15 neurons in a single hidden layer to perform data processing, and 1 neuron in the output layer to represent the *mean absolute error (MAE)* in simulation observed in each simulation run. The ANN model was then trained under supervision to learn the pattern of relationship between the normalized values of the *vehicle and driver characteristics* used, and the corresponding predicted *mean absolute errors* for 109 rows of the database.

**Table 6.28 Details on Tests Performed for Identifying the Ideal ANN Configuration**

Test Serial No.	Number of Neurons in the Hidden Layers			Mean Absolute Error (MAE) in ANN Prediction (%)	Number of training cycles for convergence
	Hidden Layer No: 1	Hidden Layer No: 2	Hidden Layer No: 3		
1	15	0	0	3.0480	24292
2	14	0	0	2.9003	19779
3	13	0	0	3.6360	22111
<b>*4</b>	<b>12</b>	<b>0</b>	<b>0</b>	<b>2.7941</b>	<b>21671</b>
5	11	0	0	3.2837	14572
6	10	0	0	3.1028	21532
7	9	0	0	3.0600	14390
8	8	0	0	2.9311	18814
9	7	0	0	2.9728	19227
10	6	0	0	2.9309	18141
11	5	0	0	2.8128	90761
12	4	0	0	2.8789	18313
12	12	12	0	3.4537	12402
13	12	11	0	3.7124	12459
14	12	10	0	3.5375	11841
15	12	9	0	3.1344	6030
<b>*16</b>	<b>12</b>	<b>8</b>	<b>0</b>	<b>2.7261</b>	<b>333502</b>
17	12	7	0	3.2525	644120
19	12	8	8	3.4021	12299
20	12	8	7	4.2761	6777
21	12	8	6	4.7326	102589
<b>*22</b>	<b>12</b>	<b>8</b>	<b>5</b>	<b>1.8532</b>	<b>500343</b>
23	12	8	4	2.1801	202849

Note:

Target error = 0.02; Learning rate = 0.7; Momentum rate = 0.8;

Number of neurons in the input layer = 14; and Number of neurons in the output layer = 1.

\*Optimum ANN configurations for the neurons organized in hidden layer 1, hidden layer 2, and hidden layer 3.



The training-errors between the values of the *mean absolute errors* predicted using the ANN model, and the same provided as input was required to be lesser than the target error of 0.02 for all the rows of the dataset. The *EasyNN-plus* software automatically optimized the learning rate to 0.7 and the momentum to 0.8 in the training phase of this study.

### 6.4.3 Method Adopted in the Study of Sensitivity Analysis

In the analysis of relative importance/ *sensitivity* of input variables for ANN structures with a single hidden layer, the Garson's algorithm (**Garson 1991**) is found to be used widely in addition to alternative approaches recommended by **Gevrey et al. (2003 & 2006)**, and **Olden and Jackson (2002)**. **Ozesmi and Ozesmi (1999)** suggested a more robust approach that could handle complex ANN structures with one, two, or more hidden layers.

**Eq.1 to Eq.5** provide details on the formulae adopted in computing the relative importance or sensitivity of input variables based on the methods recommended by **Garson (1991)**, **Gevrey et al. (2003 & 2006)**, **Olden and Jackson (2002)**, and **Ozesmi and Ozesmi (1999)** respectively. It is observed that the *EasyNN-plus* software employs a method similar to that adopted by **Ozesmi and Ozesmi (1999)** to compute the sensitivity of input variables.

**Garson's Algorithm for ANN with one hidden layer:**

$$R_i = (I_{i,j} / \sum_{i=1}^n I_{i,j}) \times 100 \quad \text{Eq.6.1}$$

**Table 6.29** provides the details on the *relative importance* or *sensitivity* of various vehicle and driver characteristics. Here, it can be seen that the *relative importance* or *sensitivity* of *average stand still distance* is 7.65%, which indicates that this variable is more sensitive when compared to other vehicle and driver characteristics. The second most sensitive variable is the *minimum look-ahead distance* bearing a *relative importance* value of 7.50%. Similarly, the third and the fourth most sensitive variables are the *multiplicative part of safety distance* and the *lower bounds for speed distributions* with *relative importance* values of 7.32% and 7.30% respectively. The characteristics such as *maximum acceleration distributions* and

*additive part of safety distance* are also found to be sensitive with the *relative importance* values of 7.23% and 7.21%, whereas, the remaining characteristics are not found to have any significant effect on the accuracy of prediction.

**Table 6.29 Values of the *Relative Importance* of Vehicle and Driver Characteristics Computed Based on the Proposed Alternative Approach**

Sl. No.	Vehicle and Driver Characteristics	Computed Values of Relative Importance (%)
1	Average Standstill Distance (m)	7.65
2	Minimum Look ahead Distance (m)	7.50
3	Multiplicative Part of Safety Distance (m)	7.32
4	Lower Bounds for Speed Distributions (km/h) (Weighted Average)	7.30
5	Maximum Acceleration Distribution (m/s <sup>2</sup> )	7.23
6	Additive Part of Safety Distance (m)	7.21
7	Desired Acceleration Distributions (m/s <sup>2</sup> )	7.12
8	Time-between Direction Changes (s)	7.12
9	Minimum Look back Distance (m)	7.03
10	Minimum Collision Time-gain (s)	7.03
11	Minimum Longitudinal Speed (km/h)	6.98
12	Upper Bounds for Speed Distributions (km/h) (Weighted Average)	6.96
13	Minimum Lateral Clearance (m)	6.83
14	Deceleration Distribution (m/s <sup>2</sup> )	6.71

In the present study, it is observed from **Table 6.29** that the, average standstill distance, minimum look-ahead distance, multiplicative part of safety distance, lower bounds for speed distributions, maximum acceleration distributions, and additive part of safety distance were sensitive when compared to other parameters.

**Otkovic et al. (2013a)** too observe that the average standstill distance, minimum/ maximum look-ahead distance, multiplicative part of desired safety distance, and the additive part of desired safety distance have a significant influence on simulation results.

Similarly, **Mathew and Radhakrishnan (2010)** also observe that the average standstill distance, multiplicative part of desired safety distance, and the additive part of desired safety distance play a major role in ensuring higher prediction accuracies.

## 6.5 EXTENDED MULTI-LEVEL CALIBRATION BASED ON RESULTS OF SENSITIVITY ANALYSIS

This section provides details on the extended multi-level calibration exercise performed using video-graphic database previously kept apart for calibration of the VISSIM Model. The observations made in the ANN-based sensitivity analysis of the vehicle and driver characteristics were used as a guiding tool in this part of the study.

### 6.5.1 Extended First Level of Simulation Based on Sensitivity Analysis

In the first level of the extended multi-level calibration exercise based on the results of the sensitivity analysis, refinements in the value of the *average standstill distance* were performed for various vehicle-types using a trial and error approach. A refined value of 0.60m was found to be ideal for all vehicle categories as shown in Table 6.30a.

**Table 6.30a Refined Value of Driving Behavior Characteristic (Car Following) Assigned**

Driving Behavior Characteristic	Modified Value	Value Previously Assigned at the End of the Main Calibration
Average Standstill Distance (m)	0.60m	1.0

**Table 6.30b Comparison of Actual and Simulated Traffic Volumes at 18 Mid-Block Locations for the First Level of Extended Multi-level Simulation**

Direction		Simulated	Observed	Observed-Simulated	Error (%)	Abs. Error (%)	GEH STATISTIC
From	To						
Jyothi	Hampankatta	2551	2580	29	1.1	1.1	0.57
Hampankatta	Jyothi	2168	2320	152	6.6	6.6	3.21
PVS	Bunts	1352	1465	113	7.7	7.7	3.01
Bunts	PVS	1431	1505	74	4.9	4.9	1.93
Navabharat	PVS	2371	2510	139	5.5	5.5	2.81
PVS	Navabharat	2306	2370	64	2.7	2.7	1.32
Hampankatta	Navabharat	2091	2225	134	6.0	6.0	2.88
Navabharat	Hampankatta	1783	2100	317	15.1	15.1	7.19
Bendoorwell	St. Theresa	1157	1205	48	4.0	4.0	1.40
St. Theresa	Bendoorwell	1062	1100	38	3.5	3.5	1.16
				<b>Average</b>	<b>5.2%</b>	<b>5.5%</b>	<b>2.34</b>

### 6.5.2 Extended Second Level of Simulation Based on Results of Sensitivity Analysis

In the second level of the extended multi-level simulation exercise based on the results of the sensitivity analysis, the values of *minimum look-ahead distances* were further refined from the existing value of 40m for various vehicle-types using a trial and

error approach. Values of 20m for motorized two-wheelers and auto-rickshaws, 25m for cars and LCVs, and 30m for buses and trucks were assigned as shown in **Table 6.31a**.

**Table 6.31b Comparison of Actual and Simulated Traffic Volumes at 18 Mid-Block Locations for the Second Level of Extended Calibration**

Direction		Simulated	Observed	Observed-Simulated	Error (%)	Abs. Error (%)	GEH STATISTIC
From	To						
Jyothi	Hampankatta	2587	2580	-7	-0.3	0.3	0.14
Hampankatta	Jyothi	2168	2320	152	6.6	6.6	3.21
PVS	Bunts	1322	1465	143	9.8	9.8	3.83
Bunts	PVS	1442	1505	63	4.2	4.2	1.64
Navabharat	PVS	2433	2510	77	3.1	3.1	1.55
PVS	Navabharat	2303	2370	67	2.8	2.8	1.39
Hampankatta	Navabharat	2095	2225	130	5.8	5.8	2.80
Navabharat	Hampankatta	1794	2100	306	14.6	14.6	6.93
Jyothi	Bunts	1942	2020	78	3.9	3.9	1.75
Bunts	Jyothi	1903	1970	67	3.4	3.4	1.52
Jyothi	Balmatta	1665	1830	165	9.0	9.0	3.95
<b>Average</b>					<b>4.9%</b>	<b>5.2%</b>	<b>2.21</b>

### 6.5.3 Extended Third Level of Simulation Based on Results of Sensitivity Analysis

In the third level of the extended multi-level simulation exercise based on the results of the sensitivity analysis, the value of *multiplicative part of safety distance* was further refined for various vehicle-types using a trial and error approach. A value of 0.45m was found to be ideal for all vehicle categories as shown in **Table 6.32a**.

**Table 6.32b Comparison of Actual and Simulated Traffic Volumes at 18 Mid-Block Locations for the Third Level of Extended Calibration**

Direction		Simulated	Observed	Observed-Simulated	Error (%)	Abs. Error (%)	GEH STATISTIC
From	To						
St. Theresa	Balmatta	816	805	-11	-1.4	1.4	0.39
Bendoorwell	Balmatta	1477	1455	-22	-1.5	1.5	0.57
Balmatta	Bendoorwell	1498	1680	182	10.8	10.8	4.57
Bendoorwell	St. Theresa	1160	1205	45	3.7	3.7	1.31
St. Theresa	Bendoorwell	1061	1100	39	3.5	3.5	1.19
<b>Average</b>					<b>4.6%</b>	<b>5.0%</b>	<b>2.12</b>

### 6.5.4 Extended Fourth Level of Simulation Based on Results of Sensitivity Analysis

In the fourth level of the extended multi-level simulation exercise based on the results of the sensitivity analysis, the *lower bound values for speed distributions* were further refined for various vehicle-types using a trial and error approach.

**Table 6.33b Comparison of Actual and Simulated Traffic Volumes at 18 Mid-Block Locations for the Fourth Level of Extended Calibration**

Direction		Simulated	Observed	Observed-Simulated	Error (%)	Abs. Error (%)	GEH STATISTIC
From	To						
Jyothi	Hampankatta	2581	2580	-1	0.0	0.0	0.02
Navabharat	Hampankatta	1797	2100	303	14.4	14.4	6.86
Jyothi	Bunts	1934	2020	86	4.3	4.3	1.93
Bunts	Jyothi	1926	1970	44	2.2	2.2	1.00
Jyothi	Balmatta	1659	1830	171	9.3	9.3	4.09
				<b>Average</b>	<b>4.3%</b>	<b>4.6%</b>	<b>1.97</b>

### 6.5.5 Extended Fifth Level of Simulation Based on Results of Sensitivity Analysis

In the fifth level of the extended multi-level refinement exercise performed based on the results of the sensitivity analysis, the vehicle characteristic *maximum acceleration distribution* for various vehicle-types was smoothed where, minor corrections to the trend-line between acceleration and speed was applied. Similar approaches were adopted by **Mathew and Radhakrishnan (2010)**, **Mehar et al. (2014)**, and **Bains et al. (2013)**.

### 6.5.6 Extended Sixth Level of Simulation Based on Results of Sensitivity Analysis

In the sixth level of the extended multi-level simulation exercise based on the results of the sensitivity analysis, the value of *additive part of safety distance* was further refined for various vehicle-types using a trial and error approach. A value of 0.35m was found to be ideal for all vehicle categories as shown in **Table 6.35a**.

**Table 6.34 Comparison of Actual and Simulated Traffic Volumes at 18 Mid-Block Locations for the Fifth Level of Extended Calibration**

Direction		Simulated	Observed	Observed-Simulated	Error (%)	Abs. Error (%)	GEH STATISTIC
From	To						
Balmatta	St. Theresa	668	710	42	5.9	5.9	1.60
St. Theresa	Balmatta	818	805	-13	-1.6	1.6	0.46
Bendoorwell	Balmatta	1472	1455	-17	-1.2	1.2	0.44
Balmatta	Bendoorwell	1501	1680	179	10.7	10.7	4.49
Bendoorwell	St. Theresa	1152	1205	53	4.4	4.4	1.54
St. Theresa	Bendoorwell	1059	1100	41	3.7	3.7	1.25
				<b>Average</b>	<b>4.2%</b>	<b>4.6%</b>	<b>1.95</b>

For the revised value for *additive part of safety distance*, the *mean absolute error* was computed as summarized in **Table 6.35b**.

**Table 6.35b Comparison of Actual and Simulated Traffic Volumes at 18 Mid-Block Locations for the Sixth Level of Extended Calibration**

Direction		Simulated	Observed	Observed-Simulated	Error (%)	Abs. Error (%)	GEH STATISTIC
From	To						
Jyothi	Hampankatta	2576	2580	4	0.2	0.2	0.08
Hampankatta	Jyothi	2166	2320	154	6.6	6.6	3.25
PVS	Bunts	1371	1465	94	6.4	6.4	2.50
Bunts	PVS	1441	1505	64	4.3	4.3	1.67
Navabharat	PVS	2417	2510	93	3.7	3.7	1.87
PVS	Navabharat	2318	2370	52	2.2	2.2	1.07
Hampankatta	Navabharat	2095	2225	130	5.8	5.8	2.80
Navabharat	Hampankatta	1777	2100	323	15.4	15.4	7.34
Jyothi	Bunts	1931	2020	89	4.4	4.4	2.00
Bunts	Jyothi	1906	1970	64	3.2	3.2	1.45
				<b>Average</b>	<b>4.6%</b>	<b>5.0%</b>	<b>2.12</b>

**Fig.6.8a** provides a graphical representation of the reduction in the *mean absolute prediction errors* for flows measured across 18 mid-block sections using the VISSIM model for the extended multi-level simulations aimed at refinement of vehicle and driver characteristics performed based on the relative sensitivity values obtained using the ANN approach.

**Fig.6.8b** provides a graphical representation of the reduction in the *mean absolute prediction errors* for flows measured across 18 mid-block sections using the VISSIM model for the calibration exercise and the extended multi-level calibration exercise aimed at refinement of vehicle and driver characteristics.

## 6.6 EXTENDED VALIDATION BASED ON RESULTS OF SENSITIVITY ANALYSIS

The refined values of vehicle and driver characteristics obtained based on the extended multi-level calibration exercise described in **Section 6.5** were incorporated in the VISSIM micro-simulation model, and the extended validation exercise was performed using the 20-minute video-graphic data kept apart for validation earlier.

### 6.6.1 Extended Validation of Volumes

The extended validation exercise was performed using the refined values of vehicle and driver characteristics in a manner similar to that described in as described in **Section 6.3**. Here, the *mean absolute error (MAE)* was found to be 9.5%, while the *GEH* value was around 2.43 as shown in **Table 6.36**. The low values of the *GEH*

statistic (lesser than 5.0) for the validation and calibration models indicate that the simulated vehicular volumes are within tolerable limits.

**Table 6.36 Extended Validation Results for Volume at 18 Mid-block Sections after Extended Calibration: Random Seed 42**

Direction		Simulated	Observed	Observed-Simulated	Error (%)	Abs. Error (%)	GEH Statistic
From	To						
Balmatta	Jyothi	857	775	-82	-10.6	10.6	2.87
Balmatta	St. Theresa	270	260	-10	-3.8	3.8	0.61
St. Theresa	Balmatta	239	250	11	4.4	4.4	0.70
Bendoorwell	Balmatta	461	455	-6	-1.3	1.3	0.28
Balmatta	Bendoorwell	574	550	-24	-4.4	4.4	1.01
Bendoorwell	St. Theresa	391	435	44	10.1	10.1	2.17
St. Theresa	Bendoorwell	332	395	63	15.9	15.9	3.30
<b>Average</b>				<b>2.8%</b>	<b>9.5%</b>	<b>2.43</b>	

Fig.6.9 provides a pictorial representation of the differences between the observed volumes and the simulated volumes for vehicular flows along the 18 mid-block sections for the extended validation using random seed 42.

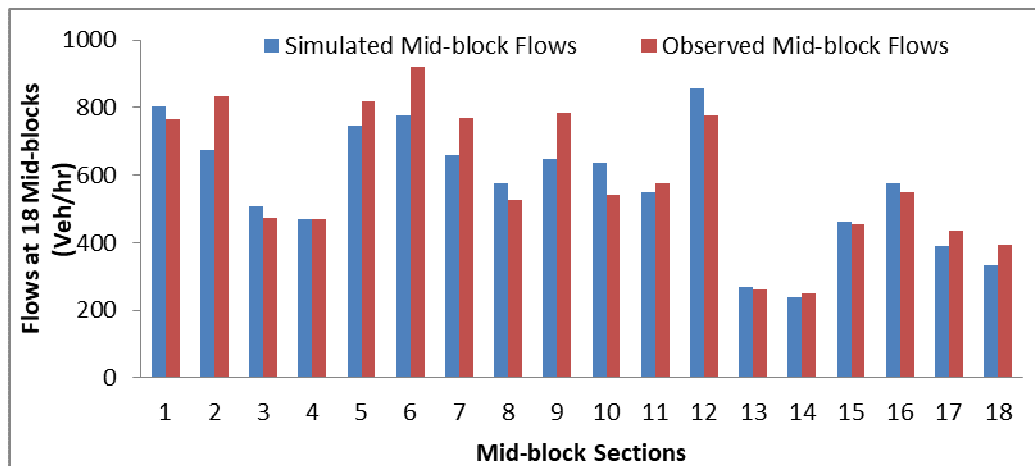


**Fig.6.9 Comparison of Observed and Simulated Flows at 18 Mid-block Locations for Extended Validation after Extended Calibration Using Random Seed 42**

## CHAPTER 7

### ANALYSES USING VISSIM FOR SHORT-TERM AND LONG-TERM IMPROVEMENTS

#### 7.1 INTRODUCTION

The details on the *basic multi-level calibration* exercises, and the *basic validation* exercises performed as part of development of the VISSIM model, were discussed in the previous chapter, in addition to details on the sensitivity analysis performed using an ANN-based approach by adopting a new *modified Garson's approach* developed as part of this study. The simulation exercises performed as part of the *extended multi-level calibration* exercise further improved upon the predictive capability of the VISSIM model which was verified using the *extended validation* exercise.

The refined VISSIM model with the improved values of vehicle and driver characteristics was found to be capable of simulating the traffic flows at 18 mid-block sections of the road network of the city, and satisfied important criteria specified by **DMRB (1996)**, **FHA (2004)** and **Wisconsin DOT (2002)**.

Having developed a reliable VISSIM model to simulate traffic flows along important traffic routes in the city, it was proposed to analyse the effect of implementation of *short-term* improvement strategies at selected locations in the city as listed below:

- ***Short-term Improvement Strategy-1:*** Widening of the road section between Karangalpady Junction and Bunt's Hostel Junction in order to facilitate the movement of vehicles towards Jyothi Junction and also towards Kadri Junction via Bunt's Hostel Junction.
- ***Short-term Improvement Strategy-2:*** Widening of the road section at Bendoorwell Junction in order to facilitate the movement of vehicles towards St. Theresa's School Junction, and also towards Balmatta Junction via Bendoorwell Junction.



The simulated volumes, simulated average stopped delays, and the simulated speeds for the above studies were then compared to the actual observations made before implementation of the *short-term improvements*.

As part of the *long-term improvement* strategy, it was proposed to include the following studies in order to examine the influence of the use of flyovers at selected road sections:

- ***Long-term Improvement Strategy-1:*** The use of a flyover in order to facilitate the movement of vehicles arriving from PVS Junction, moving towards Jyothi Junction and also towards Kadri Junction.
- ***Long-term Improvement Strategy-2:*** The use of a flyover in order to facilitate the movement of vehicles arriving from Kankanady Junction moving towards St. Theresa's School Junction.

Here too, the simulated volumes and the simulated speeds for the above studies were compared to the actual observations made before implementing the *long-term improvements*.

In these studies, the values of vehicle and driver-characteristics were adopted based on the fine-tuned values at the final stage of the *extended multi-level calibration* exercise. The following sections provide details on the analyses related to evaluation of *short-term* and *long-term* strategies.

## **7.2 ANALYSIS OF SHORT-TERM IMPROVEMENT STRATEGY-1:**

As part of *Short-Term Improvement Strategy-1*, it was proposed to analyse the effect of widening of the road section between Karangalpady Junction and Bunt's Hostel Junction in order to facilitate the movement of vehicles towards Jyothi Junction and also towards Kadri Junction via Bunt's Hostel Junction. **Fig.7.1a** provides details on the existing layout of the road section between Karangalpady Junction and Bunt's Hostel Junction. The *.net* network file used for calibration and validation exercises in *VISSIM* was modified to incorporate the proposed short-term improvements related to minor widening of the road section between Karangalpady

Junction and Bunt's Hostel Junction. The 20-minute video-graphic data kept apart for validation studies was used in this part of the study.

The width of the road section between Karangalpady Junction and Bunt's Hostel Junction was proposed to be increased to a minor extent as part of the *short-term improvement strategy* from the existing widths of 3.1-3.3m to a width of 3.8m for Link 1 and Link 2, ensuring a minimum lane width of 3.5m to conform to road geometric standards as per IRC 86 (**IRC 1983**). Also, increased the existing road width of 4.0m to a width of 5.0m for Link 3. Further widening was not possible in this road section due to site-restrictions in the built-up area, and the presence of commercial buildings in the vicinity.

As part of this strategy, it was also required to reduce the existing width of the adjoining footpath from around 1.8-2.2m to a minimum width of 1.5m as per IRC 86 (**IRC 1983**) in order to compensate for the increase in the road width. Additionally, the width of a road link close to Bunt's Hostel Junction was proposed to be widened from 4m to 5m to facilitate faster movement of vehicles.

### ***Traffic Flows from Karangalpady Junction to Jyothi Junction via Bunt's Hostel Junction***

A summary of the observations on traffic flows from Karangalpady Junction to Jyothi Junction via Bunt's Hostel Junction with respect to simulated volumes, simulated speeds, and average stopped delays is provided in **Table 7.1b**. Here, it can be observed that the simulated average stopped delays have reduced from 293.20s to 85.32s resulting in a savings of 71% in fuel loss due to idling of vehicles. The level of improvement in stopped delays for auto-rickshaws, buses, cars, and motorized two-wheelers were observed to be 59%, 81%, 71%, and 66% respectively. **Fig.7.1c** provides a pictorial representation of the comparison between the simulated delays for various vehicle types before and after widening of the road for the above-mentioned directions of traffic movement.

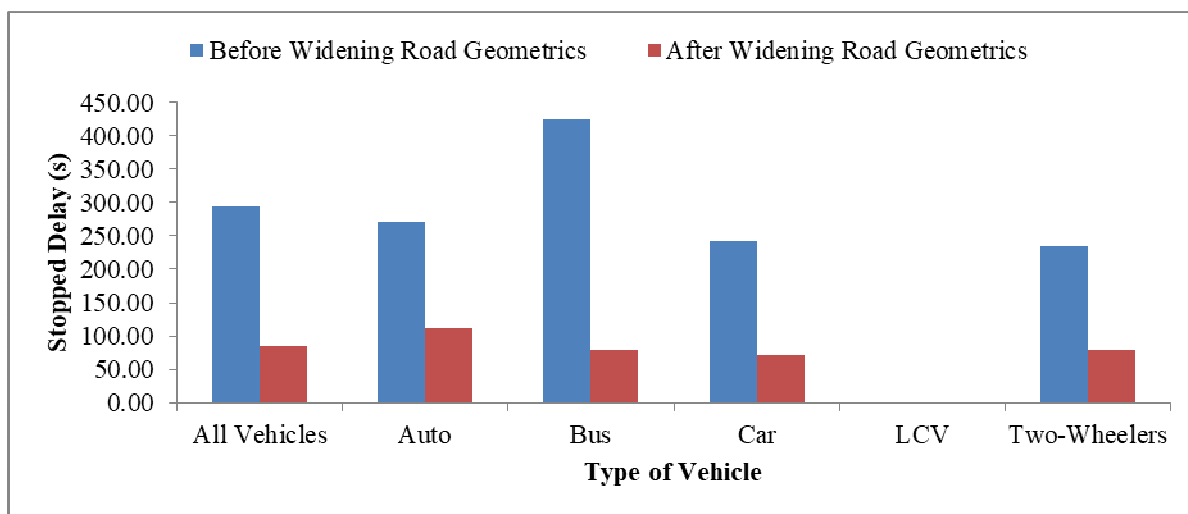


**Fig.7.1c Short-Term Improvement Strategy-1: Comparison of Simulated Stopped Delays for Flows between Karangalpady and Jyothi Junctions via Bunt’s Hostel Junction**

**Table 7.1b Short-Term Improvement Strategy-1: Comparison of Simulated Volumes, Speeds and Stopped Delays for Flows between Karangalpady and Jyothi Junction via Bunt’s Hostel Junction**

Volume and Percentage of Vehicles (veh/h)			
Vehicle Types	*Before Widening of Road Geometrics	*After Widening of Road Geometrics	Level of Improvement (%)
All Vehicles	209 (100.00%)	249 (100.00%)	19%
Auto	34 (16.27%)	44 (17.67%)	29%
Bus	16 (07.66%)	20 (08.03%)	25%
Car	53 (25.36%)	78 (31.33%)	47%
LCV	0 (00.00%)	0 (00.00%)	-
Two-Wheelers	106 (50.72%)	107 (42.97%)	1%

\* The percentages for each vehicle-type are shown in parenthesis.

It may be observed in this study that a minor widening of the road section by 0.5-1.0m has resulted in an appreciable reduction in the average stopped delays due to the reason that the vehicles were able to manoeuvre and move ahead on the road section between Karangalpady and Jyothi Junctions with minimal stoppages. This is evident in the simulation runs in terms of the increase in the simulated volumes of auto-rickshaws, buses, cars, and motorized two-wheelers by 29%, 25%, 47%, and 1% respectively.

While examining the speeds, it can be observed that the simulated space-mean speeds of all vehicles moving between Karangalpady Junction and Jyothi Junction have increased from 20.46kmph to 27.06kmph. It may be observed that the ~~space-mean speeds~~ of auto-rickshaws, buses, cars, and motorized two-wheelers have witnessed an increase in space-mean speeds by 35%, 30%, 30%, and 35% respectively as shown in **Fig.7.1e**.

***Traffic Flows from Karangalpady Junction to Kadri Junction via Bunt’s Hostel Junction***

**Table 7.1c** provides a summary of the observations for traffic flows from Karangalpady Junction to Kadri Junction via Bunt’s Hostel Junction with respect to simulated volume, simulated speeds and average stopped delays. Here too, it is observed that the simulated average stopped delays have reduced from 344.73s to 118.50s resulting in a savings of 66% in fuel loss due to idling of vehicles. The level of improvement in average stopped delays for auto-rickshaws, buses, cars, LCVs, and motorized two-wheelers were observed to be 73%, 81%, 60%, 56%, and 58% respectively.

**Table 7.1c Short-Term Improvement Strategy-1: Comparison of Simulated Volumes, Speeds and Stopped Delays for Flows between Karangalpady and Kadri Junction via Bunt’s Hostel Junction**

Volume and Percentage of Vehicles (veh/h)			
Vehicle Types	*Before Widening of Road Geometrics	*After Widening of Road Geometrics	Level of Improvement (%)
All Vehicles	389 (100.00%)	450 (100.00%)	16%
Auto	61 (15.68%)	61 (13.56%)	0%
Bus	8 (02.06%)	11 (02.44%)	38%
Car	95 (24.42%)	95 (21.11%)	0%
LCV	6 (01.54%)	11 (02.44%)	83%
Two-Wheelers	219 (56.30%)	272 (60.44%)	24%

\* The percentages for each vehicle-type are shown in parenthesis.

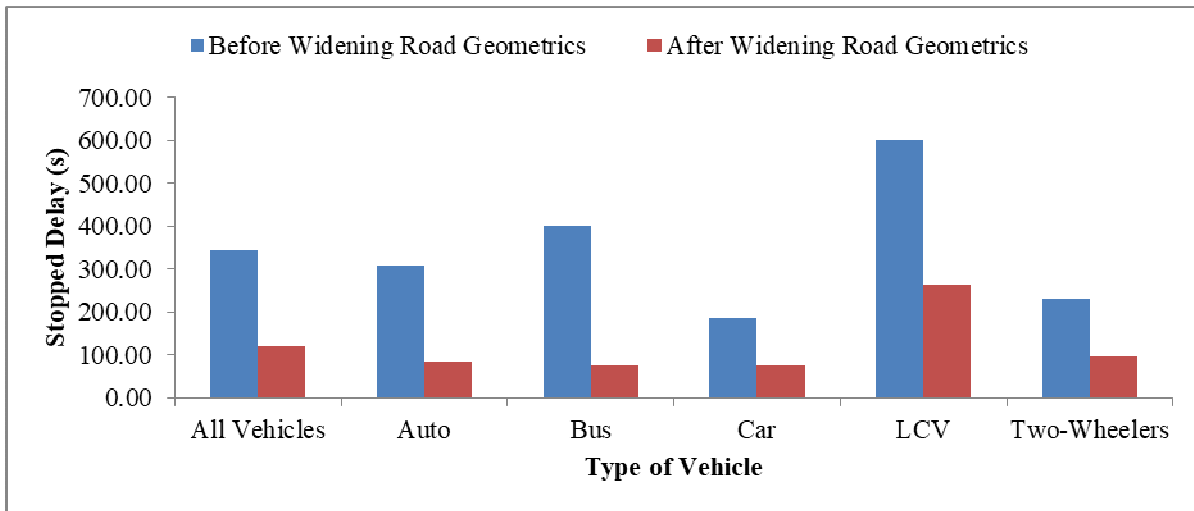


**Fig.7.1f Short-Term Improvement Strategy-1: Comparison of Simulated Stopped Delays for Flows between Karangalpady and Kadri Junctions via Bunt’s Hostel Junction**

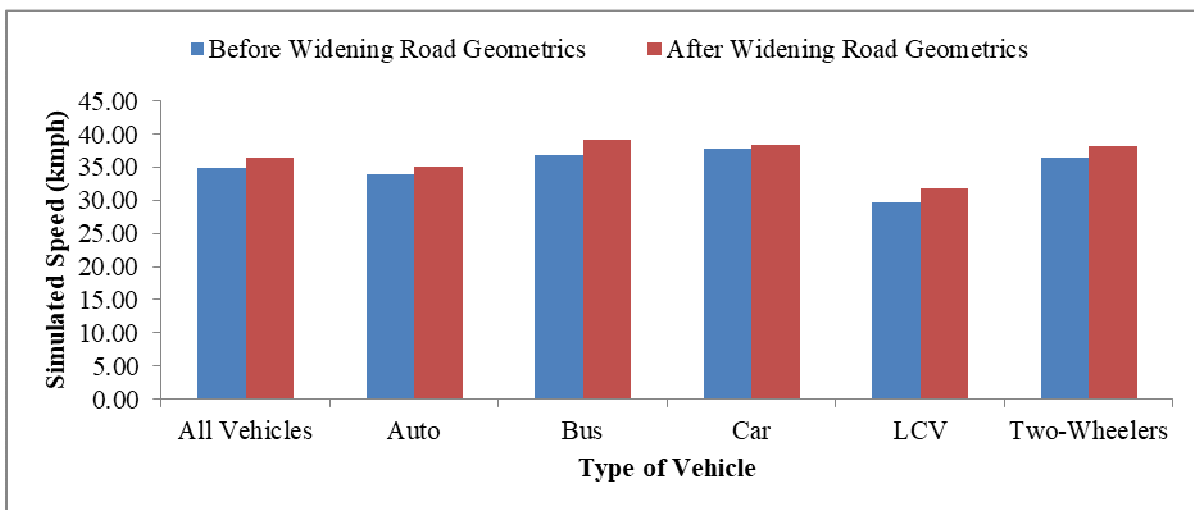


**Fig.7.1h Short-Term Improvement Strategy-1: Comparison of Simulated Speeds for Flows between Karangalpady and Kadri Junctions via Bunt’s Hostel Junction**

The reduction in average stopped delays can be attributed to a minor widening and streamlining of the existing carriageway as indicated earlier by about 0.5-1.0m. This has facilitated faster movement of motorized two-wheelers as mentioned in the case of the previous road section analysed. This is also evident from the increase in the simulated volume of buses, LCVs, and motorized two-wheelers by 38%, 83%, and 24%. **Fig.7.1g** provides a pictorial representation of the comparison between the simulated volumes for various vehicle types before and after widening the road sections. While analysing the speeds, it can be observed that the simulated space-mean speeds of all vehicles moving between Karangalpady Junction and Jyothi

Junction have increased from 34.96kmph to 36.49kmph showing an improvement of 4%.

### ***General Observations on Short-term Improvement Strategy-1***

Considering the performance of the road section for traffic flows from Karangalpady Junction to Jyothi Junction *via Bunt's Hostel Junction* as described in **Table 7.1b**, it can be seen that there is a moderate improvement in vehicular volumes by 19%, with a significant decrease in the average stopped delays by 71% for different types of vehicles as measured by *VISSIM*. With regard to the performance of the road section for traffic flows from Karangalpady Junction to Kadri Junction described in **Table 7.1c**, it can be seen that there is a considerable improvement in vehicular volumes by 16% and a significant decreased in the average stopped delays by 66% for different types of vehicles as measured by *VISSIM*.

### **7.3 ANALYSIS OF SHORT-TERM IMPROVEMENT STRATEGY-2:**

As part of *Short-Term Improvement Strategy-2*, it was proposed to analyse the effect of widening of the road sections at Bendoorwell Junction to streamline traffic flows towards St. Theresa's School Junction and Balmatta Junction. **Fig.7.2a** provides details on the existing layout of the road section between Kankanady Junction and Balmatta Junction. The *.net* network file used for calibration and validation exercises in *VISSIM* was modified to incorporate the proposed short-term improvements related to minor widening of the road sections at Bendoorwell Junction. The 20-minute video-graphic data kept apart for validation studies was used in this part of the study.

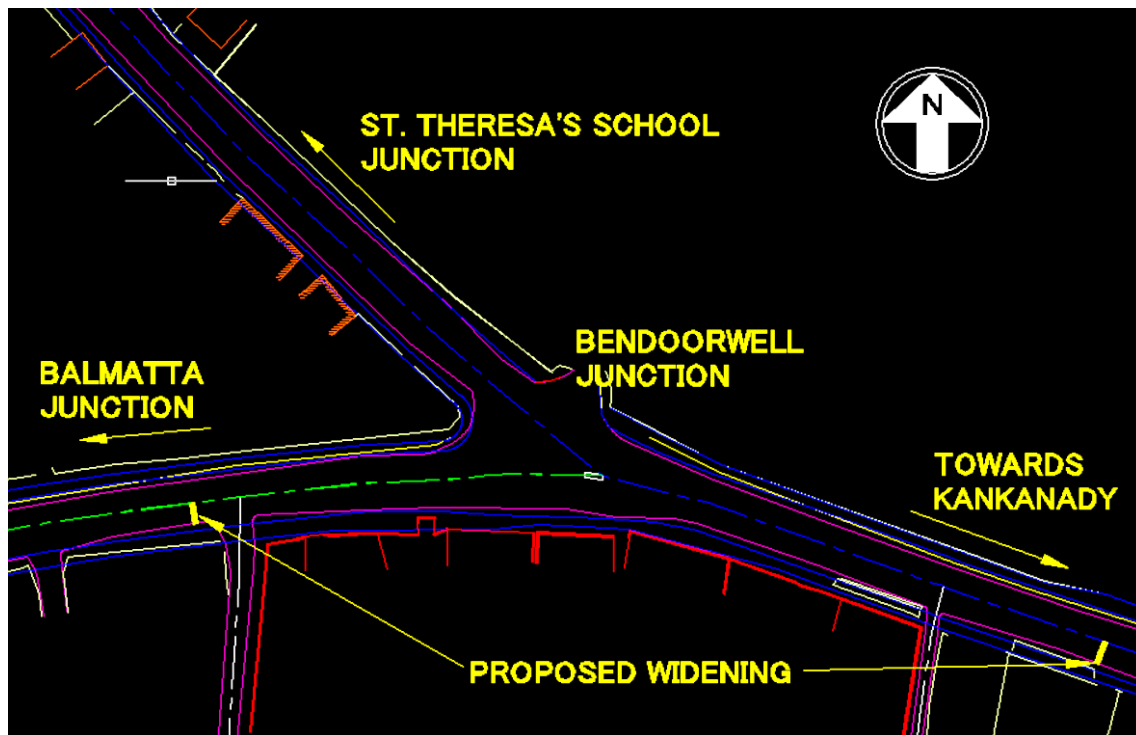


**Fig.7.2a Layout of the Existing Road Alignment at Bendoorwell Junction**

As part of this strategy, it was also required to reduce the existing width of the adjoining footpath from around 1.8-2.2m to a minimum width of 1.5m specified as per **IRC 86 (1983)** in order to compensate for the increase in the road width.

**Table 7.2a Lane-Width Measured Before and After Minor Road Widening Near Bendoorwell Junction**

	Assigned Lane	Width before Widening (m)	Width after Widening (m)
Link 1	Lane 1 (inner)	4.0	5.0
	Lane 2 (outer)	4.0	5.0
Link 2	Lane 1 (inner)	3.5	3.5
	Lane 2 (outer)	3.5	5.0

***Traffic Flows from Kankanady to St. Theresa’s School Junction via Bendoorwell Junction***

A summary of the observations on traffic flows for vehicles arriving from Kankanady Junction, moving towards St. Theresa’s School Junction via Bendoorwell Junction with respect to simulated volumes, simulated speeds, and average stopped delays is provided in **Table 7.2b**. Here, it can be observed that the simulated average stopped delays have reduced from 20.31s to 8.44s resulting in a savings of 58% in

fuel loss due to idling of vehicles. The level of improvement in average stopped delays for auto-rickshaws, buses, cars, LCVs, and motorized two-wheelers were observed to be 53%, 79%, 45%, 70%, and 33% respectively. **Fig.7.2c** provides a pictorial representation of the comparison between the simulated delays for various vehicle types before and after widening of the road for the above-mentioned directions of traffic movement.

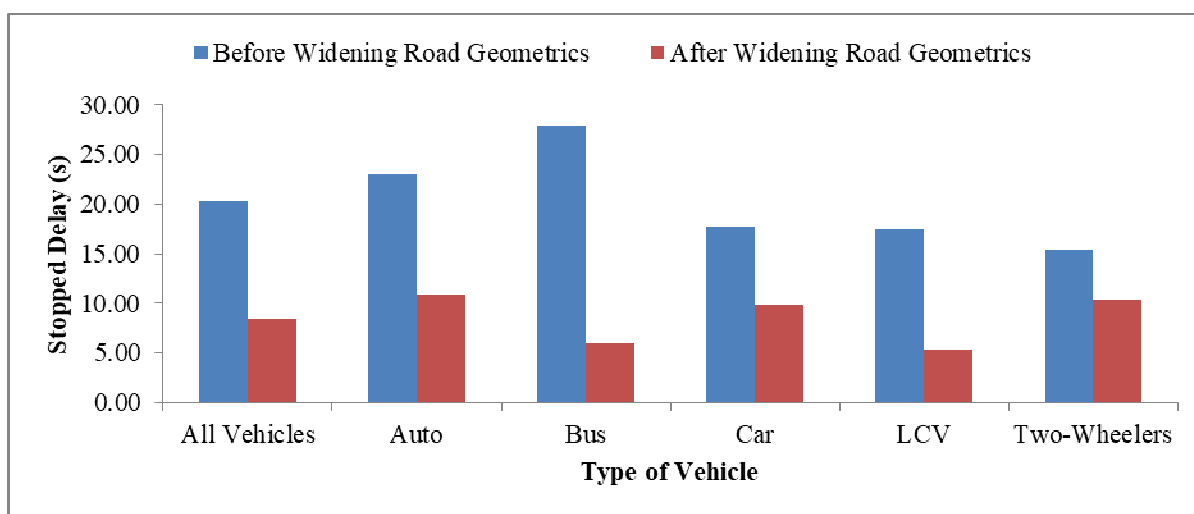


**Fig.7.2c Short-Term Improvement Strategy-2: Comparison of Simulated Stopped Delays for Flows between Kankanady and St. Theresa’s School Junction for Various Vehicle Types**

**Fig.7.2d** provides a pictorial representation of the comparison between the simulated volumes of various vehicle types before and after widening the road for the above-mentioned direction of traffic movement.

**Table 7.2b Short-Term Improvement Strategy-2: Comparison of Simulated Volumes, Speeds and Stopped Delays for Flows between Kankanady and St. Theresa’s School Junction**

Volume and Percentage of Vehicles (veh/h)			
Vehicle Types	*Before Widening of Road Geometrics	*After Widening of Road Geometrics	Level of Improvement (%)
All Vehicles	337 (100.00%)	345 (100.00%)	2%
Auto	25 (07.42%)	30 (08.70%)	20%
Bus	8 (02.37%)	9 (02.61%)	13%
Car	110 (32.64%)	119 (34.49%)	8%
LCV	7 (02.08%)	9 (02.61%)	29%
Two-Wheelers	187 (55.49%)	178 (51.59%)	-5%

\* The percentages for each vehicle-type are shown in parenthesis.



In the case of speeds, it can be observed that the simulated space-mean speeds of all vehicles approaching from Kankanady Junction, and moving towards St. Theresa's School Junction have increased marginally from 30.00kmph to 32.521kmph showing an overall improvement of 8%. It may be observed that the space-mean speeds of buses, cars, and light commercial vehicles (LCVs) have witnessed an increase by 16%, 4%, and 35% respectively, while in the case of other types of vehicles such as auto-rickshaws and motor-cycles, the simulated space-mean speeds have shown a marginal reduction as shown in **Fig.7.2e**.

***Traffic Flows from Kankanady Junction to Balmatta Junction via Bendoorwell Junction***

**Table 7.2c** provides a summary of the observations for traffic flows from Kankanady Junction to Balmatta Junction via Bendoorwell Junction with respect to simulated volume, simulated speeds and average stopped delays. Here, it is observed that the simulated average stopped delays were already much lesser, ranging between 7-10s, and that the nature of flow remained almost the same since traffic along this straight direction at the T-junction is relatively free from obstructions. With the improvement in the flows at the junction, the simulated average stopped delays have reduced to values lesser than 1.5s, resulting in an overall savings of 93% in fuel loss due to idling of vehicles. The level of improvement in average stopped delays for auto-rickshaws, buses, cars, LCVs, and motorized two-wheelers were observed to be 90%, 95%, 84%, 100%, and 94% respectively.

**Table 7.2c Short-Term Improvement Strategy-2: Comparison of Simulated Volumes, Speeds and Stopped Delays for Flows between Kankanady and Balmatta Junction**

<b>Volume and Percentage of Vehicles (veh/h)</b>			
<b>Vehicle Types</b>	<b>*Before Widening of Road Geometrics</b>	<b>*After Widening of Road Geometrics</b>	<b>Level of Improvement (%)</b>
All Vehicles	410 (100.00%)	467 (100.00%)	14%
Auto	74 (18.05%)	79 (16.92%)	7%
Bus	22 (05.37%)	21 (04.50%)	-5%
Car	152 (37.07%)	166 (35.55%)	9%
LCV	3 (00.73%)	4 (00.86%)	33%
Two-Wheelers	159 (38.78%)	197 (42.18%)	24%

\* The percentages for each vehicle-type are shown in parenthesis.

***General Observations on Short-term Improvement Strategy-2***

Considering the performance in the road section for traffic flows arriving from Kankanady Junction, moving towards St. Theresa's School Junction via Bendoorwell Junction described in **Table 7.2b**, it can be said that there is an overall improvement in the flow of vehicles by 2%, with a reduction in average stopped delays by 58% as measured using *VISSIM*.

#### **7.4 ANALYSIS OF LONG-TERM IMPROVEMENT STRATEGY-1:**

As part of *Long-Term Improvement Strategy-1*, it was proposed to analyse the effect of addition of a flyover to handle traffic arriving from PVS Junction, moving towards Jyothi Junction and from PVS Junction towards Kadri Junction via Karangalpady Junction and Bunt's Hostel Junction. **Fig.7.1a** provided in the earlier section gives details on the existing layout of Bunt's Hostel Junction.

The flyover at Bunt's Hostel Junction was proposed as part of a long-term improvement strategy to reduce the congestion at Bunt's Hostel Junction and at Karangalpady Junction which are about 100m apart.

In order to represent the traffic flows along the flyover, the base-network was modified to incorporate additional links for handling traffic arriving at Bunt's Hostel from PVS Junction, moving towards Jyothi Junction, and towards Kadri Junction.

##### ***Traffic Flows from PVS Junction to Jyothi Junction via Bunt's Hostel Junction***

A summary of the observations for traffic flows from PVS Junction moving towards Jyothi Junction via Bunt's Hostel Junction with respect to simulated volumes and speeds is provided in **Table 7.3a**. Here, it is observed that the overall simulated vehicular volumes have increased from 209 to 315 vehicles resulting in an improvement of 51%. The level of improvement in volumes for auto-rickshaws, buses, cars, and motorized two-wheelers were observed to be 76%, 19%, 25%, and 60% respectively. **Fig.7.3b** provides a pictorial representation of the comparison between the simulated volumes for various vehicle types before and after introduction of the flyover for the above-mentioned direction of traffic movement. It may be observed that stopped delays will be completely eliminated with the introduction of the flyover.

**Table 7.3a Long-Term Improvement Strategy-1: Comparison of Simulated Volumes and Speeds for Flows between PVS Junction and Jyothi Junction via Bunt’s Hostel Junction**

Volume and Percentage of Vehicles (veh/h)			
Vehicle Types	*Before providing the Flyover	*After providing the Flyover	Level of Improvement (%)
All Vehicles	209 (100.00%)	315 (100.00%)	51%
Auto	34 (16.27%)	60 (19.05%)	76%
Bus	16 (07.66%)	19 (06.03%)	19%
Car	53 (25.36%)	66 (20.95%)	25%
LCV	0 (00.00%)	0 (00.00%)	-
Two-Wheelers	106 (50.72%)	170 (53.97%)	60%

\* The percentages for each vehicle-type are shown in parenthesis.

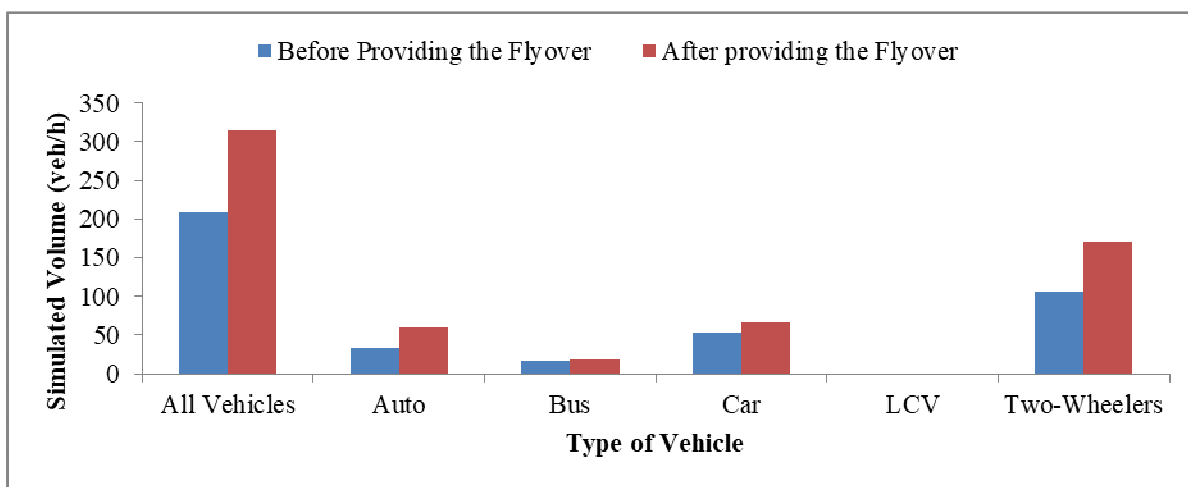


**Fig.7.3b Long-Term Improvement Strategy-1: Comparison of Simulated Volumes for Flows between PVS Junction and Jyothi Junction via Bunt’s Hostel Junction**

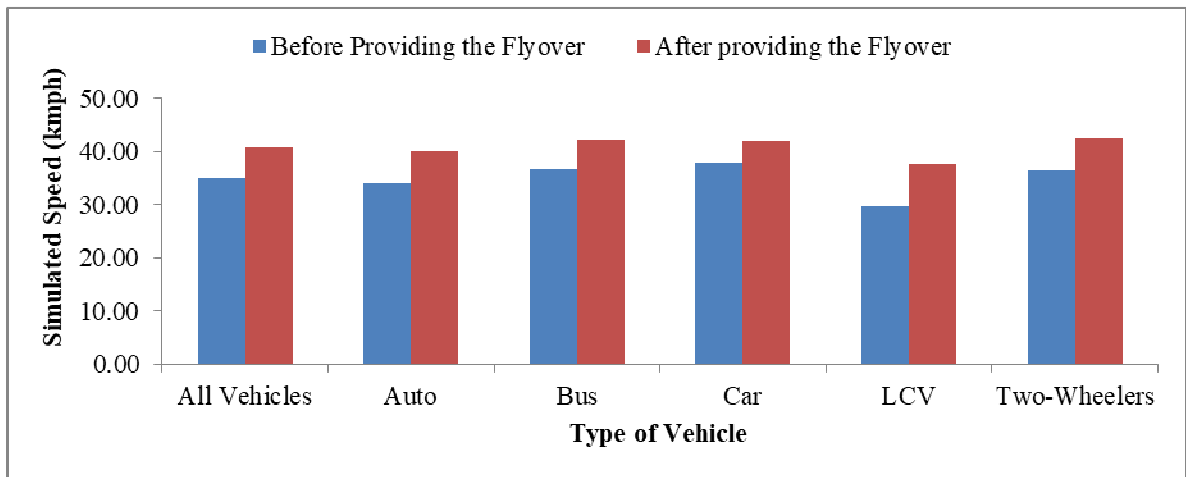
**Traffic Flows from PVS Junction to Kadri Junction via Bunt’s Hostel Junction**

Table 7.3b provides a summary of the observations for traffic flows from PVS Junction moving towards Kadri Junction via Bunt’s Hostel Junction with respect to simulated volumes and speeds. Here too, it is observed that the overall simulated vehicular volumes have increased from 389 to 444 vehicles resulting in an improvement of 14%. The level of improvement in volumes for auto-rickshaws, buses, cars, LCVs, and motorized two-wheelers were observed to be 49%, 25%, 12%, 33%, and 5% respectively. Fig.7.3d provides a pictorial representation of the comparison between the simulated volumes for various vehicle types before and after introduction of the flyover for the above-mentioned direction of traffic movement. It may be observed that stopped delays will be completely eliminated with the introduction of the flyover.

**Table 7.3b Long-Term Improvement Strategy-1: Comparison of Simulated Volumes and Speeds for Flows between PVS Junction and Kadri Junction via Bunt’s Hostel Junction**

Space Mean Speed (kmph)			
Vehicle Types	Before providing the Flyover	After providing the Flyover	Level of Improvement (%)
All Vehicles	34.96	40.85	17%
Auto	33.99	40.05	18%
Bus	36.79	42.21	15%
Car	37.78	41.92	11%
LCV	29.71	37.58	26%
Two-Wheelers	36.52	42.51	16%

\* The percentages for each vehicle-type are shown in parenthesis.



**Fig.7.3e Long-Term Improvement Strategy-1: Comparisons of Simulated Speeds for Flows between PVS Junction and Kadri Junction via Bunt’s Hostel Junction**

**General Observations on Long-term Improvement Strategy-1**

Considering the performance of a flyover for traffic flows from Karangalpady Junction to Jyothi Junction and Kadri Junction described in **Table 7.3a** and **Table 7.3b**, it can be seen that there is a considerable improvement in vehicular volumes by 51% and 14%, while the space-mean speeds increased significantly by 69% to 17% for the flows towards Jyothi Junction and also towards Kadri Junction by all vehicles as measured by VISSIM.

## **7.5 ANALYSIS OF LONG-TERM IMPROVEMENT STRATEGY-2:**

As part of *Long-Term Improvement Strategy-2*, it was proposed to analyse the effect of addition of a flyover to handle right-turning traffic arriving from Kankanady Junction, moving towards St. Theresa's School Junction via Bendoorwell Junction. **Fig.7.2a** provided in the earlier section gives details on the existing layout of Bendoorwell Junction. The *.net* network file used for calibration and validation exercises in *VISSIM* was modified to incorporate the proposed long-term improvements related to introduction of a flyover to cater to traffic moving along the above mentioned directions.

In order to represent the traffic flows along the flyover, the base-network was modified to incorporate additional links for handling the traffic movement from Kankanady towards St. Theresa's School Junction via Bendoorwell Junction. A flyover of approximately 200m length was proposed to be constructed for a single lane width of 4.5m with a gradient of 3%. The gradient specified was within the specified maximum permissible gradient of 4% as per IRC 86 (IRC 1983). **Fig.7.4a** provides details on simulated movement of vehicles on the flyover at Bendoorwell Junction.

### ***Traffic Flows from Kankanady to St. Theresa's School Junction via Bendoorwell Junction***

A summary of the observations for traffic flows from Kankanady Junction moving towards St. Theresa's School Junction via Bendoorwell Junction with respect to simulated volumes and speeds is provided in **Table 7.4**. Here, it is observed that the overall simulated vehicular volumes have increased from 337 to 415 vehicles resulting in an improvement of 23%. The level of improvement in volumes for auto-rickshaws, buses, cars, LCVs, and motorized two-wheelers were observed to be 176%, 25%, 15%, 86%, and 5% respectively.

In the case of speeds, it can be observed that the simulated space-mean speeds of all vehicles moving between Kankanady Junction and St. Theresa's School Junction have increased from 30.00kmph to 41.61kmph showing an improvement of 39%. The simulated space-mean speeds of auto-rickshaws, buses, cars, LCVs, and

motorized two-wheelers have witnessed an increase by 40%, 49%, 30%, 58%, and 23% respectively as shown in **Fig.7.4c**, **Fig.7.4d** and **Fig.7.4e** provide details on the traffic scenario at Bendoorwell Junction before and after introduction of the flyover.

**Table 7.4 Long-Term Improvement Strategy-2: Comparison of Simulated Volumes and Speeds for Flows between Kankanady and St. Theresa’s School Junction via Bendoorwell Junction**

Space Mean Speed (kmph)			
Vehicle Types	Before providing the Flyover	After providing the Flyover	Level of Improvement (%)
All Vehicles	30.00	41.61	39%
Auto	28.16	39.39	40%
Bus	29.01	43.09	49%
Car	33.11	43.17	30%
LCV	25.87	40.89	58%
Two-Wheelers	33.83	41.53	23%

\* The percentages for each vehicle-type are shown in parenthesis.

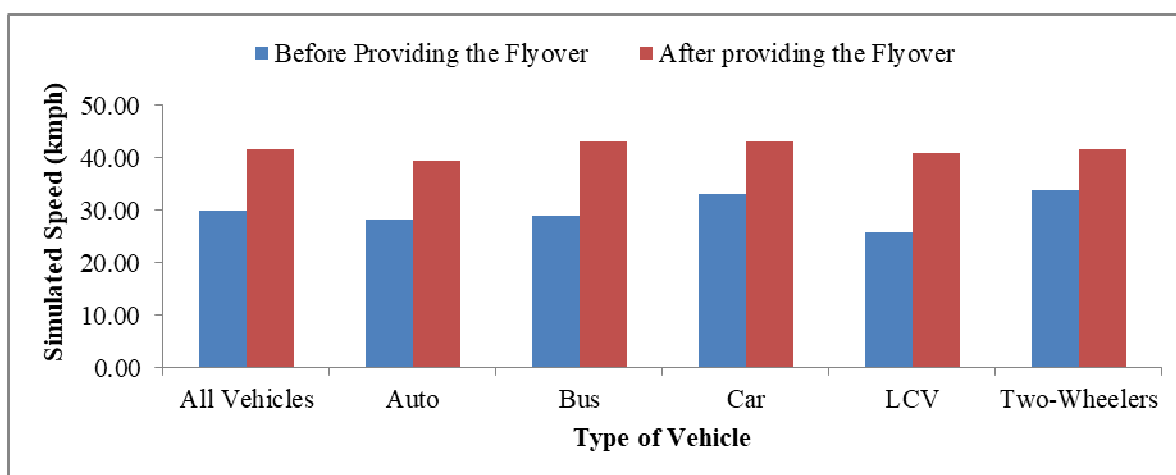


**Fig.7.4c Long-Term Improvement Strategy-2: Comparison of Simulated Speeds for Flows between Kankanady and St. Theresa’s School Junction via Bendoorwell Junction**

### **General Observations on Long-term Improvement Strategy-2**

Considering the performance of a flyover for traffic flows from Kankanady Junction to St. Theresa’s School Junction via Bendoorwell Junction described in **Table 7.4a**, it can be seen that there is a considerable improvement in vehicular volumes by 23%, while the space-mean speeds increased significantly by 39% by all vehicles as measured by *VISSIM*.

## 7.6 OTHER RELATED OBSERVATIONS

In the above study, it may be observed that stopped delays do not directly contribute towards fuel savings. A number of studies performed by **Sharma et al. (2019)**, **Kan et al. (2018)**, **Satiennam et al. (2017)**, and **Website: MERN-Ecomobile** have attempted to investigate various aspects of the relationship between traffic delays and fuel savings. However, the conclusions of these studies were not directly mapped on to the present study since the above studies suggest a deeper understanding of driving cycle behavior such as stop-go and acceleration-deceleration responses which are beyond the scope of the present study. Additionally, the expressions relating stopped delays to fuel-savings may not represent the actual scenario. This is likely to be the case as new vehicles, especially cars and motor-cycles introduced in the market have an *auto-stop* feature to save fuel consumption at signalized junctions.

## CHAPTER 8

### DESIGN OF 3-PHASE SIGNALS IN MANGALORE CITY USING *HCM 2000 METHOD AND GA APPROACH WITH VERIFICATION USING VISSIM MODEL*

#### 8.1 INTRODUCTION

*Genetic algorithm (GA)* approach is an *evolutionary optimization* technique, formulated based on the concept of *natural-selection* and *evolution*. In this approach, the solution to a problem situation is attained based on stochastic operations related to performing *selection, crossover* and *mutation* at each step focused on finding the best solution.

A *GA* has the capability to perform a search for the *global-optima* over a wider solution space, reducing the possibility of being trapped in *local-optima* (**Goldberg 2002**). This is due to the implementation of *mutation* on the set of population strings representing the solution states tested. The *genetic algorithm* based approach performs in a manner similar to the *steepest gradient* method as in classical optimization methods. However, the *GA* approach is considered to be more flexible since it does not require any information on the gradient of the objective function. It does not require the use of complex mathematical relationships, and their derivatives for arriving at the *optima*. Additionally, the *GA* is capable of handling optimization problems with *disconnected search spaces* (**Goldberg 2002**), while in simulation-based approaches, the optimal solutions can be arrived at based on a series of experiments starting with an existing feasible solution.

The *GA* approach has been widely used in various areas of the transportation-field, such as in urban transport planning, transit network design, traffic management, and accident studies. In the design of optimal signal timings, the search for the *optima* is conducted on a set of binary-bit descriptions of the signal timings in the *GA* approach. Genetic algorithm has been applied to a number of areas in engineering, and technology including the field of transportation engineering. Details on the applications of *GA* in traffic and transportation engineering were provided in



**Chapter 2**, while the fundamental aspects of *GA* operations such as *crossover*, and *mutation* were discussed in **Section 3.6**.

In the conventional *HCM 2000 design method (TRB 2000)* the green times are allocated such that the *volume/ capacity ratio* ( $X_c$ ) for critical movements in each phase are equal as explained in Chapter 16 page 100 of the TRB Manual.

In the later stages, a comparison of the delays experienced at selected junctions in Mangalore city before and after the implementation of the HCM based signal timings is also incorporated based on simulations performed using the fully calibrated and validated *VISSIM* model.

## **8.2 DESIGN OF 3-PHASE PRE-TIMED SIGNALS FOR SELECTED JUNCTIONS IN MANGALORE CITY USING HCM 2000 DESIGN METHOD**

This section provides descriptions on the design of pre-timed isolated 3-phase signals for selected junctions in Mangalore city using the *HCM 2000 design method (TRB 2000)*.

### **8.2.1 Design of 3-Phase Isolated Traffic Signal Using HCM 2000 Design Method: PVS Junction**

This sub-section provides details on the design of a 3-phase signal using the *HCM 2000 design method (TRB 2000)* for PVS Junction, one of the busiest junctions in Mangalore city. The details of turning movements of traffic flows at the junction are depicted in **Fig.8.1a**. The details on the incoming traffic flows  $q_i$  for each phase  $i$ , and the computations for the saturation volumes  $s_i$ , and the flow ratios  $y_i$  are summarized in **Table8.1a**.

In the first step in signal design, the *total lost-time per cycle* ( $L$ ) is computed as shown below, using **Eq.3.4a** discussed in **Section 3.4.1** where the lost-time for each lane group ( $t_L$ ) is assumed as 2 seconds according to HCM 2000 (**TRB 2000**):

$$L = \sum_{L=1,n} t_L = 2 + 2 + 2 = 6s$$

In the second step, it is required to determine the *minimum cycle length* ( $C_{min}$ ) to avoid over-saturation. This is computed by substituting a *critical volume/ capacity ratio* equal to 1.0 in **Eq.3.4d** which reduces to **Eq.3.4e** as reproduced below:

$$\begin{aligned}
C_{min} &= L / [1.0 - \sum_i (q_i / s_i)_c] \\
&= L / [1.0 - \sum_i y_{ci}] \\
&= L / [1.0 - (y_{c1} + y_{c2} + y_{c3})] \text{ (for 3-phase traffic signal)} \\
&= 6 (1.0) / [1.0 - (0.4263 + 0.1987 + 0.2224)] \\
&= 39.32 \approx 40 \text{ s}
\end{aligned}$$

The above computation indicates that a *critical volume/ capacity ratio* of 0.8474 cannot be implemented for the given traffic-flow demand levels for the junction since the computed cycle-length approaches infinity. Hence, it is required to increase the cycle length beyond the minimum cycle length of 40s in an iterative manner. HCM 2000 (**TRB 2000**) suggests that the cycle length assumed may be rounded to the nearest 5s for cycle lengths between 30 and 90s and to the nearest 10s for higher cycle-lengths. Let us assume a revised cycle length of 45 seconds. The actual *degree of saturation* or the actual *volume/ capacity ratio* for critical movements ( $X_c$ ) can be verified for the revised cycle-length using **Eq.3.4c** as,

$$\begin{aligned}
X_c &= C \sum_i (q_i / s_i)_c / (C-L) \\
&= C (y_{c1} + y_{c2} + y_{c3}) / (C-L) \\
&= 45 (0.4263 + 0.1987 + 0.2224) / (45-6) = 0.9778
\end{aligned}$$

Thus, for a cycle length of 45s, the timing diagrams for 3-phase traffic signal can be derived as shown in **Fig.8.1b**. The results of the analysis performed above are summarized in **Table 8.1b**.

### 8.2.2 Summary of the Design of 3-Phase Isolated Traffic Signals for the Remaining Three Junctions Using HCM 2000 Design Method

This sub-section provides a summary on the design of 3-phase pre-timed isolated traffic signals using the *HCM 2000 design method* (**TRB 2000**) for the remaining three important junctions in Mangalore city. The overall design approach adopted in **Section 8.2.1** was followed in the design of these three-phase signals too. The details of turning movements of traffic flows at Jyothi Junction, Bunt's Hostel Junction, and St. Theresa's School Junction are provided in **Fig.8.1c**, **Fig.8.1d**, and **Fig.8.1e** respectively.

of the analysis performed are provided in **Table 8.1f**, **Table 8.1g**, and **Table 8.1h**.

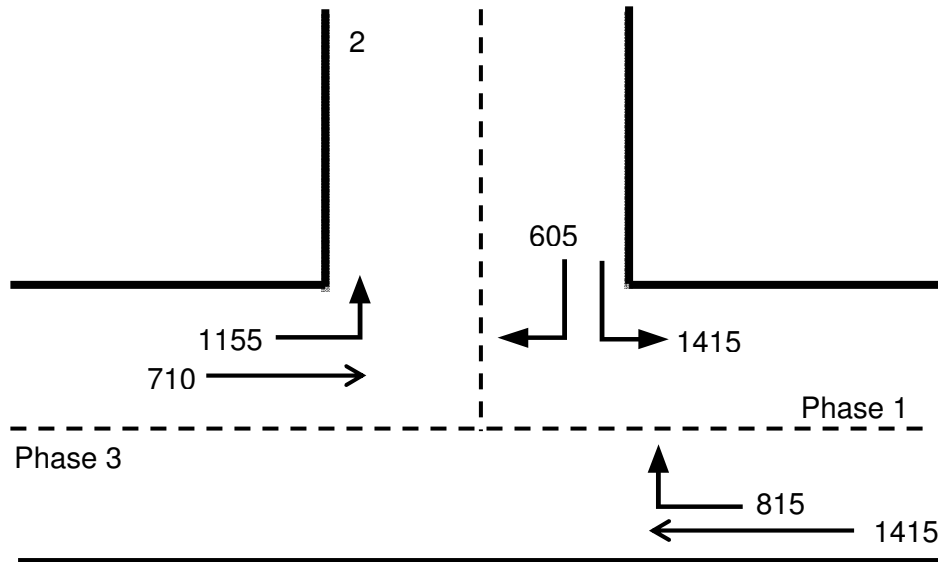


**Fig.8.1d Layout and Phasing Diagram for 3-Phase Traffic Signal: Bunt's Hostel Junction**

**Table 8.1f Details of 3 Phase Signal Timings Computed Based on HCM 2000 Design Method: Jyothi Junction**

Phase	Critical Flows Considered for Computations $q_i$	Green time ( $g_i$ ) in seconds	Cycle Length ( $C$ ) in seconds	Total Lost Time ( $L$ ) in seconds
Phase 1	870	9	40	6
Phase 2	1175	13		
Phase 3	1135	12		

**Table 8.1h Details of 3 Phase Signal Timings Computed Based on HCM 2000 Design Method: St. Theresa's School Junction**

Phase	Critical Flows Considered for Computations $q_i$	Green time ( $g_i$ ) in seconds	Cycle Length ( $C$ ) in seconds	Total Lost Time ( $L$ ) in seconds
Phase 1	775	13	35	6
Phase 2	1175	11		
Phase 3	80	5		

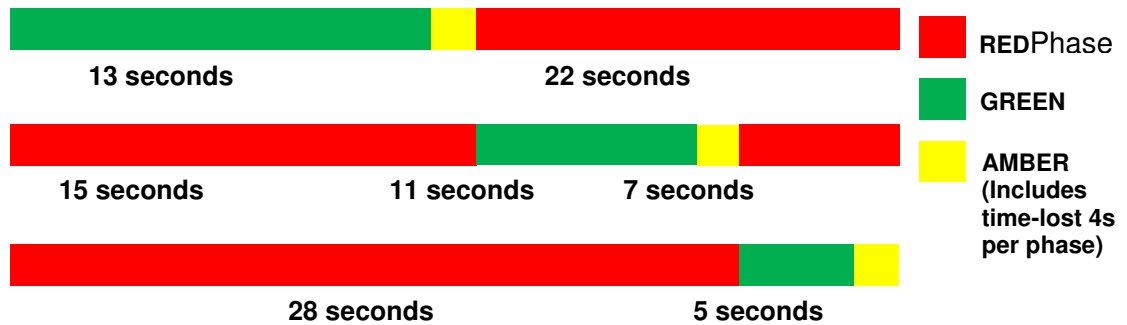


**Fig.8.1h Three Phase Signal Timing Diagram Using HCM 2000 Design Method: St. Theresa's School Junction**

### **8.3 DESIGN OF 3-PHASE ISOLATED SIGNALS FOR SELECTED JUNCTIONS USING GA APPROACH BASED ON HCM AVERAGE DELAY MODEL**

The design of three-phase isolated signals for selected junctions in Mangalore city was performed using the HCM *average delay* model discussed in **Section 3.5.3.1** in **Chapter 3**. Details on the theoretical aspects of *steady state stochastic* delays, *deterministic* (or *uniform*) delay models, and the *time-dependent stochastic* delay models were also provided in **Chapter 3**. This section provides details on the design of pre-timed isolated 3-phase signals for selected junctions in Mangalore city using the *GA* approach based on optimizing delays computed according to the *HCM average delay model* (TRB 2000).

#### **8.3.1 A Summary of Theoretical Considerations in HCM Average Delay Model**

Based on the theoretical aspects presented in **Section 3.5.3.1**, the average delays for one of the approaches to an intersection can be computed based on the *HCM average delay model* (TRB 2000) using **Eq.3.5h** reproduced below:

$$d = d_1.PF + d_2 + d_3 \quad \text{Eq.8.1a}$$

where,  $d$  = average delay per vehicle, s/veh;  $d_1$  = uniform delay assuming uniform vehicle arrivals, s/veh;  $PF$  = uniform delay progression adjustment factor which accounts for the effects of signal progression which is approximately equal to 1.0 for uncoordinated signals and not greater than 1.0 according to HCM2000 ;  $d_2$  = incremental delay (s/vehicle) to account for random vehicle arrivals and over

saturated queues for the period of analysis;  $d_3$  = supplemental delay (s/vehicle) to account for over saturation queues that might have existed just before the analysis period ( $T$ ), which may be ignored if such situations do not exist.

The expression for *uniform delay* according to HCM 2000 is given vide **Eq.3.5i** reproduced below as,

$$d_1 = C \cdot (1-g/C)^2 / \{ 2 [1 - (\text{Min}(1, X) \cdot g/C)] \} \quad \text{Eq.8.1b}$$

where,  $d_1$ = uniform delay (s/vehicle) assuming uniform vehicle arrivals;  $C$  = cycle length (s) used in pre-timed signal control, or average cycle length (s) for actuated control;  $g$  = effective green time (s) for the lane group for pre-timed signal controls, or average lane group effective green time (s) for actuated signal controls;  $X$  = volume/capacity ratio or degree of saturation for the lane group.

Also, the expression for *random delays* or *incremental delays* due to piling up of vehicles during a cycle time is given by HCM 2000 vide **Eq.3.5j** reproduced below as,

$$d_2 = 900T [(X-1) + \sqrt{(X-1)^2 + (8K \cdot I \cdot X / (c \cdot T))}] \quad \text{Eq.8.1c}$$

where,  $d_2$  = incremental delay (s/vehicle) to account for the effect of random vehicle arrivals, and over saturated queues in the duration of analysis;  $T$  = duration of analysis period (h);  $K$  = incremental delay factor to be calibrated based on the controller settings (assumed as 0.50 for pre-timed signals for random arrivals and uniform service time);  $I$  = upstream filtering/ metering adjustment factor to be calibrated based on arrivals from upstream signals (assumed as 1.0 for isolated signals);  $c$  = lane group capacity (vehicles/h), and;  $X$  = lane group volume/ capacity ratio, or degree of saturation.

### **8.3.2 Theoretical Considerations in the Formulation of the Objective Function, Constraints, and Defining of the Fitness Index for the GA Approach**

It is possible to formulate an optimization problem that minimizes the delays at intersections. A typical optimization problem comprises computation of individual parameters, testing of equality or inequality constraints, determination of the objective function value, and evaluation of fitness using a suitable fitness function (**Deb 2000**).

In the formulation of a problem on optimization of signal timings, it is required to constitute the objective function  $f(x)$  aimed at minimizing vehicular delays. One of the possible ways of formulating such an objective function is based on minimization of the average delay per vehicle as shown below:

$$\text{Min } f(x) = \text{Min } D = \text{Min} [(\sum_{i=1,n} q_i \cdot d_i) / (\sum_{i=1,n} q_i)] \quad \text{Eq.8.2a}$$

where,  $f(x) = D =$  average delay per vehicle, which is a function of  $q_i$ , the mean arrival rate of vehicles in phase  $i$ , expressed in passenger cars per second (pcu/s);  $d_i$ , the average delay per vehicle for each phase  $i$ ;  $D = [(\sum_{i=1,n} q_i \cdot d_i) / (\sum_{i=1,n} q_i)]$ ;  $d_i = d_1 \cdot PF + d_2 + d_3$  as in Eq.8.1a.

Moreover, it is also required to formulate the constraint equations related to the *cycle length*, and the *green time* in addition to the *non-negativity constraints*, in order to arrive at the best signal timing. In the design of coordinated signals for a group of signals, constraints related to the *off-set time* also may have to be considered. The details of formulation of these constraints are provided below:

### 8.3.2.1 Constraint related to cycle length:

The constraints related to cycle time can be formulated as given below:

$$C_{min} \leq C \leq C_{max} \quad \text{Eq.8.2b}$$

where,  $C =$  cycle length  $= \sum g_i + L$ ;  $g_i =$  effective green time for phase  $i$  in seconds;  $C_{min} =$  minimum cycle length  $= L / [1.0 - \sum_i (q_i / s_i)_c]$  as in Eq. 3.4d;  $L =$  lost time per cycle (s)  $= \sum_{L=1,n} t_L$ ;  $t_L =$  lost-time for each lane group  $L$ ;  $(q_i / s_i)_c =$  critical volume to saturation flow ratio for lane group  $i$ , and  $C_{max}$  can be assumed as 120 seconds as per HCM2000 (**TRB 2000**), while higher than 120 seconds is used under exceptional conditions. Also, this should not be allowed to exceed the local agency acceptable maximum cycle length. However, IRC 93(**IRC 1985**) recommends maximum cycle length of 120 seconds. Thus, the limits for  $C_{min}$  and  $C_{max}$  can be defined, while the cycle length  $C$  has to be computed as part of the GA algorithm based on the green times,  $g_1$ ,  $g_2$ , and  $g_3$ . The GA algorithm thus focuses on optimizing the *green times*.

### 8.3.2.2 Constraints related to green time:

The constraints related to effective green time are formulated as given below:

$$g_{i \min} \leq g_i \leq g_{i \max} \text{ or} \quad \text{Eq.8.2c}$$

$$g_i - g_{i \min} \geq 0; \text{ and} \quad \text{Eq.8.2d}$$

$$g_{i \max} - g_i \geq 0 \quad \text{Eq.8.2e}$$

Also, it is required to add a *phase priority constraint* that states that the phase identified with a higher vehicular flow must possess a greater value of effective green time.

### 8.3.2.3 Non-negativity constraints:

However, the effect of the non-negativity constraint for effective green time and cycle length is automatically considered while specifying the upper and lower bounds for the same in the GA algorithm.

### 8.3.2.4 Constraints related to off-set time:

The constraints related to *off-set time* are of importance only in the design of coordinated signals, and so, are not considered in the algorithm for design of isolated signals.

### 8.3.2.5 Formulation of the Constraint Violation Coefficient

In a GA approach, the focus is on identifying the best green time signal that ensures optimal signal operations. Since a GA approach is most suited to perform an unconstrained optimization, the best signal timing can be identified based on a constraint violation coefficient that indicates the extent to which the constraints remain unsatisfied when a particular signal-timing is selected. This is similar to defining a penalty function for constraint violation. Thus, the aim of a GA based approach reduces to maintaining the degree of constraint violations to a minimum.

When a constraint  $G_i(x)$  is satisfied, the constraint violation coefficient  $P_i$  can be set to a value zero. Else, if the constraint  $G_i(x)$  is violated, then the value of  $P_i$  may be set to attain the value of  $G_i(x)$ . This can be mathematically expressed for a constraint equation  $G_i(x)$  as follows:

$$P_i = G_i(x) \quad \text{if } G_i(x) \leq 0; \text{ and}$$

$$P_i = 0, \quad \text{if } G_i(x) > 0.$$

### 8.3.2.6 Formulation of the Modified Objective Function

After determining the overall constraint violations  $P$  as described above for a particular signal-timing, the value of the *objective function*  $f(x)$  has to be computed considering the effect of constraint violations. Also, since a GA-based approach is usually formulated in the form of an unconstrained optimization problem, a *modified objective function*  $F(x)$  or  $\eta(x)$  as defined below is used based on a similar approach adopted by **Rajeev and Krishnamoorthy (1992)**:

$$\eta(x) = F(x) = f(x) (1 + KP) \quad \text{Eq.8.2j}$$

where,  $\eta(x)$  = penalty function, which is defined in this investigation as equal to  $F(x)$ ;  $F(x)$  = modified objective function;  $f(x)$  = objective function;  $K$  = a *scaling constant* selected based on the required influence of the constraint violation coefficient  $P$  on the function.

### 8.3.2.7 Establishing the Fitness Index (FI)

Based on the value of the *modified objective function*  $\eta(x)$  for each string (or chromosome or individual) for the current generation, a *fitness index* is computed as given below:

$$FI_i = 1 / (1 + \eta(x)_i) \quad \text{Eq.8.2k}$$

### 8.3.2.8 Normalization of the Fitness Value (NFV) – An Alternative Approach

After computing the *fitness index* values for each of the strings, it is possible to compute the *normalized fitness index* ( $Nevis$ ) for each string by comparing with the average value of the fitness indices as given below:

$$Nevis = FI_i / Fl_{ag} \quad \text{Eq.8.2k}$$

where,  $FI_i$  = fitness index value for the string  $i$ , and  $Fl_{ag}$  = average of the fitness index values of the strings for the current generation.



The strings that possess higher normalized fitness indices are then selected for producing off-springs for the new generation of strings. However, this optional step was not adopted in the *GA* algorithm implemented as part of this study.

### 8.3.3 Design of 3-Phase Isolated Signals Using *GA*-Based Approach for Optimal Design Using *HCM Average Delay Model*: PVS Junction

This sub-section provides details on the design of a 3-phase signal using the *GA* approach based on optimizing delays computed according to the *HCM average delay model* (TRB, 2000) for PVS Junction, one of the busiest junctions in Mangalore city. The details of turning movements of traffic flows at the junction were provided earlier vide Fig.8.1a reproduced below:

#### 8.3.3.1 Input data to be assigned to the *GA* algorithm

The input data required to be provided for the determination of the optimal signal timing using the *GA*-based method for the design of a 3-phase traffic signal are listed below:

- $L$  = total lost time = 6 seconds (computed using Eq.3.4a as described in Section 3.4.1.1);
- Here, it may be observed that the computed *minimum cycle length*  $C_{min}$  based on Eq.3.4d and Eq.3.4e is 40s while the *maximum cycle length*  $C_{max}$  specified for exceptional conditions is 150s as per HCM 2000 (TRB 2000). IRC 93 (IRC 1985) recommends maximum cycle length of 120 seconds.
- The value of  $g_{i min}$  can be assumed as 5s according to HCM 2010 (TRB 2010), and the constraint equations for the same may be formulated accordingly. The value of  $g_{i max}$  can be computed as in section 8.3.2.2 above for phases 1, 2, and 3. Thus the *cycle length* including the *lost time* can be computed for each string in the population set as,  $C = g_1 + g_2 + g_3 + L$  for the optimized values of  $g_1, g_2$ , and  $g_3$ .
- For the traffic flows shown for the junction as shown as in Fig.8.1, the critical flow ( $q_1$ ) for which the signal has to be designed for Phase 1 is the right turning flow of 1620 vehicles per hour. Similarly, for Phase 2, the critical flow ( $q_2$ ) is

755 vehicles per hour, and for Phase 3, the critical flow ( $q_3$ ) is 845 vehicles per hour. The saturation flows  $s_1$ ,  $s_2$ , and  $s_3$ , for phases 1, 2, and 3 are computed assuming 1900 veh/h/ln according to HCM-2000.

### 8.3.3.2 Explanation on encoding of binary strings for a hypothetical set of binary strings and computation of actual string values based on green time variable bounds

In the next step in the GA-based optimization procedure, it is required to constitute a population of strings that can represent the initial search space. The theoretical details on encoding of the binary strings, computation of the actual string values, formulation of the objective functions and constraints, and identification of expressions for computation of delays are explained below.

In a generalized GA-based optimization approach for signal design, it may be required to compute the *effective green time*  $g_i$  that lies between the *minimum green time*  $g_{i \min}$ , and the *maximum green time*  $g_{i \max}$  as expressed in **Eq.8.2c**. Here, it is required to assign a set of binary strings for  $g_i$  that represents the initial sample space of values of effective green times that lie between the lower and upper bounds  $g_{\min}$  and  $g_{\max}$  respectively. If  $g_i$  is represented using a binary strings of  $n$  bits as  $b_{n-1}b_{n-2} b_{n-3} \dots b_{n-(n-1)}$ , then the converted value of the binary string from base 2 to base 10 is given as,

$$\zeta_{splice} = \sum_{i=0, n-1; k=0, n-1} b_{n-k} \cdot 2^i \quad \text{Eq.8.3a}$$

Based on an approach adopted by **Ceylan and Bell (2004)**, the corresponding real values of the effective green times can be computed as,

$$g_i = g_{i \min} + \{(g_{i \max} - g_{i \min}) \times \zeta(splice) / (2^8 - 1)\} \quad \text{Eq.8.3b}$$

Generally, 8-bit, 16-bit, or 24 bit binary strings are generally used in a GA-based optimization approaches depending upon the accuracy of the predicted output and the computation capability (single/two/three variable optimization). A GA-based approach randomly selects a set of binary strings and the values of the strings are computed using **Eq.8.3a**. The strings with the least and the highest values are assigned the upper and lower limiting values of the effective green time as shown in the hypothetical sample set of binary strings in **Table 8.2**, while the GA randomly selects a set of binary strings between the upper and lower limits representing green

time values in between. The green time values for each string can be computed using Eq.8.3b.

**Table 8.2 A Hypothetical Sample Solution Set of Binary Strings with Values of Effective Green Times**

Sl. No.	8 bit binary strings	Effective green time values assigned $g_i(s)$
1	00000000	$g_{i\ min} = 5$
2	00010111	10
3	00101110	15
4	01000110	20
5	01011101	25
6	01110100	30
7	10001011	35
8	10100010	40
<b>9</b>	<b>10111001</b>	<b>45</b>
10	11010001	50
11	11101000	55
12	11111111	$g_{i\ max} = 60$

**Table 8.3a Computational Details for the Initial 0<sup>th</sup> Test Generation Using the GA Approach: PVS Junction**

Sl. No.	Current Population Strings (Parent)	Green Times ' $g_i$ ' sec (Assigned by the GA)			$f(x)$ sec	$P$	$\eta(x)$	$FI_i$	New Population Strings (Offspring)
		$g_1$	$g_2$	$g_3$					
(1)	(2)	(3a)	(3b)	(3c)	(4)	(5)	(6)	(7)	(10)
1	01111111- 00111000- 01110001	27.91	9.173	14.749	125.629	0	125.629	7.897	11001111- 10111000- 01110001
2	10111100- 11111110- 10101110	38.914	23.925	20.012	33.364	3.914	1339.119	0.746	01111111- 00111011- 11101001
8	01000001- 10101001- 11000100	16.725	17.592	21.91	551.606	6.051	33929.153	0.029	01100111- 01011000- 10101110
9	10000011- 00101111- 10111100	28.631	8.502	21.22	235.094	0	235.094	4.236	11001111- 10111011- 11101001
10	01111001- 00111110- 01100001	26.827	9.62	13.369	83.302	0	83.302	11.862	10000011- 00101111- 10111100
11	01100111- 01011000- 11100001	23.58	11.557	24.412	243.089	0.831	2264.063	0.441	10101111- 11000010- 10101110
12	11110010- 10111011- 01110101	48.655	18.933	15.094	171.139	3.839	6741.536	0.148	10111100- 11111110- 11110111

**Table 8.3a** provides details on the 12 strings of the initial solution space (or 0<sup>th</sup> generation) assigned by the GA program. Here, a 24-bit string comprising 3

substrings, each of 8-bit length representing the green times  $g_1$ ,  $g_2$ , and  $g_3$  for phases 1, 2, and 3 can be defined. Thus the problem can be formulated as a *three-variable GA optimization* problem.

### 8.3.3.3 Computations in the GA for setting the proportions for effective green times

In the GA-based optimization approach adopted in this study, the cycle timing  $C$  can be computed as mentioned in **Section 8.3.3.1**, and the green times for each of the phases are required to be determined using the GA-based optimization approach.

The values of the other two substrings for the first string can be computed in a similar manner in the GA program as follows:

$$\lambda_2 = g_2/C = 9.173 / 57.832 = 0.1586$$

$$\lambda_3 = g_3/C = 14.749 / 57.832 = 0.2550$$

### 8.3.3.4 Computations in the GA for of the value of the objective function $f(x)$

The *uniform delay* according to HCM 2000 can be computed using **Eq.8.1b**as,

$$d_i = ( C ( 1 - g_i / C )^2 / \{ 2 [ 1 - ( \text{Min}(1, X_i) . g_i / C ) ] \} )$$

where,  $d_i$ = uniform delay (s/vehicle) assuming uniform vehicle arrival;  $C$  = cycle length (s) used in pre-timed signal control;  $g_i$  = effective green time (s) for the lane group  $i$  for pre-timed signal controls;  $X_i$  = volume/ capacity ratio or degree of saturation for the lane group  $i$ .

It is also required to compute the *degrees of saturation*  $X_1$ ,  $X_2$ , and  $X_3$  as part of the GA program for the phases 1, 2, and 3 using **Eq.8.1g** for input data on the corresponding flows  $q_1$ ,  $q_2$ , and  $q_3$ , and the saturation flows  $s_1$ ,  $s_2$ , and  $s_3$  for PVS Junction as shown below:

### 8.3.3.5 Computation of constraint violation coefficients for the effective green times

For a GA-based optimization problem, the limits for the minimum and maximum green times are set as in **Eq.8.2c-Eq.8.2e** as,

$$g_i \min \leq g_i \leq g_i \max$$

where,  $g_i - g_i \min \geq 0$ , and

$$g_i \max - g_i \geq 0$$

The constraint violations  $P_1, P_2, P_3, P_4, P_5$ , and  $P_6$  for the above problem can then be defined and computed

### ***8.3.3.6 Computation of constraint violation coefficient for cycle length***

For a *GA*-based optimization problem, the limits for the minimum and maximum cycle lengths are set as in **Eq.8.2b** as,

$$C_{min} \leq C \leq C_{max}$$

where,  $C - C_{min} \geq 0$  and  $C_{max} - C \geq 0$

### ***8.3.3.7 Computation of constraint violation coefficients for phase priority***

It is also required to set a phase priority constraint based on the quantity of flow in each phase of the signal. The following are the phase priority constraints compiled as per **Eq.8.2f**:

### ***8.2.3.8 Computation of constraint violation coefficient for non-negativity***

The non-negativity constraints for green time and cycle length given based on **Eq.8.2g** and **Eq.8.2h** as,

$$g_i \geq 0 \text{ and}$$

$$C \geq 0$$

However, the constraints with the negative values are not considered for the computation of constraint violation coefficient in the *GA* algorithm as only values greater than ‘zero’ are used in assigning the green times in the program.

### ***8.3.3.9 Computation of the sum of constraint violation coefficients***

The value of the sum of the constraint violations can be computed based on **Eq.8.2i** as,

$$P = \sum_{i=1,m} P_i$$

where,  $P_i$  = constraint violation coefficient for the constraint  $g_i(x) \leq 0$ ; and  $m$  = total number of constraints.

#### **8.3.3.10 Computation of the values of modified objective function $\eta(x)$ for each string**

Based on **Eq.8.2j**, the values of the modified objective function for each string can be computed as,

$$\eta(x) = F(x) = f(x) (1 + KP)$$

where,  $\eta(x)$  = penalty function, which is defined in this investigation as equal to  $F(x)$ ;  $F(x)$  = modified objective function;  $f(x)$  = objective function;  $K$  = a *scaling constant* with a value assumed as 10.

#### **8.3.3.11 Computation of the values of the fitness index (FI) for each string**

Based on **Eq.8.2k**, the values of the fitness index for each string can be computed as,

$$FI_i = 1 / (1 + \eta(x)_i)$$

where  $FI_i$  is the fitness index for each of the individual strings;  $\eta(x)_i$  is the modified objective function value for the individual string under consideration.

#### **8.3.3.12 Selection of the best string to form the next generation by the principle of elitism**

The *GA* then selects the string set with the highest *fitness index* as the most suitable value for the green times in order to form the seed for the next generation. This is called the principle of *elitism*. The remaining strings for the next generation are formed by the *GA* operations such as *cross-over* and *mutation*.

The procedure related to computation of the value of the objective function, the constraint violations, and the fitness indices are again performed in an iterative manner until a specified number of generations (assigned 30 generations in this study based on trial and error approach) of strings are tested in the initial run. The procedure was repeated for 10 runs (assigned based on trial and error approach), and the best value of the strings are identified from among all the runs.

**Table 8.3b Computational Details for the 1<sup>st</sup> Generation of the First Run Using the GA Approach: PVS Junction**

Sl. No.	Current Population Strings (Parent)	Green Times ' $g_i$ ' sec (Assigned by the GA)			$f(x)$ sec	$P$	$\eta(x)$	$FI_i$	New Population Strings (Offspring)
		$g_1$	$g_2$	$g_3$					
(1)	(2)	(3a)	(3b)	(3c)	(4)	(5)	(6)	(7)	(10)
1	11001111-10111000-01110001	42.341	18.71	14.749	135.232	3.961	5491.46	0.182	01111111-00111011-11110001
2	01111111-00111011-11101001	27.91	9.396	25.102	252.987	0	252.987	3.937	11001111-10111000-01101001
11	10101111-11000010-10101110	36.569	19.455	20.012	28.594	0	28.594	33.791	11001111-10111011-11101001
12	10111100-11111110-11110111	38.914	23.925	26.31	71.216	0	71.216	13.847	10111100-11111110-11100001

**Table 8.3c Computational Details for the 30<sup>th</sup> Generation of the First Run Using the GA Approach: PVS Junction**

Sl. No.	Current Population Strings (Parent)	Green Times ' $g_i$ ' sec (Assigned by the GA)			$f(x)$ sec	$P$	$\eta(x)$	$FI_i$
		$g_1$	$g_2$	$g_3$				
(1)	(2)	(3a)	(3b)	(3c)	(4)	(5)	(6)	(7)
1	10101111-11000010-10101001	36.569	19.455	19.58	28.276	0	28.276	34.157
6	10101111-11000010-10101001	36.569	19.455	19.58	28.276	0	28.276	34.157
7	10101111-11000010-10101001	36.569	19.455	19.58	28.276	0	28.276	34.157
10	10101111-11000010-10101001	36.569	19.455	19.58	28.276	0	28.276	34.157
11	10101111-11000010-10101001	36.569	19.455	19.58	28.276	0	28.276	34.157
12	10101111-11000010-10101001	36.569	19.455	19.58	28.276	0	28.276	34.157

**Table 8.3d Computational Details for the 4<sup>th</sup> Generation for the 10<sup>th</sup> Run for the Overall Best String among All the Test Runs Using the GA Approach: PVS Junction**

Sl. No.	Current Population Strings (Parent)	Green Times ' $g_i$ ' sec (Assigned by the GA)			$f(x)$ sec	$P$	$\eta(x)$	$FI_i$
		$g_1$	$g_2$	$g_3$				
(1)	(2)	(3a)	(3b)	(3c)	(4)	(5)	(6)	(7)
1	10011111-10001001-11010010	33.682	15.208	23.118	39.51	0	39.51	24.685
7	01110001-01011010-01010111	25.384	11.706	12.506	21.578	0	21.578	44.291
8	01110001-01011011-01011100	25.384	11.78	12.937	20.943	0	20.943	45.573
9	01110000-01101000-11100110	25.204	12.749	24.843	201.819	0	201.819	4.931
10	01110000-01101000-11101100	25.204	12.749	25.361	213.245	0.157	547.747	1.822
11	10011111-01011011-10001011	33.682	11.78	16.992	87.225	0	87.225	11.335
12	01110001-10001001-11010010	25.384	15.208	23.118	178.142	0	178.142	5.582

**Table 8.3e Details of 3-Phase Signal Timings Computed Based on the GA Approach: PVS Junction**

Phase	Green time ( $g_i$ ) in seconds	Cycle Length ( $C$ ) seconds	Total Lost Time ( $L$ ) seconds	Optimal Run Sl. No.	Optimal Generation Sl. No.
Phase 1	25	56	6	10	4
Phase 2	12				
Phase 3	13				

### 8.3.4 Results on the Design of 3-Phase Isolated Traffic Signals for the Remaining 3 Junctions Using the GA Approach

This sub-section provides a summary on the design of 3-phase pre-timed isolated traffic signals using the GA approach where the average delay computed using the HCM average delay model (TRB 2000) was optimized for the remaining three important junctions in Mangalore city. The details of turning movements of traffic flows at these three junctions in the city were provided earlier in Fig.8.1c, Fig.8.1d, and Fig.8.1e.



The details on the incoming traffic flows  $q_i$  for each phase  $i$ , and the computations for the saturation volumes  $s_i$ , and the flow ratios  $y_i$  for the remaining junctions were summarized earlier in **Table 8.1c – Table 8.1e**.

The GA-based optimization was performed as demonstrated in the above section, and the details on the optimized timings for the 3-phase traffic signals are provided in **Table 8.3f – Table 8.3h**.

**Table 8.3f 3-Phase Signal Timings Based on the GA Approach: Jyothi Junction**

Phase	Green time ( $g_i$ ) in seconds	Cycle Length ( $C$ ) seconds	Total Lost Time ( $L$ ) seconds	Optimal Run Sl. No.	Optimal Generation Sl. No.
Phase 1	16	60	6	9	14
Phase 2	19				
Phase 3	19				

**Table 8.3g 3-Phase Signal Timings Based on the GA Approach: Bunt's Hostel Junction**

Phase	Green time ( $g_i$ ) in seconds	Cycle Length ( $C$ ) seconds	Total Lost Time ( $L$ ) seconds	Optimal Run Sl. No.	Optimal Generation Sl. No.
Phase 1	49	112	6	9	0
Phase 2	36				
Phase 3	21				

**Table 8.3h 3-Phase Signal Timings Based on the GA Approach: St. Theresa's School Junction**

Phase	Green time ( $g_i$ ) in seconds	Cycle Length ( $C$ ) seconds	Total Lost Time ( $L$ ) seconds	Optimal Run Sl. No.	Optimal Generation Sl. No.
Phase 1	25	56	6	9	1
Phase 2	20				
Phase 3	5				

#### **8.4 Performing Simulations Using VISSIM and Assessment of Delays at Selected Junctions in Mangalore City**

The VISSIM model for the road network in Mangalore city was used to test the performance of the three-phase signals designed based on the *HCM2000 Design Method*, and the signal timing computed using the GA-based approach. The reduction in delays and the overall improvement in traffic flows across all the selected junctions were compared to the existing manually controlled signal timing. The details of this part of the study are provided in the sub-sections below:

#### **8.4.1 Comparisons between the Performance of Existing Manually Controlled Signal Timings Vs Signal Timings Computed Based on *HCM 2000 Design Method***

In the first step, simulations were performed for the existing signal timings using the fully calibrated and validated *VISSIM* model for the four manually operated signals, and the simulated delay/phase/vehicle, the *average delay per vehicle*, and the *total flows across the junctions* were tabulated for each of the junctions as given in **Table 8.4a**.

In the next step, the signal timings for the 3-Phase signals computed using the *HCM2000 Design Method*, summarized earlier in **Table 8.1b**, **Table 8.1f**, **Table 8.1g**, and **Table 8.1h** for the four selected junctions were then implemented in the fully calibrated and validated *VISSIM* model. The details on the simulated delay/phase/vehicle, the *average delay per vehicle*, and the *total flows across the junctions* were tabulated for each of the junctions as summarized in **Table 8.4b** along with the comparisons with the existing signal timings. Here, it can be observed that the average reduction in delays for the four junctions is around 11.62% when compared to the performance of the signals using the existing signal timings.

#### **8.4.2 Comparisons between the Performance of Existing Manually Controlled Signal Timings Vs Optimized Signal Timings Computed Using the *GA Approach***

Additionally, the signal timings were designed using the *genetic algorithm* (*GA*) approach where the delays were minimized subject to signal design constraints such as the *computed minimum cycle length* for the junction, the *upper bounds for green times* assigned separately for each phase based on the *critical flow ratios*, and the *assumed maximum cycle length* specified by the *HCM average delay model* (**TRB 2000**).

Based on the *genetic algorithm* (*GA*) approach, the search for the best green-times that optimized the delays for the four junctions were summarized earlier in **Table 8.3e**, **Table 8.3f**, **Table 8.3g**, and **Table 8.3h**. These signal timings were then implemented in the fully calibrated and validated *VISSIM* model for the four selected junctions. The details on the simulated delay/phase/vehicle, the *average delay per vehicle*, and the *total flows across the junctions* were tabulated for each of the

junctions as summarized in **Table 8.4c** along with the comparisons with the existing signal timings. Here, it can be observed that the average reduction in delays for the four junctions is around 18.50% when compared to the performance of the signals using the existing signal timings.

## CHAPTER 9

### CONCLUSIONS

#### 9.1 INTRODUCTION

Simulation models have contributed a great deal towards understanding the interdependence of various factors such as vehicle, driver, and roadway characteristics. The development of a reliable simulation model depends on adopting the right strategy for calibration and validation of vehicle and driver characteristics, while roadway characteristics remain unchanged for the period of analysis. The identification of a set of more sensitive characteristics can further assist in improving the predictive capability of simulation models. The simulation models thus calibrated and validated, can be used to simulate various traffic scenarios and can assist in streamlining the flow of traffic on the road network.

*The initial phase* of the study involved the creation of an *AutoCAD* drawing of the road network system city spread over 3.08 square km area, and the creation of a high-resolution digital *base-map* of the city created at a scale of 1:5000 by stitching together 104 screenshots. The digital *base map* was later used as a base layer in the *AutoCAD* drawing along with details on road links and junctions. Information contained in drawings prepared previously by **Dalal Consultants and Engineers Ltd. (2007)** was used to refine the *AutoCAD* drawing. The composite drawing for the road network thus prepared was imported into the VISSIM micro-simulation environment, and the details on 423 road links were provided along with turning movements at junctions, and the traffic generation points.

The previous chapters provide details on the methodology adopted in this study, collection of video-graphic data, and the details on the strategy adopted in performing the calibration and validation of the *VISSIM*-based simulation model for Mangalore city. The study also includes investigations on performing an *artificial neural network (ANN)* based sensitivity analysis on vehicle and driver characteristics in order to identify the most sensitive factors. The *ANN* used in this study for

sensitivity analysis comprised of neurons optimized in three hidden layers in addition to neurons in the input and output layers. The extended calibration and validation exercises performed based on the sensitivity analysis assisted in the development of a reliable simulation model for the road network.

Furthermore, the present study also incorporates analyses on short-term improvement strategies involving minor widening of existing road junctions, and long-term improvement strategies where the use of flyovers at selected junctions were examined. The study also included a *genetic algorithm* (GA) based traffic signal design using constraints specified based on the HCM (TRB 2000) approach. The following sections of this chapter provide details in the conclusions of the present study.

## 9.2 CONCLUSIONS BASED ON TESTING AND CALIBRATION OF VISSIM MODEL

Data on turning movements at junctions, and vehicular flows and speeds across 18 important mid-block sections of the road network were collected for 80 minutes out of the surveyed peak-hour duration between 5:00 – 6:30 pm on Tuesday 10<sup>th</sup> March 2015. 75% of the video-graphic data corresponding to 60 minutes of video-graphic data was used in the calibration study.

The preliminary calibration of the VISSIM model was performed for the selection of the best *random seed* from random seeds lying between 1 and 50. Random seeds 42 and 25 were identified as the best random seeds based on predictions of vehicular flows across 18 mid-block sections. The simulated volumes were compared to the actual volumes based on the *mean absolute error* (MAE) in prediction, and the *GEH statistic* values. The GEH values for random seeds 42 and 25 were computed as 15.79 and 15.69 respectively.

Although the *GEH* value of random seed 42 was marginally higher than that for random seed 25, the random seed 42 was considered for further simulation exercises as it was observed by Wang et al. (2012), that simulations using random seeds higher than 25 resulted in lesser standard errors. Moreover, it was found that the use of random number 42 provided reliable estimates of the actual values in a wide

variety of simulation experiments as reported by **Ishaque and Noland (2005)**, **Kamdar (2004)**, and **TJPDC (2007)**.

### 9.2.1 Conclusions Based on Multi-Stage Calibrations Performed

The calibration exercises were performed in *VISSIM* by fine-tuning vehicle characteristics and driving behavior characteristics in a number of calibration stages. The calibration studies commenced with the assigning of default values for vehicle and driver characteristics in *VISSIM*. The following observations were made during the calibration exercise performed over 14 major stages:

- ***First and Second Stages of Refinement:*** In the first stage of refinement, the values for *lateral clearances* (for standing and driving vehicles) were assigned as in **Table 6.3a** based on field observations, and also based on values adapted and modified from **Arasan and Krishnamurthy (2008)**, **Manjunatha et al. (2003)** and **Bains et al. (2013)**. In the second stage of refinement, the values for the *desired acceleration* and *maximum acceleration* were assigned based on a trial and error approach as in **Table 6.5a**, and **Table 6.5b** and also based on values suggested by **Arasan and Krishnamurthy (2008)** given in **Table 6.5c**.

Moreover, the values for the *desired deceleration* for each vehicle type as in **Table 6.5d** was computed using the Newton's laws of motion assuming a design speed of 30-40kmph for stopping distances of 30-40m based on IRC 65 (**IRC, 1976**), and IRC 86 (**IRC, 1983**). The values of computations made for 30kmph in the present study tally well with the desired deceleration rates suggested by **Mathew and Radhakrishnan (2010)** as given in **Table 6.5e**.

However, in these simulation exercises, the *mean absolute error (MAE)* between the observed and simulated volumes was found to remain same at around 33.4%, as shown in **Table 6.4** and **Table 6.6**. Also, the *GEH* statistic was unchanged at around 15.79. Here, although the refined values suggested in this stage of calibration were more realistic, the changes in values did not seem to affect the accuracy significantly.

- ***Third Stage to the Seventh Stage of Refinement:*** Further refinements in the values for the *desired accelerations*, the *maximum accelerations*, the *minimum*

*look-ahead distance*, and the *desired speed distributions* were performed from the third to the seventh stage of refinement. In these stages of refinement, the *mean absolute error (MAE)* between the observed and simulated volumes for the 18 mid-block locations was found to reduce from 33.4% to 24.5% while the *GEH* statistic reduced from 15.79 to 11.46 indicating that the assigned values provided better predictions. However, the improvement in the prediction accuracy remained mildly-moderate to marginal in most cases. See **Table 6.8**, **Table 6.10**, **Table 6.12**, **Table 6.14**, and **Table 6.16**. A *minimum look-ahead distance* of 40m came to be adopted through these stages by a trial and error process. Further changes to vehicle characteristics did not result in improving the *GEH* statistic at this stage.

- ***Eighth Stage to the Fourteenth Stage of Refinement:*** Further refinements in the values for driver behavior characteristics such as the *minimum look-back distance*, the *average stand-still distance*, the *additive part of safety distance*, the *multiplicative part of safety distance*, *time-lag between lane/ direction change*, the *minimum longitudinal speeds*, and the *minimum collision time-gain* were performed from the eighth to the fourteenth stage of refinement.

*GEH* statistic value of 2.52 was found to indicate an acceptable level of accuracy within the tolerable limits recommended by **DMRB (1996)**, **FHA (2004)**, and **Wisconsin DOT (2002)**. At the end of this multi-level calibration exercise, it was also observed that for 85% of the links considered as part of the 18 mid-block locations, the *GEH* statistic values were lesser than 5. This satisfied the second-level of criteria recommended by **DMRB (1996)**, **FHA (2004)**, and **Wisconsin DOT (2002)** to ensure reliable predictions of traffic flows.

### **9.2.2 Conclusions Based on Model Validation (after the 14<sup>th</sup> Stage of Calibration)**

The vehicle and driver characteristics refined after the fourteenth level of calibration were noted, and the validation exercise was performed using 25% of the 80 minute video-graphic data set apart for the same. Based on **Table 6.25**, the simulated vehicular volumes of the 18 mid-block locations tallied well with the observed traffic volume with a *mean absolute error (MAE)* of 10.8% and the *GEH*

statistic value of 2.71 for the validation model. The validation results also indicate that the *GEH* values of 85% of the links considered are lesser than 5, satisfying the second criteria recommended by **DMRB (1996)**, **FHA (2004)**, and **Wisconsin DOT (2002)**.

### **9.2.3 Conclusions Based on the Sensitivity Analysis**

Based on trial simulations performed in *VISSIM* as part of the calibration exercise, a database comprising 109 rows of datasets as in **Table 6.27** was prepared with details on changes applied to vehicle and driver characteristics one at a time and the corresponding changes in the values of the *mean absolute errors* in simulated traffic volumes. These datasets were normalized to lie between 0 and 1 based on the lower and upper bound values for vehicle and driver variables.

The relative importance of input variables, or the sensitivity can be determined in ANN approaches using *Garson's Algorithm* (**Garson 1991**) and its modified forms developed by **Gevrey et al. (2003 & 2006)**, and **Olden and Jackson (2002)**. However these approaches were suitable for ANNs with a single hidden layer. The approach suggested by **Ozesmi and Ozesmi (1999)** for ANNs with more than one hidden neuron considered only the weights between the input layer and the first hidden layer to compute the sensitivity of input variables. The present study proposed the use of a modified approach to compute the sensitivity based on connection weights to neurons in all the hidden layers as a modification to the Garson's approach.

The *relative importance of the variables* or the *sensitivity* was computed as in **Table 6.29**. Here, it is observed that the *relative importance* or *sensitivity* of *average stand still distance* is 7.65% indicating that this variable is more sensitive when compared to other vehicle and driver characteristics. The second most sensitive variable is the *minimum look-ahead distance* bearing a *relative importance* value of 7.50%. Similarly, the third and the fourth most sensitive variables are the *multiplicative part of desired safety distance* and the *lower bounds for speed distributions* with *relative importance* values of 7.32% and 7.30% respectively. The characteristics such as *maximum acceleration distributions* and *additive part of*



*desired safety distance* are also sensitive with the *relative importance* values of 7.23% and 7.21%, whereas, the remaining characteristics are not seen to have any significant influence on the accuracy of prediction.

#### **9.2.4 Conclusions Based on Extended Calibration after Sensitivity Analysis**

Based on the results of the sensitivity analysis, an extended multi-level calibration exercise was performed in **Section 6.5** using 75% of the video-graphic data kept apart previously for the same in a manner similar to the original calibration exercise described in **Section 6.2**.

- ***First Level to the Sixth Level of Extended Calibration:*** In the first level to the sixth level of *extended multi-level calibrations* performed after the sensitivity analysis, refinements were made to the *average stand-still distances*, the *minimum look-ahead distances*, and the *multiplicative part of safety distances* that resulted in a significant improvement in the predictive capability of the VISSIM model. These stages of extended calibrations witnessed a reduction in the *mean absolute error (MAE)* from 5.9% to 4.5%, and a reduction in the *GEH* value from 2.52 to 1.89. See **Table 6.30b**, **Table 6.31b**, **Table 6.32b**, **Table 6.33b**, **Table 6.34**, and **Table 6.35b**.

**Fig.6.8b** provides a graphical representation of the reduction in the *mean absolute prediction errors* for flows measured across 18 mid-block sections using the VISSIM model for the calibration exercise and the extended multi-level calibration exercise aimed at refinement of vehicle and driver characteristics.

The decrease in the values of the *mean absolute errors (MAE)* in the extended calibration exercise is graphically depicted as in **Fig.6.8a**, and **Table 6.29**. Here, it can be seen that the sequence followed in the extended calibration procedure based on the findings of the sensitivity analysis ensured the reduction in prediction errors as expected. Thus, the *relative importance of the variables* or the *sensitivity* as computed using the alternative approach based on a modification of the Garson's method was found to be reasonably accurate and reliable. Further refinements however, did not result in any significant improvement in the predictions.

### **9.2.5 Conclusions Based on Extended Validation after Sensitivity Analysis**

The extended validation exercise was performed using the refined values of vehicle and driver characteristics obtained based on the extended calibration exercise performed after the sensitivity analysis. This extended validation exercise was performed in **Section 6.6** in a manner similar to that described in **Section 6.3**. Here, the *mean absolute error (MAE)* was found to be 9.5%, while the *GEH* value was around 2.43 as shown in **Table 6.36**.

## **9.3 CONCLUSIONS ON SHORT-TERM AND LONG-TERM TRAFFIC MANAGEMENT STRATEGIES**

Having developed a fully refined, calibrated, and validated *VISSIM* model for the city based on the findings of the sensitivity analysis as explained in **Chapter 6**, it was proposed to analyse the effect of implementation of *short-term* and *long-term* improvement strategies at selected locations in the city.

### **9.3.1 Conclusions Based on Short-Term Improvements at Selected Locations in the City**

As part of the *short-term improvement strategy-1*, the widening of the road section between Karangalpady Junction and Bunt's Hostel Junction was proposed in order to streamline the movement of vehicles towards Jyothi Junction and also towards Kadri Junction via Bunt's Hostel Junction. Here, it was possible to obtain an increase in the flow of vehicles by 19% and 16%, accompanied by a reduction in stopped delays by 71% and 66% for the flows towards Jyothi Junction and also towards Kadri Junction by all vehicles as measured using *VISSIM*.

As part of the *short-term improvement strategy-2*, the widening of the road section at Bendoorwell Junction was proposed in order to facilitate the movement of vehicles arriving from Kankanady Junction moving to St. Theresa's School Junction, and also to Balmatta Junction via Bendoorwell Junction. Here, it was possible to obtain an increase in the flow of vehicles by 2% and 14%, and a reduction in stopped delays by 58% and 93% for flows towards St. Theresa's School Junction and towards Balmatta Junction by all vehicles as measured using *VISSIM*. Also, in the case of space mean speeds between Bendoorwell Junction and St. Theresa's School Junction,

the space-mean speeds increased by 8%, while for the existing straight-flows from Bendoorwell Junction to Balmatta Junction, the improvement was marginal at 2%.

### **9.3.2 Conclusions on Long-Term Improvements at Selected Locations in the City**

As part of the *long-term improvement strategy-1*, it was proposed to streamline the movement of vehicles arriving from PVS Junction moving towards Jyothi Junction and towards Kadri Junction via Karangalpady Junction and Bunt's Hostel Junction. Considering the performance of a flyover for traffic flows from Karangalpady Junction to Jyothi Junction and Kadri Junction described in **Table 7.3a** and **Table 7.3b**, it can be seen that there is a considerable improvement in vehicular volumes by 51% and 14%, with a significant increase in the space mean speeds by 69% and 17% for the flows towards Jyothi Junction and towards Kadri Junction by all vehicles as measured using *VISSIM*.

### **9.4 CONCLUSIONS BASED ON THE DESIGN OF 3-PHASE TRAFFIC SIGNALS USING HCM2000 DESIGN METHOD AND GENETIC ALGORITHM APPROACH FOR THE SELECTED JUNCTIONS**

In this part of this study, it was initially proposed to design three-phase signals using the *HCM2000 Design Method*(**TRB, 2000**), for four selected junctions in the city, and to compare the performance of the signal timings using the *VISSIM* model. Using the optimized green times obtained using the *HCM2000 Design Method*, the simulated delay/phase/vehicle, the *average delay per vehicle*, and the *total flows across the junctions* were computed using the *VISSIM* model as in **Table 8.4b**. Here, it can be observed that the average reduction in delays for the four junctions is around 11.62% when compared to the performance of the signals using the existing signal timings.

Here, it can be observed that the signal timings computed using the *GA*-based approach for minimization of traffic delays along with the *HCM2000* based constraints could give a better performance when compared to the *HCM2000 Design Method*, while there was a significant reduction in delays when compared to the manual operation of signals.

## **9.5 MAJOR CONTRIBUTIONS OF THE STUDY**

The major contributions of this study include the following:

1. The overall approach adopted in performing the calibration studies discussed in this work was evolved through an elaborate trial and error procedure. The basic framework for calibration and fine-tuning of vehicle and driver characteristics adopted in this study.
2. The present study incorporates the use of an *ANN* structure with hidden neurons organized in three hidden layers for which the use of an alternative *modified Garson's approach* was proposed. The sequence of relative importance of variables identified in the sensitivity analysis ensured further refinement of vehicle and driver characteristics on expected lines in the extended calibration process.

## **9.6 LIMITATIONS AND SCOPE FOR FUTURE STUDIES**

The limitations of the present study are summarized below:

1. The collection of video-graphic data for large network area during peak hours is a difficult task that requires proper synchronization in the operation of video cameras and mobile phone cameras by skilled and trained man-power.
2. Further studies on fine-tuning vehicle and driver characteristics such as, temporary lack of attention, minimum headway, safety distance reduction factor, maximum deceleration considering movement of a group of vehicles, reaction to amber signal, and the influence of power-weight ratio of vehicles can be performed.
3. The study on sensitivity analysis of vehicle and driver characteristics may be performed using other alternative approaches including statistical methods, genetic algorithm, and empirical approaches.

## REFERENCES

1. Abu-Lebdeh, G. and Benekohal, R.F. (2000). "Genetic Algorithms for Traffic Signal Control and Queue Management of Oversaturated Two-way Arterials." *Transportation Research Record*, No. 1727, 61-67.
2. Ahmed, Kazi Iftekhar (1999). "Modelling Drivers' Acceleration and Lane Changing Behavior." Thesis. Doctor of Science in Transportation Systems and Decision Sciences, Massachusetts Institute of Technology.
3. Amin, S. M., Rodin, E. Y., Liu, A. P., Rink, K., and Garcia-Ortiz, A. (1998). "Traffic Prediction and Management via RBF NeuralNets and Semantic Control." *Computer-Aided Civil and Infrastructure Engineering*, 13, 315-327.
4. Arasan, V.T. and Krishnamurthy, K. (2008). "Study of the Effect of Traffic Volume and Road Width on PCU Values of Vehicles using Microscopic Simulation." *Journal of Indian Road Congress*, Vol. 69 (2), pp. 133-149.
5. ASCI (2011). "City Sanitation Plan (CSP)." Karnataka draft report of Mangalore, Administration Staff College of India (ASCI), submitted to Director of Municipal Administration, Govt. of Karnataka, Bangalore.
6. Back, T., Fogel, David, B. and Michalewicz, Z. (1997). "Handbook of Evolutionary Computation." *Computational Intelligence Library*, Published in cooperation with the Institute of Physics, Ring-bound edition, 17<sup>th</sup> April.
7. Bains, Manaraj Singh, Bharadwaj, Anshuman, Arkatkar, S.S., and Velmurugan, S. (2013). "Effect of Speed Limit Compliance on Roadway Capacity of Indian Expressways." *Procedia Social and Behavioural Sciences*, Vol. 104, pp. 458-467.
8. Balling, N. and Hansen, T.M. (2004). "Upper mantle reflectors: modeling of seismic wave-field characteristics and tectonic implications." *Geophysics Journal*, Vol. 157, pp. 664–682.
9. Braun, R., Kemper, C. and Weichenmeier, F. (2008). "Travolution – adaptive urban traffic signal control with an evolutionary algorithm." *Proceedings of the 4th International Symposium Networks for Mobility*, Stuttgart, Germany, pp. 24–25.
10. Brilon, W. and Wu, N. (1990). "Delays at fixed-time traffic signals under time dependent traffic conditions." *Traffic Engineering and Control* Vol. 31(12), pp. 623–631.
11. Celikoglua, Hilmi Berk and Cigizoglu, Hikmet Kerem (2007). "Modelling public transport trips by radial basis function neural networks." *Mathematical and Computer Modelling* 45 (2007), pp. 480-89.

12. Ceylan, P. and Bell, M.G.H. (2004). "Traffic Signal Timing Optimisation Based on Genetic Algorithm Approach, Including Driver's Routing." *Transportation Research, Part B*, 38(4), pp. 329-342.
13. Chen, Shuyan and Wang, Wei (2006). "Traffic Volume Forecasting Based on Wavelet Transform and Neural Networks." J. Wang et al. (Eds.): *ISNN 2006*, LNCS, 3973, pp. 1 – 7.
14. Columbia River Crossing (2006). "*VISSIM Calibration and Validation*." Technical Report, Columbia River Crossing Project Office, Columbia, USA.
15. Courage, K.G. and Papapanou, P. (1977). "Delay at Traffic Actuated Signals." *Traffic signs and signals*, Florida Department of Transportation.
16. Deb, K. (2000). "Optimization for Engineering Design." Prentice Hall of India Private Ltd., New-Delhi.
17. Dick, A.C. (1966). "Speed-Flow Relationships within an Urban Area." *Traffic Engineer Control*, Vol. 8, No. 6, pp. 393-396.
18. Dion, F., Rakha, H. and Kang, Y. (2004). "Comparison of delay estimates at under-saturated and over-saturated pre-timed signalized intersections." Elsevier, *Transportation Research Part B*, pp. 99–122.
19. DMRB (1996). "Traffic Appraisal of Roads Schemes." *Design Manual for Roads and Bridges*, Vol. 12(2), UK Highways Agency, May, London.
20. Dogan, Ueruen, Edelbrunner, Hannes, and Iossifidis, Ioannis (2008). "Towards a Driver Model: Preliminary Study of Lane Change Behavior." *Proceedings of the 11<sup>th</sup> International IEEE Conference on Intelligent Transportation Systems Beijing, China, October 12-15, 2008*
21. Duncan, N.C. (1979). "A Further Look at Speed/Flow/Concentration." *Traffic Engineering and Control*, Vol. 20, No. 10, pp. 482-483.
22. Durrani, Umair, Lee, Chris, and maoh, Hanna F. (2016). "Calibrating the Wiedemann's vehicle-following model using mixed vehicle-pair interactions." *Transportation Research Part C: Emerging Technologies*, Vol. 67, pp. 227-242, Ontario, Canada. DOI: 10.1016/j.trc.2016.02.012.
23. Edie, L.C. (1961). "Car-Following and Steady-State Theory for Non-Congested Traffic." *Operations Research*, Vol. 9, No. 1, pp. 66-76.
24. *Encyclopaedia Britannica Book of the Year (1985)*. "Britannica Book of the Year: 1985." Ed. Philip W. Goetz, Encyclopaedia Britannica Ltd., London.
25. Eriskin, E., Karahancer, S., Terzi, S., and Saltan, M. (2017) Optimization of Traffic Signal Timing at Oversaturated Intersections Using Elimination Pairing System, *Procedia Engineering* 187, pp. 295 – 300, 10th International Scientific Conference Transbaltica: Transportation Science and Technology-2017.

26. Fambro, D.B. and Roupail, N.M. (1997). "Generalized delay model for signalized intersections and arterial streets." *Transportation Research Record*, No. 1572, TRB, National Research Council, Washington, DC, pp. 112–121.
27. Fellendorf, Martin and Vortisch, Peter (2001). "Validation of the Microscopic Traffic Flow Model VISSIM in Different Real-World Situations." *Proceeding*
28. Foy, M.D., Benekohal, R.F. and Goldberg, D.E. (1992). "Signal timing determination using genetic algorithms." *Transportation Research Record*, TRB. National Research Council, Washington DC, pp. 108–115.
29. Gallelli, Vincenzo and Vaiana, Rosolino (2008). "Roundabout Intersections: Evaluation of Geometric and Behavioural Features with VISSIM." *Proceeding National Roundabout Conference*, Transportation Research Board, Kansas City, Missouri, May.
30. Garson, G. D. (1991). "Interpreting neuralnetwork connection weights", *Artificial Intelligence Expert*, Vol. 6, No. 4, pp. 46–51.
31. Gartner, N.H. (1983). "A Demand-responsive Strategy for Traffic Signal Control." *OPAC*, *Transportation Research Record*, No. 906. Transportation Research Board, Washington, DC, pp. 75-81.
32. Gazis, D. C. (1964). "Optimum Control of a System of Oversaturated Intersections." *Operation Research*, Vol. 12, No. 6, pp. 815-831.
33. Gevrey, M., Dimopoulos, I., and Lek, S. (2003). "Review and comparison of methods to study the contribution of variables in artificial neural network models." *Ecological Modelling* 160, pp. 249-264.
34. Gevrey, M., Dimopoulos, I., and Lek, S. (2006). "Two-way interaction of input variables in the sensitivity analysis of neural network models." *Ecological Modelling* 195, pp. 43-50.
35. GoK (2017). "Management Information System." Public Works, Ports & Inland Water Transport Department (PWP&IWTD), Government of Karnataka, Bangalore. Available at <http://103.241.144.46:81/pdf/mis/MIS-2017.pdf>. Site last accessed on 14<sup>th</sup> April 2020.
36. GoK (2019). "Annual Report of the Transport Department for the Year 2018-19." Transport and Road Safety Department, Government of Karnataka. Website: <https://transport.karnataka.gov.in/storage/pdf-files/Annual%20Report%20Eng%202018-19.pdf>. Accessed on 17-08-2020.
37. Greenberg, H. (1959). "An Analysis of Traffic Flow." *Operations Research*, Vol. 7, pp. 79-85.
38. Habtemichael, F., and Picado-Santos, L. (2012). "Sensitivity Analysis of VISSIM Driver Behavior Parameters on Safety of Simulated Vehicles and their Interaction with Operations of Simulated Traffic." Paper presented at the 92nd

- Annual Meeting of the Transportation Research Board. Washington, DC. January 13-17, 2013.
39. Haupt, R.L. and Haupt, S.E. (1998). "Practical Genetic Algorithms." John Wiley & Sons, Inc, New York.
  40. IRC: 106 (1990). "Guidelines for Capacity of Urban Roads in Plain Areas." IRC: 106-1990, Pub: Indian Roads Congress (IRC), New-Delhi.
  41. IRC: 86 (1983). "Geometric design standards for Urban roads in plains." Indian Road Congress, New Delhi, India.
  42. IRC: 93 (1985). "Guidelines on Design and Installation of Road Traffic Signals." Indian Road Congress, New Delhi, India.
  43. Jamal, A., Raman, M. T., Al-Ahmadi, H. M., Ulla, I., and Wahid, M. (2020). "Intelligent Intersection Control for Delay Optimization: Using Meta-Heuristic Search Algorithms." *Sustainability* 2020, 12, 1896; doi:10.3390/su12051896.
  44. Kalteh A.M. (2008). "Rainfall-runoff modelling using artificial neural networks (ANNs): modelling and understanding." *Caspian Journal of Environmental Science*, Vol. 6(1), pp. 53-58.
  45. Karakikes, I., Spanglera, M. and Margreitera, M. (2017). "Designing a VISSIM-Model for a motorway network with systematic calibration on the basis of travel time measurements." *Transportation Research Procedia* 24, 171–179, 3<sup>rd</sup> Conference on Sustainable Urban Mobility, Volos, Greece.
  46. Khanna, S.K. and Justo, C.E.G. (1987). "Highway Engineering." 6<sup>th</sup> Ed., Nemchand and Bros., Roorkee.
  47. Laval, Jorge A. and Daganzo, Carlos F. (2004). "Multi-lane hybrid traffic flow model: a theory on the impacts of lane-changing manoeuvres." Paper No. 587, Presented under topic titled: Land Use Merging and Lane Changing Behavior, sponsored by the Traffic Flow Theory and Characteristics Committee, 84<sup>th</sup> TRB Annual Meeting, 9-13 Jan, 2005, Hilton Hotel, Washington, D.C.
  48. Lin, F. and Cooke, D.J. (1986). "Potential Performance Characteristics of Adaptive Control at Individual Intersections." *Transportation Research Record*, No. 1057. Transportation Research Board, Washington, DC, pp. 30-33.
  49. Liu, Henry X., Wu, Xinkai, Ma, Wenteng, and Hu, Heng (2009). "Real-time queue length estimation for congested signalized intersections." *Transportation Research Part C*, 17, 412–427.
  50. Lo, H., Chang, E. and Chan, Y.C. (2001). "Dynamic Network Traffic Control." *Transportation Research Board, Part A*, Vol. 35, No. 8, pp. 721-744.
  51. Lobo, Norbert (2001). "Patterns of Rural to Urban migration: A case study of Dakshina Kannada district." PhD thesis submitted to the department of Economics, Mangalore University, 2001. Available at <http://hdl.handle.net/10603/92095>. Site visited on 1<sup>st</sup> Dec. 2016.



52. Lownes, Nicholas E. and Machemehl, Randy B. (2010). "Exact and Heuristic Methods for Public Transit Circulator Design." *Transportation Research Part B: Methodological*, Vol. 44, No.2, pp. 309-318.
53. Manjunatha, Pruthvi, Vortisch, Peter and Mathew, Tom V. (2013). "Methodology for the Calibration of *VISSIM* in Mixed Traffic." Paper No. 13-3677, revised paper submitted for publication in TRB, 92<sup>nd</sup> Annual Meeting Compendium of Papers, Washington 2013.
54. Mathew, Tom V. and Radhakrishnan, Padmakumar (2010). "Calibration of Microsimulation Models for Non-lane-based Heterogeneous Traffic at Signalized Intersections." *Journal of Urban Planning and Development*, ASCE, Vol. 136, No. 1, pp. 59-66.
55. Miller, A.J. (1963). "Settings for fixed-cycle traffic signals." *Operations Research*, Quarterly 14, pp. 373-386.
56. Wing, Ministry of Road Transport and Highways (MoRTH), Govt. of India, New-Delhi.
57. Nakatsuyama, M., Nagahashi, H. and Nishizuka, N. (1984). "Fuzzy Logic Phase Controller for Traffic Junctions in One-way Arterial Roads." *Proceedings of the IFAC 9<sup>th</sup> Triennial World Conference*, Pergamon Press, Oxford, pp. 2865-2870.
58. Nyame-Baafi, E., Adams, C.A. and Osei, K.K. (2018). "Volume warrants for major and minor roads left-turning traffic lanes at unsignalized T-intersections: A case study using *VISSIM* modelling." *Journal of Traffic and Transportation (Engl. Ed.)*, 5(5), 417-428.
59. Olden, J.D. and Jackson, D.A. (2002). "Illuminating the "black-box": a randomization approach for understanding variable contributions in artificial neural networks." *Ecological Modelling* 154, pp. 135-150.
60. Otkovic, I. I., Tollazzi, Tomaz, and Srami, Matjaz (2013a). "Calibration of Microsimulation Traffic Model using Neural Network Approach." *Expert Systems with Applications*, 40, 5965-5974.
61. Papacostas, C.S. (1987). "Fundamentals of Transportation Engineering." Prentice-Hall International, Inc.
62. Pappis, C.P. and Mamdani, E.H. (1977). "A fuzzy logic controller for a traffic junction. *IEEE Transactions on Systems*." *Man and Cybernetics*, pp. 707-717.
63. Park, B. and Qi, H. (2005). "Development and Evaluation of Simulation Model Calibration Procedure." *Proceedings of 84<sup>th</sup> TRB Annual Meeting*, Transportation Research Board, Washington, DC, January.
64. Park, B., Messer, C. J. and Urbanik, T. (1999). "Traffic Signal Optimization Program for Oversaturated Conditions: Genetic Algorithm Approach." *Transportation Research Record*, No. 1683, pp. 133-142.

65. Pignataro, L.J., McShane, W.R., Crowley, K.W., Lee, B. and Casey, T.W. (1978). "Traffic Control in Oversaturated Street Networks." NCHRP Report 194, TRB Research Council, Washington D.C.
66. Pipes, L.A. (1967). "Car Following Models and the Fundamental Diagram of Road Traffic." *Transportation Research*, Vol. 1, No. 1, pp. 21-29.
67. PTV (2011). "VISSIM 5.30-05 User Manual." Planung Transport Verkehr (PTV) AG, Stumpfstrase 1, D-76131 Karlsruhe, Germany.
68. Rajeev, S. and Krishnamoorthy, C.S. (1992). "Discrete Optimization of Structures using Genetic Algorithm." *Journal of Structural Engineering*, Vol. 118, No. 5, ASCE, pp-1233-1250.
69. Robertson, D.I. (1979). "Traffic models and optimum strategies of control." *Proceedings of the International Symposium on Traffic Control Systems*, pp. 262–288.
70. Smith, J. and Blewitt, R. (2010). "Traffic Modelling Guidelines." TfL Traffic Manager and Network Performance Best Practice Version 3.0, Office of the Mayor of London. Available at <http://content.tfl.gov.uk/traffic-modelling-guidelines.pdf>. Site last accessed on 15<sup>th</sup> Aug. 2019.
71. Srikanth, S., Mehar, A., Praveen, K. G. N. V. (2020) "Simulation of Traffic Flow to Analyse Lane Changes on Multi-lane Highways under Non-lane Discipline", *Periodica Polytechnica Transportation Engineering*, 48(2), pp. 109–116. DOI: 10.3311/PPtr.10150
72. Srinivasan, D., Cheu, R.L., Poh, Y.P., and Ng, A.K.C. (2000). "Development of an intelligent technique for traffic network incident detention." *Engineering Applications of Artificial Intelligence*, Vol. 13, pp. 311-322.
73. Stanek, David and Milam, Ronald T. (2004). "High-Capacity Roundabout Intersection Analysis: Going Around in Circles." Fehr & Peers Associates, Inc., Roseville, California.
74. Tepley, S. (1995). "Canadian capacity guide for signalized intersections." 2<sup>nd</sup> Ed., Institute of Transportation Engineers, District 7, Canada.
75. Tian, Rongrong, and Zhang, Xu (2017) "Design and Evaluation of an Adaptive Traffic Signal Control System – A Case Study in Hefei, China". *Proc. Intl. Symposium of Transport Simulation (ISTS'16)*, Jeju City, South Korea, 23-25 June 2016. DOI: 10.1016/j.trpro.2017.03.084.
76. TJPDC (2007). "Simulation Model Development and Calibration." US-29 North Corridor Transportation Study, Technical Memorandum 5, Published by Thomas Jefferson Planning District Commission (TJPDC) Charlottesville, VA, prepared by Meyer, Mohaddes Associates, Community Design + Architecture Urban Advantage, US. Available at [http://www.tjpd.org/pdf/places\\_29/techmemos/29N%20Tech%20Memo%205%20VISSIM\\_Calibration.pdf](http://www.tjpd.org/pdf/places_29/techmemos/29N%20Tech%20Memo%205%20VISSIM_Calibration.pdf). Site accessed on 5th June 2015.

77. Toledo, Tomer, Choudhury, Charisma.F. and Ben-Akiva, Moshe E. (2005). "Lane-Changing Model with Explicit Target Lane Choice." *Journal of the Transportation Research Board*, No. 1934, pp. 157–165. DOI: 10.1177/0361198105193400117.
78. Tong, Yue, Zhao, Lei, Li, Li., and Zhang, Yi (2015). "Stochastic Programming Model for Oversaturated Intersection Signal Timing." *Transp. Res. Part C*, 58, 474 – 486.
79. TRB (2000). "Highway Capacity Manual 2000." *Transportation Research Board (TRB)*, TRB Special Report 209, National Research Council, Washington D.C.
80. TRB (2010). "Highway Capacity Manual 2010." *Transportation Research Board (TRB)*, 5<sup>th</sup> Ed., National Research Council, Washington D.C.
81. USBC (1986). "Statistical Abstract of the United States: 1987." *United States Bureau of the Censes, U S Department of commerce*, 107<sup>th</sup> Ed., Washington D.C.
82. Velez, Enrique González, Díaz, Didier M. Valdés and Villafañe, Felipe Luyanda (2006). "Evaluation of VISSIM a Dynamic Simulation Model for an Arterial Network at Mayagüez, Puerto Rico." *Proceedings of 4<sup>th</sup> LACCEI International Latin American and Caribbean Conference for Engineering and Technology (LACCET'2006), Breaking Frontiers and Barriers in Engineering: Education, Research and Practice, Mayagüez, Puerto Rico, June.*
83. Vilarinho, Cristina and Tavares J. P. (2014). "Real-time Traffic Signal Settings at an Isolated Signal Control Intersection." *17th Meeting of the EURO Working Group on Transportation, EWGT2014, Transportation Research Procedia*, 3, 1021 – 1030.
84. Wang, Yibing, Papageorgiou, Marcos and Messmer. Albert (2007). "Real-Time Freeway Traffic State Estimation Based on Extended Kalman Filter: A Case Study." *In Transportation Science*, Vol. 41, No. 2, pp. 167–181.
85. Wang, Yinhai, Lao, Yunteng, Liu, Cathy and Xu, Guangning (2012). "Simulation-Based Test bed Development for Analysing Toll Impacts on Freeway Travel." *Final Report TNW2012-16 for Research Project Agreement No. 62-0943, a report prepared for Transportation Northwest by the Dept. of Civil and Environmental Eng., University of Washington, Seattle, Washington, for the project sponsored by Transportation Northwest (TransNow), University of Washington and Washington State Department of Transportation (WSDOT), Olympia, WA, in cooperation with U.S. DoT, and FHA. Available at [http://ntl.bts.gov/lib/46...acts\\_on\\_Freeway\\_Travel.pdf](http://ntl.bts.gov/lib/46...acts_on_Freeway_Travel.pdf).*
86. Wiedemann, R. and Reiter, U. (1991). "Microscopic Traffic Simulation: The Simulation System Mission." *PTV America, Inc. website [Online]* <http://ptvag.com/download/traffic/library/Wiedemann.pdf>. Site Accessed on 11 December 2013.

87. Wisconsin DOT (2002) Freeway System Operational Assessment,” *Paramics Calibration and Validation Guidelines* (Draft), Technical Report I-33, Wisconsin DOT, District 2, Milwaukee, WI, June.
88. WSP Management Services Ltd. (2011). “A43 Corby Link Road: Best and Final Offer - Further Information.” NSTM Public Transport Local Model Validation Report - Summary, Highways, 28 May 2011, WSP Management Services Limited, London.
89. Yuan, Changliang, Yang, X., and Shen, F. (2006). “Fixed Cycle Strategy in Oversaturated Network Traffic Control.” The 6<sup>th</sup> World Congress on Intelligent Control and Automation, pp. 8674-8678.
90. Zhang, Hongjun, Ritchie, S. G., and Lo, Zhen-Ping (1997). “Macroscopic Modeling of Freeway Traffic Using an Artificial Neural Network.” *Transportation Research Record, Journal of the Transportation Research Board*, 1588(1), 110-119.
91. Zhu, J. Z., Cao, J. X., and Zhu, Y. (2014). “Traffic Volume Forecasting based on Radial Basis Function Neural Network with the Consideration of Traffic Flows at the Adjacent Intersections.” *Transportation Research Part C*, 47(2), 139–154.

#### **WEBSITES:**

1. Website: ADOT: Traffic - Frequently asked questions. Arizona Department of Transportation (ADOT), Available at <https://www.azdot.gov/business/engineering-and-construction/traffic/faq>. Site last accessed on 16<sup>th</sup> April 2016.
2. Website: CIA-2015: Roadways, CIA Factbook, Central Intelligence Agency (CIA), USA. Available at <https://www.cia.gov/library/publications/the-world-factbook/rankorder/2085rank.html>. Site last accessed on 18<sup>th</sup> Nov. 2015.
3. Website: Google\_Maps: Mangalore, Karnataka. <https://www.google.com/maps/place/Mangalore,+Karnataka/@12.9229829,74.782023,12z/data=!3m1!4b1!4m5!3m4!1s0x3ba35a4c37bf488f:0x827bbc7a74fcfe64!8m2!3d12.9141417!4d74.8559568>. Site last accessed on 14<sup>th</sup> April 2020.
4. Website: Knoema: World Data Atlas, India-Roads, Total Network. Available at <https://knoema.com/atlas/India/Road-network>. Site last accessed on 18<sup>th</sup> Oct. 2016.
5. Website: MoSPI-2018. “Statistical Year Book of India: 2018.” Ministry of Statistics and Programme Implementation (MoSPI), Motor Vehicles, Number of Motor Vehicles Registered In India. Available at [http://mospi.nic.in/sites/default/files/statistical\\_year\\_book\\_india\\_2015/Table-20.1\\_1.xlsx](http://mospi.nic.in/sites/default/files/statistical_year_book_india_2015/Table-20.1_1.xlsx). Site last accessed on 12<sup>th</sup> April 2020.

6. Website: MUDA-Govt\_of\_Karnataka, Mangalore Urban Development Authority (MUDA), <http://mudamangalore.com>. Site accessed on 30<sup>th</sup> Nov. 2016.
7. Website: NHAI: Indian Road Network and Modal Split. Available at <http://www.nhai.org/roadnetwork.htm>. Site last accessed on 15<sup>th</sup> Nov. 2015.
8. Website: The-Hindu-1, Revised Master Plan for Mangalore, <http://www.thehindubusinessline.com/todays-paper/tp-investmentworld/revised-master-plan-for-mangalore/article1086350.ece>. Pub. On Dec. 13, 2009. Site accessed on 30<sup>th</sup> Nov. 2016.
9. Website: Virtual-Mangalore: About Mangalore, A product of Sequoya Software Solutions. Available at <http://www.virtualmangalore.com/know-mangalore.html#top>. Site last accessed on 14<sup>th</sup> April 2020.
10. Website: Wiki-land-area: By\_area, [https://en.wikipedia.org/wiki/List\\_of\\_countries\\_and\\_dependencies](https://en.wikipedia.org/wiki/List_of_countries_and_dependencies). Site accessed on 19<sup>th</sup> Nov. 2015.

## LIST OF PUBLICATIONS

**Marsh M. Bandi**

**(Reg. No. 138005CV13F06)**

1. George, Varghese, and Bandi, Marsh M. (2015). "A Demonstration of a Single Variable Genetic Algorithm Optimization for a 2-Phase Traffic Signal." Proc. Second International Conference on Information Technology, Science, Engineering, and Management (ICITSEM-215), held at Hyatt Place, Al-Rigga, Dubai, UAE. 25-26 Feb, pp.34-39. Received Best Paper Award and Gold Medal.
2. George, Varghese, Purumala, Snehith, Tamhane, Ishan S., Reddy, Sreeja, Ranjusha, P.G., Bandi, Marsh M., and Anand, Akash (2016). "Fitting Statistical Distributions for Speeds and Headways for Peak and Non-Peak Mixed Traffic Flows in Mangalore City Karnataka, India." International Journal of Earth Sciences and Engineering, Vol. 9, No. 2, pp. 512-520. ISSN 0974-5904. Scopus Indexed Journal 2010-16. H-Index: 9, Impact Factor: 0.13.
3. Bandi, Marsh M., and George, Varghese (2020). "An Isolated Traffic Signal Design using a GA-based Optimization Technique." International Journal of Recent Technology and Engineering (IJRTE), Vol. 8, Issue5, pp. 2598-2604. ISSN: 2277-3878 (Online). Not Indexed in Scopus Since 2020. DOI:10.35940/ijrte.E6261.018520.
4. Bandi, Marsh M., and George, Varghese (2020). "Microsimulation Modelling in VISSIM on Short-term and Long-term Improvements for Mangalore City Road Network." Transportation Research Procedia, 48, Pub. Elsevier, pp. 2725-2743. ISSN: 2352-1465 (Online). Scopus Indexed Journal from 2014 to present, H-Index: 25, CiteScore: 2.5, Source Normalized Impact per Paper (SNIP): 0.945, SCImago Journal Rank (SJR): 0.476. DOI: 10.1016/j.trpro.2020.08.243.
5. Bandi, Marsh M., and George, Varghese (2020). "Calibration of Vehicle and Driver Characteristics in VISSIM and ANN-based Sensitivity Analysis." International Journal of Microsimulation, Vol. 0(0), Research Article, ISSN: 1747-5864. Scopus Indexed Journal from 2015 to Present, H-Index: 4, CiteScore: 0.9, Source Normalized Impact per Paper (SNIP): 0.510, SCImago Journal Rank (SJR): 0.213. DOI: <https://doi.org/10.34196/ijm.00219>.



## BIO-DATA

**Marsh M. Bandi**



Registration No. : 138005CV13F06  
Date of Registration : 23-12-2013  
Date of Re-registration : 14-11-2017  
Address for Communication : Shirur Park, Vidyanagar,  
Hubli - 580021  
Email : marsh\_cv13f06@nitk.edu.in  
marsh.band@gmail.com  
Contact Details : +91-9535142092  
Academic Qualifications :

<i>Qualification</i>	<i>Discipline/ Specialization</i>	<i>School/ College</i>	<i>University</i>	<i>Year of passing</i>	<i>% marks/CG PA</i>
M-Tech.	Transportation Systems Engineering	NITK Surathkal	Deemed	2013	8.69
B.E	Civil Engineering	S.D.M College of Engg & Tech, Dharwad.	V.T.U Belgaum	2010	69.44%
PUC-II	Science + PCMB Stream	CHE TAN P.U.Science College, Hubli.	P.U.E. Bangalore	2006	65.83%
SSLC	Kannada	K.L.E Society H.F.Kattimani School Hubli.	K.S.E.E.B. Bangalore	2004	73.12%



## APPENDIX I

Vehicle and Driver Characteristics Investigated in this Study	
Minimum lateral Clearance	This is the minimum distance to be maintained between vehicles when overtaking vehicles within the lane while keeping a safe distance to vehicles in the adjacent lanes. The default value is 1 m.
Desired Acceleration Distribution	This is the distribution of desired accelerations for different vehicle types required to increase the speed from 0 kmph to 100 kmph, which is lesser than maximum acceleration.
Maximum Acceleration Distribution	This is the distribution of maximum accelerations for different vehicle types required to increase the speed from 0 kmph to 100 kmph.
Deceleration Distribution	This is the distribution of decelerations for different vehicle types required to reduce the speed from 100 kmph to 0 kmph.
Lower-bound for Desired Speed	This is the minimum speed of different vehicle types on the road network.
Upper-bound for Desired Speed	This is the maximum speed of different vehicle types on the road network.
Minimum look-ahead distance	This is defined as the minimum distance that a vehicle can see forward in within the same link in order to overtake. This is of special importance when modeling lateral movement of vehicles. A value greater than 0.00, and around 20-30m can be specified if a number of vehicles can be overtaken within the lane.
Minimum longitudinal speed for lateral movement (MinSpeedForLat)	It is the minimum longitudinal speed which permits vehicles to move laterally. The default value is 1 kmph.
Minimum collision time gain (MinCollTimeGain)	This is defined as the minimum reaction time required to perform a lateral movement (to the adjacent lane) such that the driver can move ahead of the next vehicle in the traffic stream without collision. This depends upon the speed of the vehicle. The default value for collision time gain is 2 seconds.